Folia Histochemica et Cytobiologica

Scientific quarterly devoted to problems of histochemistry, cytochemistry and cell & tissue biology

www.fhc.viamedica.pl

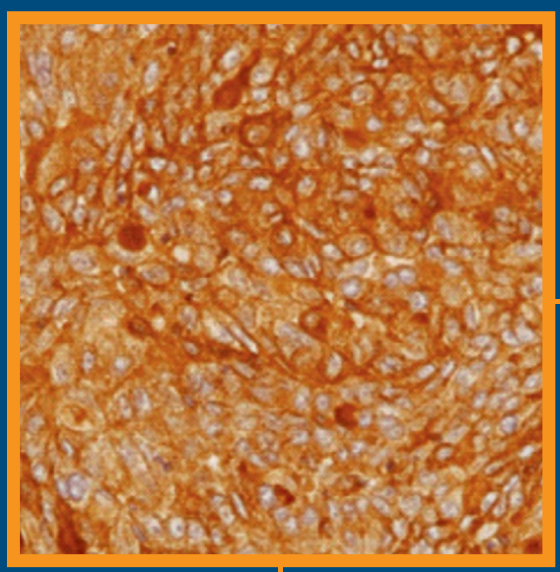

Vol. 57
No. 3
2019

ISSN 0239-8508

VIA MEDICA

Folia Histochemica et Cytobiologica

Scientific quarterly devoted to problems of histochemistry,
cytochemistry and cell & tissue biology
www.fhc.viamedica.pl

EDITOR-IN CHIEF:
Z. Kmiec (Gdansk, Poland)

EDITORS:
M. Piasecka (Szczecin, Poland)
M.Z. Ratajczak (Louisville, USA)
J. Thekkiniath (New Haven, USA)

EDITORIAL BOARD:
C.E. Alpers (Seattle, USA)
B. Bilinska (Cracow, Poland)
I.-D. Caruntu (Iassi, Romania)
J.R. Couchman (Copenhagen, Denmark)
M. Dietel (Berlin, Germany)
P. Dziegiel (Wroclaw, Poland)
T. Fujimoto (Nagoya, Japan)
J. Kawiak (Warsaw, Poland)
J.Z. Kubiak (Rennes, France)
J.A. Litwin (Cracow, Poland)
C. Lucini (Naples, Italy)
A. Lukaszyk (Poznan, Poland)
Z. Mackiewicz (Vilnius, Lithuania)
A. Mazur (Clermont-Ferrand, France)
I. Petersen (Jena, Germany)
A.T. Slominski (Memphis, USA)
C.J.F. van Noordan (Amsterdam, Netherlands)
Y. Wegrowski (Reims, France)
S. Wolczynski (Bialystok, Poland)
M. Zabel (Poznan, Poland)
V. Zinchuk (Kochi, Japan)
M. J. Zeromski (Poznan, Poland)
M.A. Zmijewski (Gdansk, Poland)

MANAGING EDITOR:
C. Kobierzycki (Wroclaw, Poland)

PUBLISHER EDITOR:
I. Hallmann (Gdansk, Poland)

EDITORIAL OFFICE:
Department of Histology
Medical University of Gdansk
Debinki St. 1, 80–210 Gdansk, Poland
tel.: + 48 58 349 14 37
fax: + 48 58 349 14 19
e-mail: zkmiec@gumed.edu.pl
http://www.fhc.viamedica.pl

Folia Histochemica et Cytobiologica (pISSN 0239–8508, eISSN 1897–5631) is published quarterly, one volume a year, by the Polish Society for Histochemistry and Cytochemistry at VM Media sp. z.o.o VM Group sp.k., Gdansk.
Indexed in: Index Medicus/MEDLINE, Excerpta Medica/EMBASE, Chemical Abstracts/CAS, SCI Expanded, SciSearch, Biochemistry & Biophysics Citation Index, ISI Alerting Services, Biosis Previews Index Copernicus, Biological Abstracts, SCOPUS, Research Alert, ProQuest, EBSCO, DOAJ, Ulrich's Periodicals Directory.

POLISH SOCIETY FOR HISTOCHEMISTRY AND CYTOCHEMISTRY STATEMENT OF FOLIA HISTOCHEMICA ET CYTOBIOLOGICA EDITORIAL POLICY

Folia Histochemica et Cytobiologica is an international, English-language journal devoted to the rapidly developing fields of histochemistry, cytochemistry, cell and tissue biology.

The Folia Histochemica et Cytobiologica publishes papers that meet the needs and intellectual interests of medical professionals, basic scientists, college and university teachers and students. Prospective authors should read most recent issues of FHC to determine the appropriateness of a possible contribution. However, such an examination does not provide an infallible guide because editorial policy is always under review. Technical correctness is necessary, but it is not the only condition for acceptance. Clarity of exposition and potential interest of the readers are important considerations; it is the reader, not the author, who must receive the benefit of the doubt.

Folia Histochemica et Cytobiologica publishes review articles, original articles, short communications and proceedings of scientific congresses/symposia. Fields of particular interests include development and application of modern techniques in histochemistry and cell biology, cell biology and pathology, cell-microenvironment interactions, tissue organization and pathology.

Manuscripts announcing new theoretical or experimental results, or manuscripts questioning well-established and successful theories, are highly desirable and are a subject for evaluation by specialists. Manuscripts describing original research that clarifies past misunderstandings or allows a broader view of a subject are acceptable. Manuscripts that demonstrate new relations between apparently unrelated areas of fields of interests are appropriate. Manuscripts that show new ways of understanding, demonstrating, or deriving familiar results are also acceptable. Such manuscripts must provide some original cytobiological insight and not just a clever derivation.

Regularly, review or tutorial articles are published, often of a length greater than that of the average article. Most of these articles are a subject of a review; authors planning such articles are asked to consult with the editors at an early stage.

Most readers of a particular article will be specialists in the subject matter presented; the context within which the paper is presented should be established in the order given in Instructions for Authors. Manuscripts must be technically correct and must take proper cognizance of previous work on the same subject regardless of where it may have appeared. Such referencing is especially important for reminders of once well known ideas, proofs, or techniques that may have again become useful to readers. It is the responsibility of the author to provide adequate references; editors and referees will not do the literature search that should have been done by the authors. The references are a matter of review though.

Contributions considered include: Regular Articles (Papers), Short Communications, Review Articles, Conference Proceeding, Book Reviews and Technical Notes, which describe new laboratory methods or substantial improvements of the existing techniques. Regular articles should be about five journal pages or less in length. Short communications are usually confined to the discussion of a single concept and should be about two journal pages in length. Review articles are confined to a broad discussion and should contain the most recent knowledge about the subject.

Instructions concerning the preparation of manuscripts are given in the Information for Authors. Care in following those instructions will permit editors and referees to devote more time to thoughtful evaluation of contributions and will ultimately lead to a better, more interesting Journal.

Copying information, in part or in whole by any means is prohibited without a written permission from the owner.

SUBSCRIPTION

Folia Histochemica et Cytobiologica is available for paper subscription (print on demand).
To read and download articles for free as pdf document, visit http://czasopisma.viamedica.pl/fhc

Publisher: VM Media sp. z o.o. VM Group sp.k., Swietokrzyska St. 73, 80–180 Gdansk, http://www.viamedica.pl, wap.viamedica.pl

Illustration on the cover: *RCAS1 immunoreactivity in epithelial ovarian cancer cells* (see: Sebastian Szubert *et al.*, pp. 116–126)

Legal note: http://czasopisma.viamedica.pl/fhc/about/legalNote

© Polish Society for Histochemistry and Cytochemistry

18-0228.003.001

Folia Histochemica et Cytobiologica

Scientific quarterly devoted to problems of histochemistry, cytochemistry and cell & tissue biology

www.fhc.viamedica.pl

Vol. 57
No. 3
2019

Official Journal of the Polish Society for Histochemistry and Cytochemistry

FOLIA HISTOCHEMICA ET CYTOBIOLOGICA
Vol. 57, No. 3, 2019
pp. 101–115

REVIEW

VIA MEDICA

Pancreatic β-cell replacement: advances in protocols used for differentiation of pancreatic progenitors to β-like cells

Muhammad Waseem Ghani[1], Li Ye[1], Zhao Yi[1], Hammad Ghani[2], Muhammad Waseem Birmani[1], Aamir Nawab[1], Lang Guan Cun[1], Liu Bin[1], Xiao Mei[1]

[1]Department of Livestock Production and Management, Agricultural College, Guangdong Ocean University, Zhanjiang, Guangdong, China

[2]Nawaz Sharif Medical College University of Gujrat, Punjab, Pakistan

Abstract
Insulin-producing cells derived from *in vitro* differentiation of stem cells and non-stem cells by using different factors can spare the need for genetic manipulation and provide a cure for diabetes. In this context, pancreatic progenitors differentiating to β-like cells garner increasing attention as β-cell replacement source. This kind of cell therapy has the potential to cure diabetes, but is still on its way of being clinically useful. The primary restriction for *in vitro* production of mature and functional β-cells is developing a physiologically relevant *in vitro* culture system which can mimic *in vivo* pathways of islet development. In order to achieve this target, different approaches have been attempted for the differentiation of pancreatic stem/progenitor cells to β-like cells. Here, we will review some of the state-of-the-art protocols for the differentiation of pancreatic progenitors and differentiated pancreatic cells into β-like cells with a focus on pancreatic duct cells. *(Folia Histochemica et Cytobiologica 2019, Vol. 57, No. 3, 101–115)*

Key words: β-cell replacement; transdifferentiation; pancreatic duct cells; acinar cells; centroacinar cells; endocrine cells; mesenchymal stem cells; β-like cells

Abbreviations:

3D — three-dimensional; Akt — protein kinase 1; ALDH1 — aldehyde dehydrogenase 1; ALK3 — activin-like kinase 3; ARIP — adult rat pancreatic ductal epithelial cell line; Arx — aristaless-related homeobox; Ascl1b — achaete-scute homolog 1b; BLCs — beta-like cells; BMP7 — bone morphogenetic protein 7; B-PMSCs — bovine pancreatic MSCs; BrdU — bromodeoxyuridine; CACs — centroacinar cells; CK19 — cytokeratin 19; CNF — ciliary neurotrophic factor; Dnmt1 — DNA methyltransferase 1; DT — diphtheria toxin; DTZ — dithizone; E12.5 — embryonic day 12.5; eBCs — enriched β-clusters; EGF — epidermal growth factor; EGFP — enhanced green fluorescent protein; EGF-R — EGF receptor; EMT — epithelial-to-mesenchymal transition; Ex-4 — exendin-4; FACS — fluorescence-activated cell sorting; FGF — fibroblast growth factor; Fstl3 — follistatin-like 3; GABA — gamma-aminobutyric acid; GFP — green fluorescent protein; GH — growth hormone; GLP-1 — glucagon-like peptide-1; HA — hyaluronic acid; HDAC — histone deacetylase; HDACi — histone deacetylase inhibitor; Hes-1 — Hairy/Enhancer of split-1; HGF — hepatocyte growth factor; hNEPT — human non-endocrine pancreatic tissue; Hnf6 — hepatocyte nuclear factor 6; ICCs — islet-like cell clusters; IDX-1 — islet duodenal homeobox-1; INS — insulin; IPCs — insulin-producing cells; KGF — keratinocyte growth factor; KO — knockout; LIF — leukemia inhibiting factor; MafA/B — musculoaponeurotic fibrosarcoma oncogene A/B; MSCs — mesenchymal stem cells; NeuroD — neurogenic differentiation; Ngn3 — neurogenin 3; Nkx6.1 — NK6 homeobox 1; NPPCs — nestin-positive progenitor cells; NOD — non-obese diabetic;

Correspondence address: Xiao Mei
Department of Livestock Production and Management, Agricultural College, Guangdong Ocean University, Zhanjiang 524088, Guangdong, China
e-mail: xiao0812@126.com

©Polish Society for Histochemistry and Cytochemistry

NOD-SCID — non-obese diabetic-severe combined immunodeficiency; p16INK4a — tumor suppressor gene; PANC-1 — human pancreatic cancer cell line; PAX4 — paired box 4; PDEC — pancreatic duct epithelial cell; PDL — partial duct ligation; PDSCs — pancreatic duct stem cells; Pdx1 — pancreatic and duodenal homeobox 1; PI-MSCs — pancreatic islet-derived mesenchymal stem cells; PLGA — poly-lactic co-glycolic acid; PP — pancreatic polypeptide; PRL — prolactin; Px — pancreatectomy; RSPO1 — R-spondin-1; SCs — stem cells; siRNA — small interfering RNA; Sox9 — sex determining region Y box 9; STAT3 — signal transducer and activator of transcription 3; STZ — streptozotocin; Tcf2 — transcription factor 2; TF — transcription factor; T3 — tri-iodothyronine; TGF — transforming growth factor; YFP — yellow fluorescent protein.

Introduction

In recent decades, the occurrence of diabetes has increased globally, with over 425 million diabetic people living worldwide whose number is expected to be 629 million in 2045 [1]. Diabetes is a form of metabolic disorder characterized by dysfunction and loss of β-cell mass resulting in chronic hyperglycemia [2, 3]. Regarding the treatment of diabetes, exogenous insulin can only control blood glucose levels without amending the devastating consequences of diabetes. Islet transplantation also has potential and is a clinical method for restoring normoglycemia, however, not without problems related to donor shortage and immune rejection for which long term immune suppression therapy is necessary [4]. Alternatively, a stem-cells-based β-cell replacement can resolve most disease-related problems of diabetic patients [5, 6].

The pancreas is composed of exocrine (acinar, centroacinar and ductal cells) and endocrine compartments (islet of Langerhans) [7, 8]. Regarding the regeneration, most of the adult tissues are composed of the differentiated cells making them dependent on stem cells for repair and regeneration [9]. However, some tissues like adult pancreas lack the existence of true stem cells, undifferentiated cells which are dedicated for providing an unlimited supply of freshly differentiated cells when these are lost, discarded, or needed in greater numbers, and rely on the unipotent and/or multipotent facultative progenitors [10]. The facultative progenitors are differentiated cells responsible for particular functions, but they retain the ability to de-differentiate [11], proliferate and eventually redifferentiate towards another cell type [12] for repairing the tissue after injury [13].The plasticity of differentiated pancreatic cells enables them to serve as a facultative progenitor in a tissue which lacks true stem cells [14, 15].

For the maintenance of β-cell mass, pancreatic β-cells can duplicate themselves [16], but this proliferation is not enough to withhold the excessive loss of β-cells in stress conditions. Recently, Domínguez-Bendala *et al.* reported that in the adult murine and human pancreas, when normal turnover of β-cells is required, β-cells are formed by the replication of existing β-cells or can also be formed by de-differentiated α-cells through an intermediate cell stage called 'virgin β-cell' [17]. The existence of 'virgin β-cell', which serves as an intermediate stage for transdifferentiation of α-cells to β-cells, as a neogenic niche at the periphery of pancreatic islets of mice was confirmed by Meulen *et al*. through single-cell transcriptome analysis [18]. It has been suggested by studies in mice that during metabolic stress, β-cell de-differentiation, and then redifferentiation mechanisms regenerate the islets [19]. However, when the pancreas is damaged excessively then ductal cell progenitors' regenerate islets [17]. The *in vivo* and *in vitro* studies have shown that pancreatic duct epithelial cells (PDECs), acinar cells, and centroacinar cells were the source for neogenesis of β-like cells (BLCs) [20–22]. The main characteristics of BLCs involve the ability to synthesize insulin; however, in most cases, the secretion of insulin stimulated by glucose and other agents is usually lower than in beta cells isolated from pancreatic islets. The *in vitro* studies on endocrine cells showed that replication of β-cells and transdifferentiation of α and δ cells are possible sources of insulin producing β-like cells [23–25]. Additionally, the pancreatic islet-derived mesenchymal stem cells also show some potential for *in vitro* development of β-like cells [26]. Added to their role as a β-cell replacement, *in vitro* derived BLCs can be used as a model to study diabetes pathology [27] and can also provide a consistent and uniform supply for the screening of pharmaceutical drugs for improving β-cell function and survival [28, 29]. However, for the success of these *in vitro* stem cell culture approaches imitation of *in vivo* islet milieu is required.

In this review, we summarized different protocols used for the differentiation of pancreatic progenitors to β-like cells. Furthermore, the available cell sources within the pancreas were also assessed for their potential as the progenitors of β-cells.

Pancreatic exocrine cells as a source of β-cell/β-like cells

The exocrine part of the pancreas is more than 95% in rodents and the pancreas in humans also have more than 95% to 98% of the exocrine part [7, 30]. It includes the acinar cells — secreting digestive enzymes, centroacinar cells — secreting bicarbonate

©Polish Society for Histochemistry and Cytochemistry

ions and mucins, and pancreatic ducts — transferring these secretions to the duodenum [7]. All types of exocrine cells in the pancreas have been used *in vitro* for expansion into β-cells in different studies which will be discussed shortly.

Pancreatic ductal epithelial cell's induction to β-cell/β-like cells

Lessons from classical animal models of β-cells regeneration

These models include mainly partial duct ligation (PDL) of the pancreatic duct, partial pancreatectomy (Px) and targeted β-cells damage by diphtheria toxin (DT) and streptozotocin (STZ). The PDL method used by Xu *et al.* [31] and Inada *et al.* [32] in adult mouse showed the presence of multipotent islet progenitors in ductal linings. Injury-induced by PDL caused the β-cell mass expansion. This β-cell mass expansion needed the activation of Nuerogenin3 (Ngn3) gene expression which they believed to be the response for the inflammatory damage and loss of acinar cells due to injury [31, 32]. Inada *et al.* used carbonic anhydrase II-Cre-lineage tracing to explore the source of new β-cells [32]. Pancreatectomy model of 90% Px in adult rats by Li *et al.* [33] illustrates that mature epithelial duct cells can be dedifferentiated and become facultative progenitors which then differentiate to both exocrine and endocrine cell types. During dedifferentiation resulting from pancreatectomy, the duct cells lost Hnf6, a ductal differentiation marker [34, 35], and expressed Pdx1, Tcf2, and Sox9 transcription factors, markers for embryonic pancreatic epithelium [36–38]. These pancreatic epithelial cells acted as progenitors and differentiated to $Ngn3^+$ cells. Differentiation and maturation of $Ngn3^+$ progenitor cells led in the growing pancreas to the formation of $MafA^+$, $insulin^+$ cells [33]. In another murine model, the 60% pancreatectomy was used for finding the source of β-cell regeneration. The $Sox9^+$ viral lineage tracing confirmed that in young, but not adult, mice and humans intra-islet pancreatic ducts are the source of β-cell regeneration [39]. In an adult mouse model, diphtheria toxin (DT) was used to ablate β-cells to show that epithelial cells within the pancreatic ducts contribute to the regeneration of endocrine and acinar cells. The results of lineage tracing in DT-induced ablated β-cell mouse model showed that β-cells were regenerated from pancreatic ductal cells [40]. In another study, a model of streptozotocin-induced diabetic mice was used. The *in vivo* differentiation of oligopotent progenitors, which can differentiate into pancreatic ductal and endocrine cell types including β-cells, was investigated and it was confirmed that after STZ-induced diabetes new β-cells were formed through differentiation of oligopotent progenitors [41].

We have learned from these models that pancreas has the facultative multipotent progenitors, which are activated by a specific type of injury to the pancreas. Pancreatic ductal epithelial cells, particularly, are believed to be these multipotent progenitors which can give rise to either endocrine or exocrine cells depending on the severity of injury to the pancreas. However, the source of β-cell regeneration under physiological conditions is not confirmed hitherto.

In vitro β-cell expansion using pancreatic duct cells

Pancreatic duct epithelial cells can dedifferentiate when there is stress or injury to the pancreas and can re-differentiate to endocrine or exocrine cells depending on the severity of the injury. As described in classical models of differentiation, in the pancreas of adult mice, pancreatic duct epithelial cells (PDECs) can contribute to the regeneration of endocrine and exocrine cell types. The regenerative pathways and cell types that contribute to this process depend upon the severity of injury [40]. Therefore, most researchers have used pancreatic duct cells in their studies to find a potential cell therapy for diabetes. Here, we summarize some protocols used in different studies for the differentiation of PDECs to islet cells or, particularly, insulin-secreting β-like cells.

$Sox9^+$ ductal cells in the adult pancreas can be differentiated to β-cells *in vitro,* but this way of *in vivo* conversion remained controversial until the Zhang group reported first *in vivo* study to resolve this controversy [42]. Using lineage-tracing, Zhang *et al.* proved that genetically labeled $Sox9^+$ adult rat pancreatic ductal cells could be induced to insulin-secreting cells *in vivo*. They used hyperglycemia in combination with long-term, low-dose epidermal growth factor (EGF) infusion as synergistic stimulants for the induction of duct cells to insulin-secreting β-cells. This treatment resulted in normoglycemia in non-autoimmune diabetic mice [42]. Recently, Shaotang *et al*. found the multipotency of adult rat pancreatic ductal epithelial cells by inducing their differentiation into pancreatic islets, nerve cells, adipose cells, and osteoblasts [43]. The development of these target cells was made possible by respective culture protocols for directing the differentiation of PDECs [43]. Furthermore, Qadir *et al.* confirmed the existence of pancreatic progenitors in human exocrine pancreas and ductal epithelial cells were confirmed as pancreatic progenitors [8]. The human exocrine pancreas is a reservoir of multipotent cells expressing PDX1, an important transcription factor expressed by pancreatic endocrine progenitors [44] and ALK3,

©Polish Society for Histochemistry and Cytochemistry

and BMP receptor 1A which is associated with the regeneration of tissues [45], mostly found in major pancreatic ducts. Qadir *et al.* also showed that BMP7, which binds to ALK3 could stimulate pancreatic progenitor cells proliferation [8].

Suarez-Pinzon *et al.* studied the effect of the combination of epidermal growth factor (EGF) and gastrin on inducing β-cells from pancreatic duct stem cells, both in human and mice [46]. Treatment with EGF and gastrin for two weeks in non-obese diabetic (NOD) mice with autoimmune diabetes (NOD-SCID) resulted in normoglycemia as the β-cell mass was expanded from 15 to 47% of normal cell mass. Immunosuppressive therapy was not done as the combination of EGF and gastrin reduced insulitis, showing that this treatment could also stop autoimmune destruction of β-cells in NOD-SCID mice [46]. On the other hand, the glucagon-like peptide-1 analog, exendin-4, reversed hyperglycemia in diabetic NOD mice; though, this required synchronized immunosuppressive treatment with anti-lymphocyte serum [47]. In their next experiment, Suarez-Pinzon *et al.* showed that β-cell mass in adult human pancreatic islets was increased after combination therapy with EGF and gastrin both *in vitro* and *in vivo*, and this was as a result of the induction of β-cell neogenesis from pancreatic duct cells [48]. In both studies by Suarez-Pinzon*et al.*, the mechanism which initiated the neogenesis of β-cells from pancreatic duct cells was not elucidated. However, the authors suggested that EGF caused an increase in the proliferation of CK19-positive duct cells while gastrin induced the expression of Pdx1 and differentiation of $Pdx1^+$ cells to insulin-positive β-like cells [48]. Likewise, the importance of EGF was reported that the perturbation of EGF-R-mediated signaling resulted in delayed β-cell development in EGF-R deficient $(-/-)$ mice [49]. These studies showing regeneration of β-cell mass through the use of EGF and gastrin combination, not only reveal the role of these peptides in the differentiation of pancreatic progenitors to β-cells in the damaged pancreas but also support the concept that pancreatic ducts contain the progenitor cells which can give rise to β-cells through epithelial-to-mesenchymal (EMT) cell transition [50]. The EMT requires some inducing stimuli, provision of which can cause *in vivo* regeneration of β-cells and also can cause the *in vitro* production of insulin-producing cells (IPCs) from pancreatic ductal epithelial cells.

Hui *et al.* investigated the effect of glucagon-like peptide-1 (GLP-1) on inducing differentiation of pancreatic ductal epithelial cells into insulin-secreting cells [51]. To test the effect of GLP-1, rat (ARIP) and human (PANC-1) cell lines, both derived from the pancreatic ductal epithelium, were used. Using fluorescence-activated cell sorting (FACS) analysis, they showed that GLP-1 induced the differentiation of ARIP cells into insulin-synthesising cells, although it did not affected the phenotype of PANC-1 cells. The expression of Glut2, insulin, and glucokinase transcripts was increased respectively in ARIC cells after GLP-1 treatment. GLP-1 was found to be associated with cause of this differentiation of ARIP cells by inducing the expression of β-cell differentiation marker, islet duodenal homeobox-1 (IDX-1). Albeit, the transfection of IDX-1 gene into PANC-1 cells made them responsive to GLP-1 treatment. The effect of GLP-1 on differentiation was confirmed by using exendin-9, a GLP-1 receptor antagonist, which inhibited the expression of β-cell-specific genes from ARIP and PANC-1 cell line pancreatic epithelial cells [51]. In an attempt to improve the efficiency of GLP-1-induced differentiation, Li *et al.* used sodium butyrate ($C_4H_7NaO_2$), histone deacetylase inhibitor (HDACi), along with GLP-1 to differentiate the FACS-sorted nestin-EGFP-positive progenitor cells (NPPCs) of transgenic (nestin and EGFP) mice into insulin-producing cells *in vitro* [52]. The treatment of purified nestin-EGFP-positive cells with a combination of sodium butyrate and HDACs resulted in increased levels of transcripts which encoded for pancreatic development factors and insulin. The population of insulin-secreting cells and volume, almost 65 ng when exposed to 25 mM glucose, of insulin secretion, both increased as a consequence. The addition of sodium butyrate resulted in de-condensation of chromatin whereas GLP-1 caused the increased expression of Pdx1 which by binding to the insulin gene promoted its transcription [52]. Additional evidence showed that HDACs treatment promoted $Ngn3^+$ proendocrine lineage, obtained from rat embryo, differentiation to an increased pool of endocrine progenitors [53]. Treatment with trichostatin A and sodium butyrate, inhibitors of both class I and II HDACs enhanced the mass of the β-cell as assessed by quantification after immunohistological staining against insulin. These results also suggest that HDACs are one of the critical key factors in endo- and exocrine pancreatic differentiation [53].

Another study conducted by Chen *et al.* reported the protocol to expand and differentiate rat PDECs into insulin-secreting islet-like cell clusters in a dynamic three-dimensional (3D) cell culture system [54]. They cultured cells for 14 days in serum-free culture media supplemented with nicotinamide, keratinocyte growth factor (KGF), and β-fibroblast growth factor (β-FGF) which resulted in the formation of islet-like cell clusters.

©Polish Society for Histochemistry and Cytochemistry

These islet-like cellular clusters were positive for insulin detection in the extracellular fluid and cytoplasm after 14 days of differentiation. However, the obtained insulin-secreting cells were not as functional like human islet cells [54]. In a recent study, Tan *et al.* used fibroblast-coated Poly-lactic acid-co-glycolic acid (PLGA) diaphragm to form a biological membrane [20]. They cultured nestin-positive pancreatic stem cells isolated from Wistar rats and, using two-step induction method, pancreatic stem cells were induced into insulin-secreting cells. A two-step induction method was used: in the first step, pancreatic stem cells were cultured in a media supplemented with bFGF and nicotinamide. After the detection of islet-like cell mass in culture media, activin-A, β-catenin, and exendin-4 (Ex-4) were used as supplements. The results showed that the number of nuclei was higher in induced cells and cells in this group were aggregated. The amount of insulin secreted upon stimulation was also significantly higher in the induced group as compared to the normal group but was not the same as of islet β-cells [20].

A summary of these and other factors used in different studies by various researchers for the differentiation of pancreatic duct stem cells into insulin-secreting BLCs is given in Table 1.

To sum up, till now we have learned that pancreatic ducts have the progenitors residing in their epithelium which can be differentiated *in situ* and *ex vivo* into BLCs by inducing their differentiation with a combination of different factors.

Acinar to β-cell neogenesis

Acinar cells are differentiated cells with a specialized function but have the plasticity to dedifferentiate towards duct-like endocrine progenitor cell phenotype which further differentiates towards β-cells [13, 55]. In pathological terms, this is referred to as metaplasia which is important for tissue repair after the injury. Owing to the abundance of their number and their ability to give rise to β-cells, the acinar cells are also a reliable candidate for β-cell regeneration and replacement. The transformation capability of acinar cells is mainly influenced by the type and extent of the pancreatic injury as confirmed by the lineage-tracing studies [40, 56].

Baeyens *et al.* showed that administration of EGF and ciliary neurotrophic factor (CNF) to adult STZ-induced diabetic mice stimulated the conversion of acinar cells to BLCs. The neo-β-like cells were glucose-responsive and restored normoglycemia. This conversion was dependent on the expression of Ngn3 which in turn was mediated by the Stat3 signaling [57]. The overexpression of three transcription factors (TFs), MafA, Pdx1, and Ngn3 in the acinar cells of transgenic mice *in vivo* resulted in acinar to β-cell reprogramming [58]. The overexpression of these three TFs caused the reprogramming-induced inflammation, which resulted in ductal cell metaplasia of acinar cells. The metaplasia of acinar to ductal cell phenotype resulted in the conversion of ductal cell phenotype to neo-β-cells. The neo-β-cells reversed diabetes in these mice and these results suggest that the expression of β-cell-specific transcription factors are the key to the transition of acinar cells to β-cells [58]. However, the viral vector system for the overexpression of TFs used in this study makes this approach less feasible for clinical application.

The *in vitro* culture of acinar cells, isolated from adult Wistar rats, in the presence of EGF and leukaemia inhibiting factor (LIF) inhibited the Notch1 signaling resulting in neogenesis of β-like cells [59]. The inhibition of Notch1 signaling caused the dedifferentiation of adult rat acinar cells to a state in which they expressed endocrine progenitor transcription factor, Ngn3, and afterwards differentiated with β-like cells. However, the newly formed β-cells were immature as compared to islet β-cells but they became mature phenotypically and resembled islet β-cells when transplanted at the ectopic site, under the kidney capsule of nude mice [59]. The presence of tri-iodothyronine (T3) receptors in murine embryonic pancreas laid the foundation for *ex vivo* culture of acinar cells in the presence of T3 to develop β-like cells [60]. Culturing of embryonic day 12.5 (E12.5) mouse embryonic pancreas tissue with T3 induced ductal phenotype at the expense of acinar tissue. Furthermore, T3 induced the endocrine fate in murine E12.5 pancreatic explant culture and also in the mouse acinar cell line 266-6. The T3-mediated conversion of acinar to β-cells was dependent upon the Akt signaling pathway and the T3-mediated effects were abrogated by Akt inhibitors [60]. These results confer that acinar cells can be converted to β-like cells by the addition of T3 in culture media. Dagmar Klein *et al.* [21] showed that exposure of adult human non-endocrine pancreatic tissue (hNEPT) to BMP-7 resulted in the conversion of the Pdx1-positive ductal cells to insulin-expressing cells. BMP-7 exposure instigated the ectopic expression of endocrine transcription factors in the exocrine cells which triggered this conversion. The use of *in vitro* lineage tracing confirmed that insulin-secreting cells were derivatives of mature ductal cells [21].

Summarily, the transformation of acinar to β-cell/ /β-like cells is possible as evidenced in many studies reported. This transformation was not direct from acinar to β-cell, instead, it was mediated by $Ngn3^+$ endocrine precursor cell phenotype. Thus, it may be

©Polish Society for Histochemistry and Cytochemistry

Table 1. Factors which caused the differentiation of pancreatic duct epithelial cells to β-cell/β-like cells [20, 39, 42, 46, 48, 51, 52, 54, 112–119]

Model and protocol used	Main obtained results	Reference
***In vitro* studies**		
Rat (ARIP*) and human (PANC-1) pancreatic ductal epithelial cells treated with GLP-1	ARIP cells were differentiated to insulin synthesizing cells while PANC-1 cells phenotype was not affected	51
Human islet cells containing endocrine and duct cells cultured for 4 weeks in media with EGF and gastrin	The number of CK19 positive duct cells expressing Pdx1, insulin, and C-peptide was significantly increased (+678%) with increased β-like cells (+118%). Thus, CK19 positive pancreatic ductal cells were a source of new β-cells	48
FACS-sorted PDECs from adult mouse cultured with bFGF	bFGF caused the differentiation of these cells to insulin-secreting cells	112
Murine FACS-sorted NPPCs exposed to GLP-1 and sodium butyrate	The NPPCs were differentiated to insulin-producing cells	52
Culture of human pancreatic duct-rich populations with Ex-4, nicotinamide, KGF, Pdx-1 and NeuroD proteins	After two weeks of culture, human pancreatic progenitors were differentiated to insulin-producing cells	113
Pancreatic ductal fragments from mouse pancreas grown in RSPO1-based 3D cultures	The fragments developed to organoids able to differentiate into ductal as well as endocrine cells upon transplantation under kidney capsule of immunodeficient mice	114
Progenitors from human and mouse embryonic pancreas stimulated by the Wnt agonist RSPO1, FGF10 and/or EGF in 3D cultures	Pancreatic progenitors were expanded to duct-like structures in the presence of EGF and were differentiated to cyst-like structures containing insulin, glucagon, and somatostatin-positive cells in the absence but not presence of EGF	115
Rat PDSCs were cultured in a 3D cell culture system in media supplemented with nicotinamide, FGF, and KGF	Rat PDSCs were differentiated to islet-like cell clusters which expressed insulin as detected by DTZ staining	54
Adult mouse pancreatic progenitor-like cells were cultured in media supplemented with insulin, transferrin, selenium, glucose, and nicotinamide	After two weeks of culture small dense cell clusters were formed and insulin presence in these clusters was confirmed by DTZ staining	116
Rat NPPCs cultured in PLGA membranes in media supplemented with bFGF, nicotinamide, activin-A, β-catenin, and exendin-4	Nestin-positive cells were differentiated mainly to insulin-secreting cells but the amount of insulin released was lower than in primary β-cell cultures	20
***In vivo* studies**		
Human fetal pancreatic cells were transplanted to rats treated with KGF	The ductal cells proliferated and differentiated to β-cells resulting in increased β-cell mass	117
NOD diabetic mice treated with EGF and gastrin	After 2 weeks of treatment, normoglycemia was achieved and β-cell mass was expanded from 15% to 47% of normal cell mass as a result of neogenesis from pancreatic ductal networks	46
The human betacellulin-adenoviral vector was retrogradely injected to mice pancreatic duct	The betacellulin gene transduction resulted in the formation of insulin-positive cells in the duct linings or associated islet-like cell clusters	118
STZ-diabetic rats were treated with GLP-1/ /exendin-4	The number of small cell clusters in pancreatic ducts was increased which improved glucose tolerance in diabetic rats	119
The partly pancreatectomized transgenic mice overexpressing TGF-β used to find the source of β-cells	Intraislet pancreatic ductal networks were present in transgenic but not in wild type mice and lineage tracing confirmed that neo-β-cells were derivatives of duct cells	39
In non-autoimmune diabetic C57BL/6 mice hyperglycemia was induced by alloxan and mice were treated for 56 days with low dose EGF and gastrin	Lineage tracing showed that $Sox9^+$ cells differentiated into insulin-producing β-cells which normalized blood glucose levels	42

*The abbreviations are explained at the beginning of the paper

concluded that first acinar cells dedifferentiate back to progenitor phenotype and then redifferentiate to insulin-secreting cells.

Centroacinar cells as a source of β-cells

Centroacinar cells (CACs) are a type of the exocrine pancreas cell and are present at the centre of acini in

©Polish Society for Histochemistry and Cytochemistry

juxtaposition to the terminal pancreatic ducts. CACs have a unique cell morphology and express the endocrine differentiation marker Sox9 [61–64]. Beer *et al.* reported that centroacinar cells (CACs) are a type of ductal pancreatic cell which possesses the progenitor properties and replaces β-cells in zebrafish [65].

The centroacinar cells in zebrafish led to the secondary islet formation after inhibition of Notch signaling [66]. The Nkx6.1-transgenic zebrafish showed fluorescent markers for endocrine progenitor cell phenotype under the Notch-inhibition. The Notch-responsive cells were centroacinar cells, which showed a pancreatic endocrine progenitor phenotype and led to the regeneration of endocrine cells after Notch-inhibition [66]. In order to further assess the ability of centroacinar cells for endocrine pancreas regeneration in adult zebrafish, Delaspre *et al.* established the transcriptome of adult CACs. Then, through the use of gene ontology and *in situ* hybridization, they found that CACs were enriched in pancreatic progenitor markers. Moreover, new β-cells arose from CACs after β-cell ablation or partial pancreatectomy as confirmed by the lineage tracing [22]. Another group also used the β-cell ablation model of zebrafish to show the progenitor properties of CACs. Ghaye *et al.* [67] developed the transgenic lines of Nkx6.1 and Ascl1b-positive cells expressing GFP. In the near complete β-cell ablation model of adult zebrafish, the Nkx6.1 cells were traced as progenitors of pancreatic tissue while Ascl1b-positive cells only gave rise to endocrine cells. These Nkx6.1 cells were present at the end to a ductal tree and were responsive to Notch signaling showing their centroacinar phenotype [67]. The findings of both of these studies suggest that adult CACs are similar to larval CACs and retain the ability for β-cell neogenesis. Thus, it is safe to say that CACs are the progenitors of endocrine cells, especially β-cells in larval as well as adult zebrafish.

For the probing of the progenitor capabilities of centroacinar cells in mammals Rovira *et al.* used the mouse as a model animal in their study [68]. They found that centroacinar and terminal ductal cells showed high levels of ALDH1 enzymatic activity which was used for FACS-based isolation of these cells. The transcription analysis of FACS-isolated cells revealed that they were not the differentiated cells but rather were enriched for markers associated with pancreatic endocrine progenitor population. Moreover, the culturing of CACs in suspension culture resulted in pancreatosphere formation which displayed the pancreatic endocrine and exocrine cell differentiation capacity along with glucose-responsive insulin secretion. For pancreatosphere formation assays on CACs, cells were grown for 5–7 days in cultures

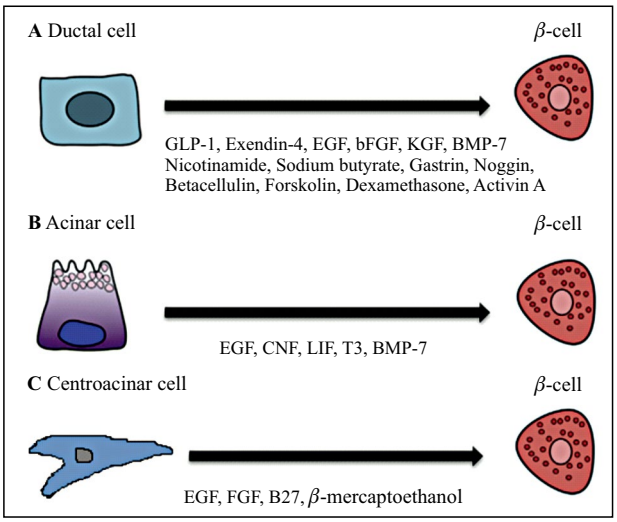

Figure 1. Some of the factors used for in vitro differentiation of pancreatic ductal (A), acinar (B) and centroacinar cells (C). The ductal and acinar cells do not directly transit to β-cell phenotype but instead first attain a progenitor stage and then redifferentiate to insulin-secreting cells.

enriched with EGF, FGF-2, B-27 cell culture supplement, β-mercaptoethanol, nonessential amino acid, and LIF. Furthermore, the CACs and terminal ductal cells also showed intense expansion under chronic epithelial injury conditions [68]. These findings support the reported zebrafish studies and suggest that CACs cells are certainly adept of progenitor's task to provide the upkeep of tissue homeostasis in the adult mouse pancreas.

In summary, so far, we have well understood that centroacinar cells are a type of progenitor cells in the pancreas with the ability of pancreatic exocrine and endocrine tissue regeneration according to the conditions. The findings of the studies mentioned above also support the β-cell neogenesis pathway for the regeneration of β-cell mass. These CACs cells can also be sorted *in vitro* for the expansion of islets or only β-cells to provide a source of β-cells replacement.

Figure 1 shows different factors used for *in vitro* differentiation of pancreatic ductal, acinar and centroacinar cells to β-cell.

Endocrine cells giving rise to β-cells

The endocrine pancreas has various endocrine cell types secreting different hormones which are α-cells (glucagon), β-cells (insulin), δ-cells (somatostatin), ε-cells (ghrelin), and PP cells (pancreatic polypeptide) [7]. These hormone-secreting cells are found in condensed structures in the pancreas called islet of

©Polish Society for Histochemistry and Cytochemistry

Langerhans. Islet β-cells sense the glucose-in-blood concentration, synthesize and secrete insulin into blood circulation which is responsible for regulating glucose metabolism in the body [69]. The pancreatic islet is likely the dwelling to search for cellular sources of new β-cells because of the common developmental lineage between the different endocrine cells in the islet of Langerhans [70]. The possibilities of islet cells as progenitors will be discussed in this section.

Potential of β-cell replication for its replenishing

The primary mechanism for expansion of β-cell mass during the neonatal period of growth is the proliferation of existing β-cells [71]. Lineage tracing studies confirmed that the replication of preexisting β-cells is the main mechanism accountable for normal β-cell turnover in adult mice [16, 72] and also for regeneration of β-cell mass following β-cell ablation [73, 74]. So, in rodents, the major source for expansion of β-cell mass is the replication of existing β-cells [75]. Though the increase in β-cell mass of neonates occurs by replication of preexisting β-cell, this mechanism disappears after 2 years in humans [71, 76]. Under the physiological conditions in adult humans, the regeneration of β-cells is rare, and so it is not confirmed hitherto from where comes the β-cells in normal conditions [7, 76]. However, the increased regenerative ability of β-cells in conditions of pregnancy [77] and obesity [78] gives us a clue about the replication of existing insulin-producing cells. Nonetheless, replication of existing β-cells and their *in vitro* expansion ability is a well-studied mechanism for restoring β-cell mass of diabetics [10, 79].

Dhawan *et al.* [23] reported that the likely reason for the decreased regenerative capacity of adult β-cells was an accumulation of p16INK4a which caused inhibition of the cell cycle ending up in the limited regenerative capacity of adult endocrine cells. Additionally, they found that TGF-β signaling maintained the p16INK4a through Smad3 which joined in with trithorax to maintain and activate the p16INK4a levels to prevent the replication of β-cells. Thus, the inhibition of TGF-β signaling with different chemical inhibitors resulted in the repression of p16INK4a locus ending up in increased replication of β-cells in adult mice [23]. Recently, Puri *et al.* studied the role of c-Myc in β-cell replication [80]. They used c-Myc transgenic mice and INS-1 cells with c-Myc overexpression (siRNA) which were cultured with L-glutamine, sodium pyruvate and 2-mercaptoethanol. They showed that increased expression of c-Myc resulted in increased proliferation of β-cells but the cells produced were immature. The transcriptome analysis validated the immaturity of new β-cells as the proliferating cellular transcripts were increased and transcripts of the mature β-cells phenotype were decreased which resembled development of islets [80]. Moreover, the genetic deletion of c-Myc resulted in a ~50% decline in the proliferative cell pool during postnatal expansion, which showed the importance of this protein during the replication of β-cells. The authors concluded that the adult β-cells retain a balance between functional and proliferative properties as the proliferation of β-cells leads to functional immaturity [80].

Nielsen *et al*. reviewed the possible factors used for enhancement of β-cell replication in *in vivo* culture. Cytokines such as GLP-1, growth hormone (GH) and prolactin (PRL) were proposed as the tangible factors for the uplifting of *in vitro* β-cell replication. These factors worked best when the cells were dedifferentiated and entered the proliferative phase [81]. *In vitro* expansion of β-cells using adult human islets was successfully attempted by Ouziel-Yahalo *et al*. [82]. The culturing conditions included activin A, betacellulin, and exendin 4 as differentiation-inducing factors. After seven days of culture, the number of β-cells was doubled as measured by BrdU labeling. The dedifferentiation of β-cells resulted in their increased size and redifferentiation to β-cell phenotype, especially in betacellulin supplemented media. However, the functionality of replicated β-cells was not high compared to the primary islet β-cells [82].

In summary, these studies suggest that β-cell replication is a possible mechanism and it involves the dedifferentiation of mature β-cells to cells with less mature phenotype which further proliferate to form new β-cells.

α- to β-cell transdifferentiation

Mature islet cell's plasticity has remained a puzzle until lineage tracing models in mouse [83] and zebrafish [84] confirmed the transdifferentiation ability of α-cells by the transition to β-cells given the conditions of severe β-cell loss [83, 84]. As we already know, adult β-cells have a long lifespan, and they replicate rarely, though they have the self-duplication ability [16, 72]. However, this self-duplication cannot counterbalance the excessive loss of β-cells and for compensating the excessive loss of β-cells, mature glucagon secreting α-cells have been traced to differentiate to β-cells [85]. This kind of cellular transition is possible because α- and β-cells are formed from the same multipotent progenitors during pancreatic islet development [70, 86].

Lineage tracing in diphtheria-toxin induced total β-cell ablation mouse model showed that α-cells were the source of β-cell regeneration [83]. In another

©Polish Society for Histochemistry and Cytochemistry

in vivo model of β-cell regeneration, Chung *et al.* used partial duct ligation and alloxan for ablation of existing β-cells [85]. After two weeks it was found that neogenic β-cells came from α-cells. The authors documented that in this model α-cells were not directly converted to β-cells, but instead, they passed through an intermediate stage in which they express the markers for both α-and β-cells and secrete both glucagon and insulin after one week of β-cell ablation [85]. However, after two weeks of PDL plus alloxan combination, the glucagon secretion was minute, and the cells resembled β-cells in phenotype and the expression of MafA was also high [85]. In another study, zebrafish was used as a model for lineage tracing of β-cell regeneration using near total ablation of existing β-cells [84]. The expression of glucagon was increased after the injury suggesting its role in α- to β-cell transdifferentiation. These results, in favor of previous studies, showed that α-cells serve as a reservoir pool for the β-cell regeneration [84] and imply the plasticity of the α-cells to be converted into β-cells [70].

Andrzejewski *et al.* reported the role of activin signaling in α-to β-cell phenotype transition. They treated α-and β-cell lines and also sorted mouse islet cells with activin [24]. In αTC1-6 α-cell line, the expression of α-cell genes, Aristaless-related homeobox (Arx), glucagon, and MafB was suppressed following the treatment with activin A or B. In INS-1E β-cell line, the expression of Pax4 and insulin was increased following the activin A treatment [24]. Furthermore, the exposure to activin A suppressed the expression of α-cell genes and enhanced the expression of β-cell genes in sorted primary islet cells. These results suggest that activin signaling destabilized the α-cell phenotype whereas promoted a β-cell fate in cultured cells [24]. To further verify the hypothesis of activin mediated α- to β-cell transdifferentiation, Brown *et al.* developed Fstl3 knockout mouse labeled with Gluc-Cre/yellow fluorescent protein (YFP) for lineage tracing [87]. Follistatin-like 3 (Fstl3) is the antagonist of activin, and its inactivation resulted in the expansion of β-cell mass and improved glucose homeostasis [88]. The number of Ins^+/YFP^+ cells was significantly increased in Fstl3 KO mice compared with wild type mice. The treatment of isolated islets with activin resulted in a significantly increased number of YFP^+/ /Ins^+ cells [87]. These pieces of evidence suggested that transdifferentiation of α-cells to β-cells was influenced by activin signaling and contributed substantially to β-cell mass [87].

Chakravarthy *et al.* deciphered another possible mechanism for the conversion of α-cells to β-cells in adult mice [89]. The inactivation of two regulators of α-cell functionality, Arx and DNA methyltransferase 1 (Dnmt1), resulted in the conversion of α-cells to β-cells. This conversion took three months, and the newly formed β-cells were similar to native β-cells when checked for gene expression using RNA-sequence. The neogenic β-cells also secreted insulin upon glucose stimulation [89]. In 2017, two remarkable reports showed the role of gamma-aminobutyric acid (GABA), a neurotransmitter found in the nervous system and also in the endocrine pancreas [90], in α-to β-cell transition [91, 92]. In the first report Ben-Othman *et al.* reported that GABA induces the α-cell-mediated β-cell neogenesis *in vivo* in mice after three months of treatment with GABA. The newly produced β-cells were functional and could replace the native β-cells. When newly transplanted human islets were treated with GABA, they showed an increased number of β-cells at the cost of α-cells [91]. In a similar report, Li *et al.* [92] tested artemisinin, an antimalarial drug which enhances GABA signaling by binding to $GABA_A$ receptors, for β-cell neogenesis from α-cells. Artemisinin repressed the master regulator of glucagon-secreting α-cells, Arx, by causing its displacement to the cytoplasm. Thus, the α-cells lost their identity and were transdifferentiated to β-cells in zebrafish, rodents and primary human pancreatic islets [92]. However, a recent study by Ackermann *et al.* contradicted the role of both GABA and antimalarial drug in the α- to β-cells conversion [93]. They treated mice for three months with artesunate and GABA and showed by cell-specific genetic lineage tracing that no α- to β-cells transdifferentiation happened and insulin secretion was also not stimulated [93]. In another recent report, Shin *et al.* used rhesus monkey to translate the rodent β-cell regeneration model [94]. They used STZ for β-cell ablation followed by porcine islet transplantation to maintain normoglycemia, but in both conditions, there was no increase in β-cell number or serum C-peptide level. They also checked the *in vivo* and *in vitro* transdifferentiation ability of α- to β-cells by GABA treatment, and yet again no β-cell regeneration was found [94]. Eizirik and Gurzov [95] proposed four main reasons for the contrary results of the reported papers [91–94] and first of them was the use of different experimental models: zebrafish, rodents and primary human pancreatic islands [92], a single mice model [93], mice model that was confirmed in human and rat [91], rhesus monkey [94]. Secondly, Ackerman *et al.* used tamoxifen-induced lineage-tracing for following the adult α- to β-cell transition [93] whereas Ben-Othman *et al.* used Glucagon-Cre mice which can also detect the β-cell neogenesis from a transient and putative cell state expressing glucagon [91]. Thirdly, the GABA used in those experiments was not made for purpose of *in*

©Polish Society for Histochemistry and Cytochemistry

vivo use and finally, the diet and housing conditions were different in those laboratories which could have affected the murine microbiome and ultimately drug metabolism and systemic mouse metabolism [95].

Thus, we come to know that under the severe loss of β-cells due to metabolic stress or injury, the transition of α-cells to β-cells becomes stimulated. The regulation of this conversion is possible due to the genetic programming which involves the repression of α-cell genes and activation of β-cell genes. Therefore, different factors which can repress the α-cell signature genes and/or enhance the β-cell signature genes in α-cells can be used for designing a fruitful protocol for *in vitro* generation of β-like cells from α-cells.

δ-cells transdifferentiation to β-cells

Delta cells are found in the islets of Langerhans and they are responsible for somatostatin secretion [96]. The attempts to find the source of new β-cells and location of dedicated or facultative progenitors in adult mammals led to the studies for δ- to β-cell transdifferentiation following the models of α- to β-cell transdifferentiation [97]. Chera *et al.* administered diphtheria toxin (DT) to postnatal two week-old mice and adult mice for ablation of β-cells [25]. The administration of DT resulted in 99% ablation of β-cells; however, afterwards mice regenerated β-cells from other islet cells. The lineage tracing revealed that in the adult mice the induction of post-DT β-cell regeneration was by transdifferentiation of α-cells while in mouse pups the δ-cells were dedifferentiated and reprogrammed to β-cells. The dedifferentiated cells showed fewer somatostatin transcripts, and high insulin transcripts and no polyhormonal cells were found [25]. Druelle *et al.* generated and characterized Cre-LoxP transgenic mice that express *Pax4* specifically in somatostatin-expressing δ-cells cells [97]. They demonstrated that the ectopic expression of *Pax4* in δ cells is sufficient to induce their conversion into functional β-like cells that can partly reverse chemically-induced diabetes and induce β-like cell hyperplasia [97].

Although more work is needed for validation of δ-cells as the source of *in vivo* β-cell expansion, these results favor the plasticity of islet cells for their transdifferentiation into β-cells.

The summary of some factors used for the differentiation of pancreatic endocrine cells to β-like cells is presented in Figure 2.

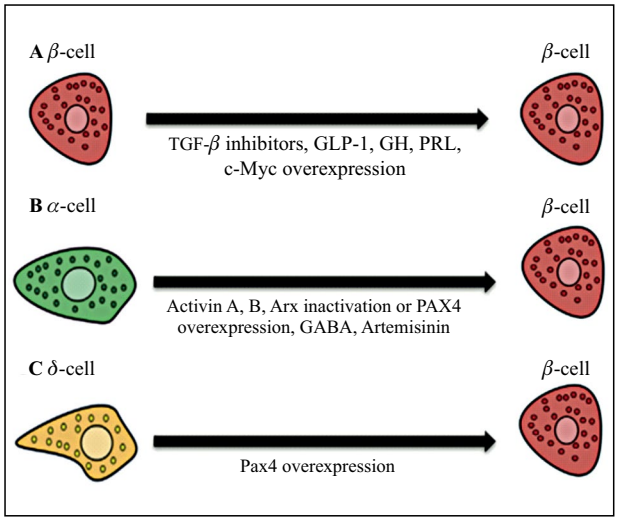

Figure 2. Some factors used for in vitro β-cell replication (A) as well as α-cell (B) and δ-cell (C) transdifferentiation to β-cell

Pancreatic islet-derived mesenchymal stem cells giving rise to β-like cells

Mesenchymal stem cells (MSCs) can differentiate into many target cells depending upon the applied conditions [98–100]. It was shown that transplantation of bone marrow-derived [101] and adipose tissue-derived [102] MSCs enhanced the regeneration of pancreatic islet and decreased the blood glucose levels of diabetic animals [103]. Furthermore, MSCs have shown a decent safety profile in clinical trials with limited risk of tumor formation [104]. The pancreatic islet also has mesenchymal stem cells (PI-MSCs) which play important roles as a source of ECM and during pancreatic islet injury. Here, we will shortly report studies showing the use of these PI-MSCs as a source of insulin-producing cells.

The quest for finding the stem or progenitor cells in the pancreas has led the researchers to search for these cells in different compartments of the pancreas. Zulewski *et al*. showed that rat and human pancreatic islets contain the distinct population of cells positive for neural stem-cell-specific marker nestin [105]. Apart from the islets of Langerhans, pancreatic ducts also contain the nestin-positive cells with the capability of giving rise to β-cells as we have discussed earlier. In *in vitro* culture, the nestin-positive cells have shown boundless proliferation and differentiation abilities as these cells were differentiated to acinar, ductal, and endocrine phenotype cells [105]. These findings suggested that the pancreatic islets have the progenitor cells with the ability to regenerate the islets of Langerhans [105]. Karaoz *et al.* isolated stem cells (SCs) from pancreatic islets and characterized their stem cell properties [106]. They found that the pancreatic islets SCs expressed the markers of embryonic SCs (Oct-4, Sox-2, and Rex-1) and also showed the high proliferation ability coinciding with the

©Polish Society for Histochemistry and Cytochemistry

bone marrow MSCs. Furthermore, these pancreatic islets SCs expressed the differentiation markers of adipo-, chondro-, neuro-, myo-, and osteogenic cells [106]. Thus, pancreatic islets contain stem cell with the ability to be expanded *in vivo* for replacement therapy of diabetes [106]. Gong *et al.* found that the CD117-positive cells were very few in normal pancreatic tissue, but their number increased after induction of pancreatitis [107]. In this model of pancreatic inflammation, the CD117-positive cells were only present in the pancreatic islet and participated only in the repair of islets of Langerhans but not in the repair of extra-islet pancreatic tissue. Thus, these findings suggested that the CD117 positive progenitor cells are not the true stem cells, but merely a type of islet progenitor or precursor cells [107].

It has been shown that microenvironment is important for the regulation of stem cells proliferation and differentiation [26]. Use of glycated collagen in culture media resulted in the induction of rat pancreatic islet-derived mesenchymal stem cells differentiation to insulin-secreting cells. PI-MSCs were induced by using glucose, hEGF, nicotinamide, activin-A, exendin-4, hHGF, and pentagastrin [26]. The differentiation efficiency and insulin expression in collagen cultures were higher than in control cultures; however, glucagon was also present in media showing the presence of α-cells [26]. Coskun *et al.* showed that valproic acid, class-I histone deacetylase inhibitor (HDACi) and glucose induced the differentiation of PI-MSCs to insulin-secreting cells with a fair efficiency, however, the newly formed β-cells were non-functional [108].

Gao *et al.* were the first to culture bovine pancreatic MSCs of (B-PMSCs) for differentiation to insulin-producing cells [109]. Growth kinetics of B-PMSCs revealed their decent *in vitro* self-renewal capability. Retinoic acid, HGF, and EGF were used for the induction of stem cells to insulin-secreting clusters. After 21 days of culture, the DTZ staining showed the presence of β-cells which were positive for glucose-stimulated insulin-secretion in culture media [109]. Most recently, the differentiation of MSCs from different sources into IPCs within 3D alginate matrices was performed by Cañibano-Hernández *et al.* [5]. MSCs from different sources were used, but the quantity of insulin released was high in IPCs differentiated from pancreatic islet-derived MSCs. Moreover, the amount of insulin secreted was increased after adding hyaluronic acid (HA) in alginate microcapsules [5].

The β-like cells developed *in vitro* in the presence of cytokines and/or inhibitors mentioned above were less in number and also were not functional enough to serve as the β-cell replacement source. In order to achieve the maturation of *in vitro* produced β-like cells, Nair *et al.* elegantly reported a reliable method for the maturation of *in vitro* generated β-like cells [110]. They recapitulated the culture conditions mimicking *in vivo* pancreatic islet organogenesis and β-cell maturation. In these conditions, the immature β-like cells were isolated and reaggregated in the form of islet-size enriched β-cell clusters (eBCs) — each eBCs comprised by aggregation of 1000 β-like cells mimicking the number of cells present in human islet [110]. After seven days, eBCs showed the properties of mature β-cells. The physiological properties exhibited by eBCs presented dynamic insulin secretion, increased calcium signaling in response to secretagogues, and improved mitochondrial energetics resembling primary human β-cells. Unlike previous studies in which long time was required for insulin secretion [28, 111], within three days of transplantation in mice, eBCs showed glucose-stimulated insulin secretion [110]. However, some dual-hormone cells, the likely progenitors of glucagon-secreting α-cells were also present in the clusters produced.

Conclusions

Attempts to control the diabetic epidemic have resulted in the development of many strategies for the replacement of β-cells. Still, to the best of our knowledge, *in vitro* development of functional islets or insulin-producing cells is not efficient enough to be used as a routine clinical option for curing diabetes due to many problems. These problems include production in low number, immature β-cell production, secretion of low amount of insulin, polyhormonal nature of cells, the impurity of cells, and the high cost of factors used in protocols for *in vitro* differentiation. While developing *in vitro* protocol, tactics like the recapitulation of *in vivo* conditions can warrant the production of an ample number of mature and functional β-cells. However, for mirroring *in vivo* conditions, first, we need to have vibrant knowledge about pancreas development which is instead a convoluted process and not fully understood yet. Though, the use of three-dimensional culture systems and tools like single-cell transcriptome analysis can help us understand the cellular and molecular mechanisms of pancreatic development assisting in the development of viable protocols for *in vitro* production of *bona fide* β-like cells.

Acknowledgment

The authors are highly indebt to Professor Zbigniew Kmiec (Gdansk, Poland) for critical reading of the manuscript and editorial assistance.

©Polish Society for Histochemistry and Cytochemistry

Conflict of interest

The authors hereby declare that they do not have any conflicting interest.

References

1. International Diabetes Federation. IDF 2017. WwwDiabetesatlasOrg. 2017; 8: 1–2.
2. Zimmet P, Alberti KG, Magliano DJ, et al. Diabetes mellitus statistics on prevalence and mortality: facts and fallacies. Nat Rev Endocrinol. 2016; 12(10): 616–622, doi: 10.1038/nrendo.2016.105, indexed in Pubmed: 27388988.
3. Afelik S, Rovira M, Afelik S, et al. Pancreatic β-cell regeneration: advances in understanding the genes and signaling pathways involved. Genome Med. 2017; 9(1): 42, doi: 10.1186/s13073-017-0437-x, indexed in Pubmed: 28511717.
4. Jacobson EF, Tzanakakis ES. Human pluripotent stem cell differentiation to functional pancreatic cells for diabetes therapies: Innovations, challenges and future directions. J Biol Eng. 2017; 11: 21, doi: 10.1186/s13036-017-0066-3, indexed in Pubmed: 28680477.
5. Cañibano-Hernández A, Saenz Del Burgo L, Espona-Noguera A, et al. Hyaluronic Acid Promotes Differentiation of Mesenchymal Stem Cells from Different Sources toward Pancreatic Progenitors within Three-Dimensional Alginate Matrixes. Mol Pharm. 2019; 16(2): 834–845, doi: 10.1021/acs.molpharmaceut.8b01126, indexed in Pubmed: 30601665.
6. Peng BY, Dubey NK, Mishra VK, et al. Addressing Stem Cell Therapeutic Approaches in Pathobiology of Diabetes and Its Complications. J Diabetes Res. 2018; 2018: 7806435, doi: 10.1155/2018/7806435, indexed in Pubmed: 30046616.
7. Zhou Q, Melton D. Pancreas regeneration. Nature. 2018; 557(7705): 351–358, doi: 10.1038/s41586-018-0088-0.
8. Qadir MM, Álvarez-Cubela S, Klein D, et al. P2RY1/ALK3-Expressing Cells within the Adult Human Exocrine Pancreas Are BMP-7 Expandable and Exhibit Progenitor-like Characteristics. Cell Rep. 2018; 22(9): 2408–2420, doi: 10.1016/j.celrep.2018.02.006, indexed in Pubmed: 29490276.
9. Alberts B. Secialized Tissues, Stem Cells, and Tissue Renewal. In: Molecular Biology of The Cell 5th Edition. Garland Science; 2008: 1417–1486.
10. Afelik S, Rovira M. Pancreatic β-cell regeneration: Facultative or dedicated progenitors? Mol Cell Endocrinol. 2017; 445: 85–94, doi: 10.1016/j.mce.2016.11.008, indexed in Pubmed: 27838399.
11. Tata PR, Mou H, Pardo-Saganta A, et al. Dedifferentiation of committed epithelial cells into stem cells in vivo. Nature. 2013; 503(7475): 218–223, doi: 10.1038/nature12777, indexed in Pubmed: 24196716.
12. Slack JM, Tosh D. Transdifferentiation and metaplasia-switching cell types. Curr Opin Genet Dev. 2001; 11(5): 581–586, indexed in Pubmed: 11532402.
13. Storz P. Acinar cell plasticity and development of pancreatic ductal adenocarcinoma. Nat Rev Gastroenterol Hepatol. 2017; 14(5): 296–304, doi: 10.1038/nrgastro.2017.12, indexed in Pubmed: 28270694.
14. Puri S, Hebrok M. Cellular plasticity within the pancreas--lessons learned from development. Dev Cell. 2010; 18(3): 342–356, doi: 10.1016/j.devcel.2010.02.005, indexed in Pubmed: 20230744.
15. Migliorini A, Bader E, Lickert H. Islet cell plasticity and regeneration. Mol Metab. 2014; 3(3): 268–274, doi: 10.1016/j.molmet.2014.01.010, indexed in Pubmed: 24749056.
16. Dor Y, Brown J, Martinez OI, et al. Adult pancreatic β-cells are formed by self-duplication rather than stem-cell differentiation. Nature. 2004; 429(6987): 41–46, doi: 10.1038/nature02520, indexed in Pubmed: 15129273.
17. Domínguez-Bendala J, Qadir MM, Pastori RL. Pancreatic Progenitors: There and Back Again. Trends Endocrinol Metab. 2019; 30(1): 4–11, doi: 10.1016/j.tem.2018.10.002, indexed in Pubmed: 30502039.
18. van der Meulen T, Mawla AM, DiGruccio MR, et al. Virgin Beta Cells Persist throughout Life at a Neogenic Niche within Pancreatic Islets. Cell Metab. 2017; 25(4): 911–926.e6, doi: 10.1016/j.cmet.2017.03.017, indexed in Pubmed: 28380380.
19. Talchai C, Xuan S, Lin HV, et al. Pancreatic β-cell dedifferentiation as a mechanism of diabetic β cell failure. Cell. 2012; 150(6): 1223–1234, doi: 10.1016/j.cell.2012.07.029, indexed in Pubmed: 22980982.
20. Tan J, Liu L, Li B, et al. Pancreatic stem cells differentiate into insulin-secreting cells on fibroblast-modified PLGA membranes. Mater Sci Eng C Mater Biol Appl. 2019; 97: 593–601, doi: 10.1016/j.msec.2018.12.062, indexed in Pubmed: 30678946.
21. Klein D, Álvarez-Cubela S, Lanzoni G, et al. BMP-7 Induces Adult Human Pancreatic Exocrine-to-Endocrine Conversion. Diabetes. 2015; 64(12): 4123–4134, doi: 10.2337/db15-0688, indexed in Pubmed: 26307584.
22. Delaspre F, Beer RL, Rovira M, et al. Centroacinar Cells Are Progenitors That Contribute to Endocrine Pancreas Regeneration. Diabetes. 2015; 64(10): 3499–3509, doi: 10.2337/db15-0153, indexed in Pubmed: 26153247.
23. Dhawan S, Dirice E, Kulkarni RN, et al. Inhibition of TGF-β Signaling Promotes Human Pancreatic β-Cell Replication. Diabetes. 2016; 65(5): 1208–1218, doi: 10.2337/db15-1331, indexed in Pubmed: 26936960.
24. Andrzejewski D, Brown ML, Ungerleider N, et al. Activins A and B Regulate Fate-Determining Gene Expression in Islet Cell Lines and Islet Cells From Male Mice. Endocrinology. 2015; 156(7): 2440–2450, doi: 10.1210/en.2015-1167, indexed in Pubmed: 25961841.
25. Chera S, Baronnier D, Ghila L, et al. Diabetes recovery by age-dependent conversion of pancreatic δ-cells into insulin producers. Nature. 2014; 514(7523): 503–507, doi: 10.1038/nature13633, indexed in Pubmed: 25141178.
26. Duruksu G, Aciksari A. Guiding the Differentiation Direction of Pancreatic Islet-Derived Stem Cells by Glycated Collagen. Stem Cells Int. 2018; 2018: 6143081, doi: 10.1155/2018/6143081, indexed in Pubmed: 30057625.
27. Balboa D, Saarimäki-Vire J, Otonkoski T. Concise Review: Human Pluripotent Stem Cells for the Modeling of Pancreatic β-Cell Pathology. Stem Cells. 2019; 37(1): 33–41, doi: 10.1002/stem.2913, indexed in Pubmed: 30270471.
28. Pagliuca FW, Millman JR, Gürtler M, et al. Generation of functional human pancreatic β-cells in vitro. Cell. 2014; 159(2): 428–439, doi: 10.1016/j.cell.2014.09.040, indexed in Pubmed: 25303535.
29. Pokrywczynska M, Lanzoni G, Ricordi C, et al. From Adult Pancreatic Islets to Stem Cells. In: Atala A. et al. (eds.). Principles of Regenerative Medicine. 3rd ed., Academic Press; 2018.
30. Avolio F, Pfeifer A, Courtney M, et al. From pancreas morphogenesis to β-cell regeneration. Curr Top Dev Biol. 2013; 106: 217–238, doi: 10.1016/B978-0-12-416021-7.00006-7, indexed in Pubmed: 24290351.
31. Xu X, Bonne S, Leu N De, Xiao X, Hoker JD, Stange G, et al. Beta cells can be generated from endogenous progenitors in injured adult mouse pancreas. Cell. 2008;132(2):

©Polish Society for Histochemistry and Cytochemistry

197–207. Available from: http://www.ncbi.nlm.nih.gov/pubmed/18243096.
32. Inada A, Nienaber C, Katsuta H, et al. Carbonic anhydrase II-positive pancreatic cells are progenitors for both endocrine and exocrine pancreas after birth. Proc Natl Acad Sci U S A. 2008; 105(50): 19915–19919, doi: 10.1073/pnas.0805803105, indexed in Pubmed: 19052237.
33. Li WC, Rukstalis JM, Nishimura W, et al. Activation of pancreatic-duct-derived progenitor cells during pancreas regeneration in adult rats. J Cell Sci. 2010; 123(Pt 16): 2792–2802, doi: 10.1242/jcs.065268, indexed in Pubmed: 20663919.
34. Pierreux CE, Poll AV, Kemp CR, et al. The transcription factor hepatocyte nuclear factor-6 controls the development of pancreatic ducts in the mouse. Gastroenterology. 2006; 130(2): 532–541, doi: 10.1053/j.gastro.2005.12.005, indexed in Pubmed: 16472605.
35. Zhang H, Ables ET, Pope CF, et al. Multiple, temporal-specific roles for HNF6 in pancreatic endocrine and ductal differentiation. Mech Dev. 2009; 126(11-12): 958–973, doi: 10.1016/j.mod.2009.09.006, indexed in Pubmed: 19766716.
36. Seymour PA, Freude KK, Tran MN, et al. SOX9 is required for maintenance of the pancreatic progenitor cell pool. Proc Natl Acad Sci U S A. 2007; 104(6): 1865–1870, doi: 10.1073/pnas.0609217104, indexed in Pubmed: 17267606.
37. Maestro MA, Boj SF, Luco RF, et al. Hnf6 and Tcf2 (MODY5) are linked in a gene network operating in a precursor cell domain of the embryonic pancreas. Hum Mol Genet. 2003; 12(24): 3307–3314, doi: 10.1093/hmg/ddg355, indexed in Pubmed: 14570708.
38. Christensen AA, Gannon M. The Beta Cell in Type 2 Diabetes. Curr Diab Rep. 2019; 19(9): 81, doi: 10.1007/s11892-019-1196-4, indexed in Pubmed: 31399863.
39. El-Gohary Y, Wiersch J, Tulachan S, et al. Intraislet Pancreatic Ducts Can Give Rise to Insulin-Positive Cells. Endocrinology. 2016; 157(1): 166–175, doi: 10.1210/en.2015-1175, indexed in Pubmed: 26505114.
40. Criscimanna A, Speicher JA, Houshmand G, et al. Duct cells contribute to regeneration of endocrine and acinar cells following pancreatic damage in adult mice. Gastroenterology. 2011; 141(4): 1451–62, 1462.e1, doi: 10.1053/j.gastro.2011.07.003, indexed in Pubmed: 21763240.
41. Skurikhin EG, Ermakova NN, Khmelevskaya ES, et al. Differentiation of pancreatic stem and progenitor β-cells into insulin secreting cells in mice with diabetes mellitus. Bull Exp Biol Med. 2014; 156(6): 726–730, doi: 10.1007/s10517-014-2434-z, indexed in Pubmed: 24824681.
42. Zhang M, Lin Q, Qi T, et al. Growth factors and medium hyperglycemia induce Sox9+ ductal cell differentiation into β-cells in mice with reversal of diabetes. Proc Natl Acad Sci U S A. 2016; 113(3): 650–655, doi: 10.1073/pnas.1524200113, indexed in Pubmed: 26733677.
43. Shaotang Y, Yuxian Y, Jiang W, et al. Multipotent of Monoclonal Epithelial Stem Cells Derived from Pancreatic Duct. Chinese J Cell Biol. 2018; 40(1): 41–6.
44. Gagliardino JJ, Del Zotto H, Massa L, et al. Pancreatic duodenal homeobox-1 and islet neogenesis-associated protein: a possible combined marker of activateable pancreatic cell precursors. J Endocrinol. 2003; 177(2): 249–259, doi: 10.1677/joe.0.1770249, indexed in Pubmed: 12740013.
45. Sugimoto H, LeBleu VS, Bosukonda D, et al. Activin-like kinase 3 is important for kidney regeneration and reversal of fibrosis. Nat Med. 2012; 18(3): 396–404, doi: 10.1038/nm.2629, indexed in Pubmed: 22306733.
46. Suarez-Pinzon WL, Yan Y, Power R, et al. Combination therapy with epidermal growth factor and gastrin increases β-cell mass and reverses hyperglycemia in diabetic NOD mice. Diabetes. 2005; 54(9): 2596–2601, doi: 10.2337/diabetes.54.9.2596, indexed in Pubmed: 16123347.
47. Ogawa N, List JF, Habener JF, et al. Cure of overt diabetes in NOD mice by transient treatment with anti-lymphocyte serum and exendin-4. Diabetes. 2004; 53(7): 1700–1705, doi: 10.2337/diabetes.53.7.1700, indexed in Pubmed: 15220193.
48. Suarez-Pinzon WL, Lakey JRT, Brand SJ, et al. Combination therapy with epidermal growth factor and gastrin induces neogenesis of human islet β-cells from pancreatic duct cells and an increase in functional β-cell mass. J Clin Endocrinol Metab. 2005; 90(6): 3401–3409, doi: 10.1210/jc.2004-0761, indexed in Pubmed: 15769977.
49. Miettinen PJ, Huotari M, Koivisto T, et al. Impaired migration and delayed differentiation of pancreatic islet cells in mice lacking EGF-receptors. Development. 2000; 127(12): 2617–2627, indexed in Pubmed: 10821760.
50. Corritore E, Lee YS, Sokal EM, et al. β-cell replacement sources for type 1 diabetes: a focus on pancreatic ductal cells. Ther Adv Endocrinol Metab. 2016; 7(4): 182–199, doi: 10.1177/2042018816652059, indexed in Pubmed: 27540464.
51. Hui H, Wright C, Perfetti R. Glucagon-like peptide 1 induces differentiation of islet duodenal homeobox-1-positive pancreatic ductal cells into insulin-secreting cells. Diabetes. 2001; 50(4): 785–796, doi: 10.2337/diabetes.50.4.785, indexed in Pubmed: 11289043.
52. Li Li, Lili R, Hui Qi, et al. Combination of GLP-1 and sodium butyrate promote differentiation of pancreatic progenitor cells into insulin-producing cells. Tissue Cell. 2008; 40(6): 437–445, doi: 10.1016/j.tice.2008.04.006, indexed in Pubmed: 18573514.
53. Haumaitre C, Lenoir O, Scharfmann R. Histone deacetylase inhibitors modify pancreatic cell fate determination and amplify endocrine progenitors. Mol Cell Biol. 2008; 28(20): 6373–6383, doi: 10.1128/MCB.00413-08, indexed in Pubmed: 18710955.
54. Chen XC, Liu H, Li H, et al. In vitro expansion and differentiation of rat pancreatic duct-derived stem cells into insulin secreting cells using a dynamicthree-dimensional cell culture system. Genet Mol Res. 2016; 15(2), doi: 10.4238/gmr.15028808, indexed in Pubmed: 27420984.
55. Means AL, Meszoely IM, Suzuki K, et al. Pancreatic epithelial plasticity mediated by acinar cell transdifferentiation and generation of nestin-positive intermediates. Development. 2005; 132(16): 3767–3776, doi: 10.1242/dev.01925, indexed in Pubmed: 16020518.
56. Pan FC, Bankaitis ED, Boyer D, et al. Spatiotemporal patterns of multipotentiality in Ptf1a-expressing cells during pancreas organogenesis and injury-induced facultative restoration. Development. 2013; 140(4): 751–764, doi: 10.1242/dev.090159, indexed in Pubmed: 23325761.
57. Baeyens L, Lemper M, Leuckx G, et al. Transient cytokine treatment induces acinar cell reprogramming and regenerates functional beta cell mass in diabetic mice. Nat Biotechnol. 2014; 32(1): 76–83, doi: 10.1038/nbt.2747, indexed in Pubmed: 24240391.
58. Clayton HW, Osipovich AB, Stancill JS, et al. Pancreatic Inflammation Redirects Acinar to β-Cell Reprogramming. Cell Rep. 2016; 17(8): 2028–2041, doi: 10.1016/j.celrep.2016.10.068, indexed in Pubmed: 27851966.
59. Baeyens L, Bonné S, Bos T, et al. Notch signaling as gatekeeper of rat acinar-to-β-cell conversion in vitro. Gastroenterology. 2009; 136(5): 1750–60.e13, doi: 10.1053/j.gastro.2009.01.047, indexed in Pubmed: 19208356.
60. Aïello V, Moreno-Asso A, Servitja JM, et al. Thyroid hormones promote endocrine differentiation at expenses of

©Polish Society for Histochemistry and Cytochemistry

exocrine tissue. Exp Cell Res. 2014; 322(2): 236–248, doi: 10.1016/j.yexcr.2014.01.030, indexed in Pubmed: 24503054.
61. Seymour PA. Sox9: a master regulator of the pancreatic program. Rev Diabet Stud. 2014; 11(1): 51–83, doi: 10.1900/RDS.2014.11.51, indexed in Pubmed: 25148367.
62. Manfroid I, Ghaye A, Naye F, et al. Zebrafish sox9b is crucial for hepatopancreatic duct development and pancreatic endocrine cell regeneration. Dev Biol. 2012; 366(2): 268–278, doi: 10.1016/j.ydbio.2012.04.002, indexed in Pubmed: 22537488.
63. Seymour PA, Freude KK, Dubois CL, et al. A dosage-dependent requirement for Sox9 in pancreatic endocrine cell formation. Dev Biol. 2008; 323(1): 19–30, doi: 10.1016/j.ydbio.2008.07.034, indexed in Pubmed: 18723011.
64. Shih HP, Kopp JL, Sandhu M, et al. A Notch-dependent molecular circuitry initiates pancreatic endocrine and ductal cell differentiation. Development. 2012; 139(14): 2488–2499, doi: 10.1242/dev.078634, indexed in Pubmed: 22675211.
65. Beer RL, Parsons MJ, Rovira M. Centroacinar cells: At the center of pancreas regeneration. Dev Biol. 2016; 413(1): 8–15, doi: 10.1016/j.ydbio.2016.02.027, indexed in Pubmed: 26963675.
66. Parsons MJ, Pisharath H, Yusuff S, et al. Notch-responsive cells initiate the secondary transition in larval zebrafish pancreas. Mech Dev. 2009; 126(10): 898–912, doi: 10.1016/j.mod.2009.07.002, indexed in Pubmed: 19595765.
67. Ghaye AP, Bergemann D, Tarifeño-Saldivia E, et al. Progenitor potential of nkx6.1-expressing cells throughout zebrafish life and during beta cell regeneration. BMC Biol. 2015; 13: 70, doi: 10.1186/s12915-015-0179-4, indexed in Pubmed: 26329351.
68. Rovira M, Scott SG, Liss AS, et al. Isolation and characterization of centroacinar/terminal ductal progenitor cells in adult mouse pancreas. Proc Natl Acad Sci U S A. 2010; 107(1): 75–80, doi: 10.1073/pnas.0912589107, indexed in Pubmed: 20018761.
69. Ghazalli N, Wu X, Walker S, et al. Glucocorticoid Signaling Enhances Expression of Glucose-Sensing Molecules in Immature Pancreatic Beta-Like Cells Derived from Murine Embryonic Stem Cells In Vitro. Stem Cells Dev. 2018; 27(13): 898–909, doi: 10.1089/scd.2017.0160, indexed in Pubmed: 29717618.
70. Shih HP, Wang A, Sander M. Pancreas organogenesis: from lineage determination to morphogenesis. Annu Rev Cell Dev Biol. 2013; 29: 81–105, doi: 10.1146/annurev-cellbio-101512-122405, indexed in Pubmed: 23909279.
71. Georgia S, Bhushan A. β-cell replication is the primary mechanism for maintaining postnatal β-cell mass. J Clin Invest. 2004; 114(7): 963–968, doi: 10.1172/JCI22098, indexed in Pubmed: 15467835.
72. Teta M, Rankin MM, Long SY, et al. Growth and regeneration of adult β-cells does not involve specialized progenitors. Dev Cell. 2007; 12(5): 817–826, doi: 10.1016/j.devcel.2007.04.011, indexed in Pubmed: 17488631.
73. Nir T, Melton DA, Dor Y. Recovery from diabetes in mice by β-cell regeneration. J Clin Invest. 2007; 117(9): 2553–2561, doi: 10.1172/JCI32959, indexed in Pubmed: 17786244.
74. Cano DA, Rulifson IC, Heiser PW, et al. Regulated β-cell regeneration in the adult mouse pancreas. Diabetes. 2008; 57(4): 958–966, doi: 10.2337/db07-0913, indexed in Pubmed: 18083786.
75. Desgraz R, Bonal C, Herrera PL. β-cell regeneration: the pancreatic intrinsic faculty. Trends Endocrinol Metab. 2011; 22(1): 34–43, doi: 10.1016/j.tem.2010.09.004, indexed in Pubmed: 21067943.
76. Gregg BE, Moore PC, Demozay D, et al. Formation of a human β-cell population within pancreatic islets is set early in life. J Clin Endocrinol Metab. 2012; 97(9): 3197–3206, doi: 10.1210/jc.2012-1206, indexed in Pubmed: 22745242.
77. Rieck S, Kaestner KH. Expansion of β-cell mass in response to pregnancy. Trends Endocrinol Metab. 2010; 21(3): 151–158, doi: 10.1016/j.tem.2009.11.001, indexed in Pubmed: 20015659.
78. Henquin JC, Rahier J. Pancreatic β-cell mass in European subjects with type 2 diabetes. Diabetologia. 2011; 54(7): 1720–1725, doi: 10.1007/s00125-011-2118-4, indexed in Pubmed: 21465328.
79. Venkatesan V, Gopurappilly R, Goteti SK, et al. Pancreatic progenitors: The shortest route to restore islet cell mass. Islets. 2011; 3(6): 295–301, doi: 10.4161/isl.3.6.17704, indexed in Pubmed: 21934353.
80. Puri S, Roy N, Russ HA, et al. Replication confers β-cell immaturity. Nat Commun. 2018; 9(1): 485, doi: 10.1038/s41467-018-02939-0, indexed in Pubmed: 29396395.
81. Nielsen JH, Galsgaard ED, Møldrup A, et al. Regulation of β-cell mass by hormones and growth factors. Diabetes. 2001; 50 Suppl 1: S25–S29, doi: 10.2337/diabetes.50.2007.s25, indexed in Pubmed: 11272193.
82. Ouziel-Yahalom L, Zalzman M, Anker-Kitai L, et al. Expansion and redifferentiation of adult human pancreatic islet cells. Biochem Biophys Res Commun. 2006; 341(2): 291–298, doi: 10.1016/j.bbrc.2005.12.187, indexed in Pubmed: 16446152.
83. Thorel F, Népote V, Avril I, et al. Conversion of adult pancreatic alpha-cells to beta-cells after extreme beta-cell loss. Nature. 2010; 464(7292): 1149–1154, doi: 10.1038/nature08894, indexed in Pubmed: 20364121.
84. Ye L, Robertson MA, Hesselson D, et al. Glucagon is essential for alpha cell transdifferentiation and beta cell neogenesis. Development. 2015; 142(8): 1407–1417, doi: 10.1242/dev.117911, indexed in Pubmed: 25852199.
85. Chung CH, Hao E, Piran R, et al. Pancreatic β-cell neogenesis by direct conversion from mature α-cells. Stem Cells. 2010; 28(9): 1630–1638, doi: 10.1002/stem.482, indexed in Pubmed: 20653050.
86. Cierpka-Kmiec K, Wronska A, Kmiec Z. In vitro generation of pancreatic β-cells for diabetes treatment. I. β-like cells derived from human pluripotent stem cells. Folia Histochem Cytobiol. 2019; 57(1): 1–14, doi: 10.5603/FHC.a2019.0001, indexed in Pubmed: 30869153.
87. Brown ML, Andrzejewski D, Burnside A, et al. Activin Enhances α- to β-Cell Transdifferentiation as a Source For β-Cells In Male FSTL3 Knockout Mice. Endocrinology. 2016; 157(3): 1043–1054, doi: 10.1210/en.2015-1793, indexed in Pubmed: 26727106.
88. Brown ML, Bonomi L, Ungerleider N, et al. Follistatin and follistatin like-3 differentially regulate adiposity and glucose homeostasis. Obesity (Silver Spring). 2011; 19(10): 1940–1949, doi: 10.1038/oby.2011.97, indexed in Pubmed: 21546932.
89. Chakravarthy H, Gu X, Enge M, et al. Converting Adult Pancreatic Islet α Cells into β Cells by Targeting Both Dnmt1 and Arx. Cell Metab. 2017; 25(3): 622–634, doi: 10.1016/j.cmet.2017.01.009, indexed in Pubmed: 28215845.
90. Adeghate E, Ponery AS. GABA in the endocrine pancreas: cellular localization and function in normal and diabetic rats. Tissue Cell. 2002; 34(1): 1–6, doi: 10.1054/tice.2002.0217, indexed in Pubmed: 11989965.
91. Ben-Othman N, Vieira A, Courtney M, et al. Long-Term GABA Administration Induces Alpha Cell-Mediated Beta-like Cell Neogenesis. Cell. 2017; 168(1-2): 73–85.e11, doi: 10.1016/j.cell.2016.11.002.

©Polish Society for Histochemistry and Cytochemistry

92. Li J, Casteels T, Frogne T, et al. Artemisinins Target GABA Receptor Signaling and Impair α Cell Identity. Cell. 2017; 168(1-2): 86–100.e15, doi: 10.1016/j.cell.2016.11.010, indexed in Pubmed: 27916275.
93. Ackermann AM, Moss NG, Kaestner KH. GABA and Artesunate Do Not Induce Pancreatic α-to-β Cell Transdifferentiation In Vivo. Cell Metab. 2018; 28(5): 787–792.e3, doi: 10.1016/j.cmet.2018.07.002, indexed in Pubmed: 30057067.
94. Shin JS, Kim JM, Min BH, et al. Absence of spontaneous regeneration of endogenous pancreatic β-cells after chemical-induced diabetes and no effect of GABA on α-to-β cell transdifferentiation in rhesus monkeys. Biochem Biophys Res Commun. 2019; 508(4): 1056–1061, doi: 10.1016/j.bbrc.2018.12.062, indexed in Pubmed: 30553443.
95. Eizirik DL, Gurzov EN. Can GABA turn pancreatic α-cells into β-cells? Nat Rev Endocrinol. 2018; 14(11): 629–630, doi: 10.1038/s41574-018-0101-6, indexed in Pubmed: 30254299.
96. Muraro MJ, Dharmadhikari G, Grün D, et al. A Single-Cell Transcriptome Atlas of the Human Pancreas. Cell Syst. 2016; 3(4): 385–394.e3, doi: 10.1016/j.cels.2016.09.002, indexed in Pubmed: 27693023.
97. Druelle N, Vieira A, Shabro A, et al. Ectopic expression of in pancreatic δ cells results in β-like cell neogenesis. J Cell Biol. 2017; 216(12): 4299–4311, doi: 10.1083/jcb.201704044, indexed in Pubmed: 29025873.
98. Damia E, Chicharro D, Lopez S, et al. Adipose-Derived Mesenchymal Stem Cells: Are They a Good Therapeutic Strategy for Osteoarthritis? Int J Mol Sci. 2018; 19(7), doi: 10.3390/ijms19071926, indexed in Pubmed: 29966351.
99. Mendes Filho D, Ribeiro PDC, Oliveira LF, et al. Therapy With Mesenchymal Stem Cells in Parkinson Disease: History and Perspectives. Neurologist. 2018; 23(4): 141–147, doi: 10.1097/NRL.0000000000000188, indexed in Pubmed: 29953040.
100. Badimon L, Oñate B, Vilahur G. Adipose-derived Mesenchymal Stem Cells and Their Reparative Potential in Ischemic Heart Disease. Rev Esp Cardiol (Engl Ed). 2015; 68(7): 599–611, doi: 10.1016/j.rec.2015.02.025, indexed in Pubmed: 26028258.
101. Carlsson PO, Schwarcz E, Korsgren O, et al. Preserved β-cell function in type 1 diabetes by mesenchymal stromal cells. Diabetes. 2015; 64(2): 587–592, doi: 10.2337/db14-0656, indexed in Pubmed: 25204974.
102. Okura H, Komoda H, Fumimoto Y, et al. Transdifferentiation of human adipose tissue-derived stromal cells into insulin-producing clusters. J Artif Organs. 2009; 12(2): 123–130, doi: 10.1007/s10047-009-0455-6, indexed in Pubmed: 19536630.
103. Boumaza I, Srinivasan S, Witt WT, et al. Autologous bone marrow-derived rat mesenchymal stem cells promote PDX-1 and insulin expression in the islets, alter T cell cytokine pattern and preserve regulatory T cells in the periphery and induce sustained normoglycemia. J Autoimmun. 2009; 32(1): 33–42, doi: 10.1016/j.jaut.2008.10.004, indexed in Pubmed: 19062254.
104. Cantarelli E, Pellegrini S, Citro A, et al. Bone marrow-and cord blood-derived stem cell transplantation for diabetes therapy. CellR4. 2015; 3(1): e1408.
105. Zulewski H, Abraham EJ, Gerlach MJ, et al. Multipotential nestin-positive stem cells isolated from adult pancreatic islets differentiate ex vivo into pancreatic endocrine, exocrine, and hepatic phenotypes. Diabetes. 2001; 50(3): 521–533, doi: 10.2337/diabetes.50.3.521, indexed in Pubmed: 11246871.
106. Karaoz E, Ayhan S, Gacar G, et al. Isolation and characterization of stem cells from pancreatic islet: pluripotency, differentiation potential and ultrastructural characteristics. Cytotherapy. 2010; 12(3): 288–302, doi: 10.3109/14653240903580296, indexed in Pubmed: 20230222.
107. Gong J, Zhang G, Tian F, et al. Islet-derived stem cells from adult rats participate in the repair of islet damage. J Mol Histol. 2012; 43(6): 745–750, doi: 10.1007/s10735-012-9447-6, indexed in Pubmed: 22972433.
108. Coskun E, Ercin M, Gezginci-Oktayoglu S. The Role of Epigenetic Regulation and Pluripotency-Related MicroRNAs in Differentiation of Pancreatic Stem Cells to Beta Cells. J Cell Biochem. 2018; 119(1): 455–467, doi: 10.1002/jcb.26203, indexed in Pubmed: 28597969.
109. Gao F, Wu Y, Wen H, et al. Multilineage potential research on pancreatic mesenchymal stem cells of bovine. Tissue Cell. 2019; 56: 60–70, doi: 10.1016/j.tice.2018.12.001, indexed in Pubmed: 30736905.
110. Nair GG, Liu JS, Russ HA, et al. Recapitulating endocrine cell clustering in culture promotes maturation of human stem-cell-derived β-cells. Nat Cell Biol. 2019; 21(2): 263–274, doi: 10.1038/s41556-018-0271-4, indexed in Pubmed: 30710150.
111. Rezania A, Bruin JE, Arora P, et al. Reversal of diabetes with insulin-producing cells derived in vitro from human pluripotent stem cells. Nat Biotechnol. 2014; 32(11): 1121–1133, doi: 10.1038/nbt.3033, indexed in Pubmed: 25211370.
112. Wang CY, Gou SM, Liu T, et al. Differentiation of CD24-pancreatic ductal cell-derived cells into insulin-secreting cells. Dev Growth Differ. 2008; 50(8): 633–643, doi: 10.1111/j.1440-169X.2008.01061.x, indexed in Pubmed: 18657167.
113. Noguchi H, Naziruddin B, Shimoda M, et al. Induction of insulin-producing cells from human pancreatic progenitor cells. Transplant Proc. 2010; 42(6): 2081–2083, doi: 10.1016/j.transproceed.2010.05.097, indexed in Pubmed: 20692413.
114. Huch M, Bonfanti P, Boj SF, et al. Unlimited in vitro expansion of adult bi-potent pancreas progenitors through the Lgr5/R-spondin axis. EMBO J. 2013; 32(20): 2708–2721, doi: 10.1038/emboj.2013.204, indexed in Pubmed: 24045232.
115. Bonfanti P, Nobecourt E, Oshima M, et al. Ex Vivo Expansion and Differentiation of Human and Mouse Fetal Pancreatic Progenitors Are Modulated by Epidermal Growth Factor. Stem Cells Dev. 2015; 24(15): 1766–1778, doi: 10.1089/scd.2014.0550, indexed in Pubmed: 25925840.
116. Ma D, Tang S, Song J, et al. Culturing and transcriptome profiling of progenitor-like colonies derived from adult mouse pancreas. Stem Cell Res Ther. 2017; 8(1): 172, doi: 10.1186/s13287-017-0626-y, indexed in Pubmed: 28747214.
117. Movassat J, Beattie GM, Lopez AD, et al. Keratinocyte growth factor and beta-cell differentiation in human fetal pancreatic endocrine precursor cells. Diabetologia. 2003; 46(6): 822–829, doi: 10.1007/s00125-003-1117-5, indexed in Pubmed: 12802496.
118. Tokui Y, Kozawa J, Yamagata K, et al. Neogenesis and proliferation of beta-cells induced by human betacellulin gene transduction via retrograde pancreatic duct injection of an adenovirus vector. Biochem Biophys Res Commun. 2006; 350(4): 987–993, doi: 10.1016/j.bbrc.2006.09.154, indexed in Pubmed: 17046717.
119. Xu G, Kaneto H, Lopez-Avalos MD, et al. GLP-1/exendin-4 facilitates beta-cell neogenesis in rat and human pancreatic ducts. Diabetes Res Clin Pract. 2006; 73(1): 107–110, doi: 10.1016/j.diabres.2005.11.007, indexed in Pubmed: 16406191.

Submitted: 19 April, 2019
Accepted after reviews: 6 August, 2019
Available as AoP: 9 August, 2019

©Polish Society for Histochemistry and Cytochemistry

FOLIA HISTOCHEMICA ET CYTOBIOLOGICA
Vol. 57, No. 3, 2019
pp. 116–126

ORIGINAL PAPER

VIA MEDICA

Cytoplasmic and membranous receptor-binding cancer antigens expressed on SiSo cells (RCAS1) immunoreactivity in epithelial ovarian cancer cells represent differing biological function of RCAS1

Sebastian Szubert[1, 2], Wojciech Jozwicki[3], Lukasz Wicherek[1], Krzysztof Koper[4]

[1]2nd Department of Obstetrics and Gynecology, Medical Centre of Postgraduate Education, Warsaw, Poland
[2]Clinical Department of Gynecological Oncology, Franciszek Lukaszczyk Oncological Center, Bydgoszcz, Poland
[3]Department of Tumor Pathology and Pathomorphology, Ludwik Rydygier Collegium Medicum in Bydgoszcz, Nicolaus Copernicus University in Torun, Torun, Poland
[4]Department of Chemotherapy, Franciszek Lukaszczyk Oncological Center, Bydgoszcz, Poland

Abstract

Introduction. Receptor-binding cancer antigen expressed on SiSo cells (RCAS1) is a selective suppressor of the immune response that has been linked to the evasion of immune surveillance by cancer cells. However, the exact prognostic impact of RCAS1 on epithelial ovarian cancer (EOC) has not been fully elucidated. The main aim of our study was to evaluate the influence of RCAS1 immunoreactivity (RCAS1-Ir) in EOC cells and in tumor stroma cells on patient overall survival. We also focused on RCAS1-Ir and the structure of the tumor stroma.
Material and methods. RCAS1-Ir was evaluated by means of immunohistochemistry in 67 patients with EOC. We distinguished cytoplasmic and membranous immunoreactivity patterns.
Results. We found that high cytoplasmic RCAS1-Ir in cancer cells was associated with more than a two-time shortened period of overall survival. Membranous RCAS1-Ir in cancer cells, as well as in tumor stroma macrophages and fibroblasts, did not correlate with patient survival. RCAS1-Ir in the cytoplasm of cancer cells was positively correlated with the degree of tumor stroma infiltration by fibroblasts and macrophages, but not with RCAS1-Ir in these cells. On the other hand, membranous RCAS1-Ir in cancer cells was positively correlated with RCAS1-Ir in fibroblasts and macrophages, but not with their quantity.
Conclusions. Due to their different impacts on patient prognosis and tumor stroma structure, it seems that cytoplasmic and membranous RCAS1-Ir in EOC cells may have different biological functions. *(Folia Histochemica et Cytobiologica 2019, Vol. 57, No. 3, 116–126)*

Key words: RCAS1; receptor-binding cancer antigen expressed on SiSo cells; epithelial ovarian cancer; tumor stroma; tumor microenvironment

Introduction

Epithelial ovarian cancer (EOC) is still the leading cause of death from gynecological malignancies in the Western world [1]. Patient prognosis depends on the stage of the disease, patient age at diagnosis, the histological type of the tumor, and the first-line chemotherapy [2]. Current data suggests that the residual disease after primary debulking surgery is the most important prognostic factor in EOC [3, 4] the prognostic role of complete and so-called optimal and suboptimal debulking and its interaction with biological factors has not been not fully defined. Exploratory analysis was conducted of 3 prospective

Correspondence address: Krzysztof Koper, MD, PhD, Department of Chemotherapy, Franciszek Lukaszczyk Oncological Center Romanowska Street 2, Bydgoszcz 85–796, Poland, e-mail: krzyskoper@gmail.com

©Polish Society for Histochemistry and Cytochemistry

randomized trials (AGO-OVAR 3, 5, and 7. However, patient prognosis may be influenced by the structure and function of the tumor stroma [5, 6]. Chen *et al*. showed that stroma-rich ovarian cancer patients had a worse prognosis and higher risk of relapse compared to patients who had tumors with poorly developed stroma [7].

In 1996, Sonoda *et al*. discovered receptor-binding cancer antigen expressed on SiSo cells (RCAS1) as a membrane protein on uterine cervix cancer cells [8, 9]. RCAS1 has strong immunosuppressive activity and is linked with the evasion of immune surveillance by cancer cells. RCAS1 is responsible for the inhibition of both cytotoxic lymphocytes and natural killer (NK) cell activity [10]. Furthermore, RCAS1 may induce Fas-independent apoptosis of both T-cells and NK cells infiltrating the tumor microenvironment [11]. RCAS1 staining was also found on numerous noncancerous cells infiltrating the tumor stroma, such as tumor-associated macrophages (TAMs) and cancer-associated fibroblast (CAFs) [12]. Therefore, RCAS1 expression on cancer stroma cells may be responsible for the immune evasion of cancer cells and the development of a more cancer-permissive microenvironment facilitating tumor growth [12, 13]. By stimulating the expression of vascular endothelial growth factor (VEGF), RCAS1 also indirectly stimulates angiogenesis [14]. RCAS1 expression was also associated with the increased secretion of matrix metalloproteinase 1 (MMP-1) and laminin-5 in cervical cancer [15]. Additionally, in their study, Sonoda *et al*. found that RCAS1 expression was negatively correlated with the number of vimentin-positive stromal cells in EOCs [16, 17]. Taken together, such evidence suggests that RCAS1 may participate in the rebuilding of the tumor stroma.

RCAS1 expression in cancer cells has been shown to be a negative prognostic factor in patients with numerous types of human neoplasms, including gynecological malignancies [9, 18–20]. However, the exact role of RCAS1 in the survival of EOC patients is not fully understood. Furthermore, although RCAS1 expression has been observed in tumor stroma macrophages and fibroblasts, there is sparse data concerning its influence on patient overall survival. Therefore, the main aim of our study was to evaluate the impact of RCAS1 immunoreactivity in both cancer and tumor stroma cells on EOC patient survival. Secondly, our goal was to observe whether RCAS1 immunoreactivity influenced select features of the tumor stroma, such as fibroblast, macrophage, and lymphocyte infiltration or tumor stroma cellularity.

Material and methods

Characteristics of patients. The study group consisted of 67 samples of primary EOCs collected from women treated in the Clinical Department of Gynecological Oncology of the Lukaszczyk Oncological Center, Bydgoszcz, Poland, from 2005 through 2010. The median patient age was 58 years (range 38–86). The median age of pre- and postmenopausal women was 49 years (range 39–56) and 59 years (48–84), respectively. The samples were obtained during primary cytoreductive surgery, and all patients achieved optimal cytoreduction (residual tumors each measuring 1 cm or less in maximum diameter). The study group included 52 high-grade serous adenocarcinomas, 4 clear cell adenocarcinomas, and 11 endometrioid adenocarcinomas. Twelve tumors were graded as G2, and 55 as G3 cancers. EOCs were classified according to the then-current International Federation of Gynecology and Obstetrics (FIGO) system. Patients were subdivided according to the FIGO stage of the disease as follows: 16 stage II patients, and 51 stage III patients. The median follow-up for our patients was 35 months (range 0–160 months). This study received the Jagiellonian University Ethical Committee approval (KBET/89/B/2005 and DK/KB/CM/0031/447/2010) and all patients gave written informed consent).

Immunohistochemistry. Immunohistochemical (IHC) reactions were performed using anti-RCAS1 (human) mAb (dilution 1:1000) purchased from Medical & Biological Laboratories Co., Ltd., Nagoya, Japan, Code No.: D060-3. All IHC studies were performed on 4 μm-thick sections taken from cancerous tumors fixed in 4% buffered-formalin and embedded in paraffin blocks. The specimens for IHC staining were selected according to routine histopathological protocols. Thus, among multiple tumor sections evaluated in hematoxylin and eosin (H&E) staining we selected the most representative specimen with the highest tumor volume and without necrosis. Paraffin sections were placed on Knittel Glass adhesive slides and incubated for 2 h in a chamber thermostat at 60°C. Prior to the automatic performance of the study, tissue sections were subjected to the dewaxing procedure followed by the thermal epitope detection (HIER) in a PT Link device using EnVision™ FLEX Target Retrieval Solution, High pH (50x) (K8002) (Dako, Carpinteria, CA, USA). Finally, the preparations were dehydrated in a series of alcohols and enclosed in a medium (Consul Mount, Thermo Fisher Scientific Inc., Waltham, MA, USA). This method was performed at room temperature (RT). In each instance, a control preparation was added to a series of patient samples. According to the recommendation by the antibody manufacturer breast cancer sections were used as a positive control. The sections were viewed in Nikon

©Polish Society for Histochemistry and Cytochemistry

Eclipse 80i microscope (Nikon Instruments Europe BV, Badhoevedorp, The Netherlands).

Evaluation of RCAS1 immunoreactivity. The RCAS1 immunoreactivity (RCAS1-Ir) in cancer cell cytoplasm and cancer cell membranes was evaluated separately. The evaluation of RCAS1-Ir was based on the Immunoreactive Score (IRS) and included the simultaneous assessment of the number of RCAS1-positive cells and the intensity of the immunoreactivity. Staining intensity was evaluated as negative (0) or positive with a grade of 1+ (pale brown), 2+ (brown), or 3+ (dark brown). The percentage of stained cells was evaluated using the subjective method of the succeeding approximations as previously described [21]. The IRS with the simultaneous assessment of staining intensity and the percentage of positive cells was conducted as follows: If the intensity of RCAS1-Ir in the cancer cell cytoplasm was assessed as 3+ in 70% of cells, while 30% had RCAS1-Ir evaluated as 2+, we calculated the immunoreactivity score (IRS) according to the formula: $[(3 \times 70) + (2 \times 30)]/100 = 2.7$, where one hundred refers to 100 analyzed cells. The combined result of the staining intensity and the percentage of positive cells equaled 2.7 (range 0 to 3.0). The cut-offs to separate "low" and "high" RCAS1-Ir, were determined following Receiver Operating Characteristic (ROC) curve analysis with the endpoint (death) as a classification variable. Therefore, the cut-offs for cancer cell cytoplasm and membranous RCAS1-Ir were 1.125 and 0.5, respectively.

The evaluation of stromal cellularity was done by counting the number of tumor stroma cells in the microscopic High Power Field (HPF). The cellularity was assessed as low (1+), moderate (2+), or high (3+). Similarly, using HPF, we have evaluated the number of fibroblasts, macrophages, and the degree of lymphocyte infiltration. The tumor stroma cells were differentiated solely based on cell morphology. The parameters mentioned above were quantified as follows: absent (lack of examined cells), low number (1+), moderate number (2+), or high number (3+). The RCAS1-Ir in macrophages and fibroblasts was very homogenous; thus we used only staining intensity for the evaluation. Staining intensity was evaluated as negative (0) and positive staining was graded as 1+ (pale brown), 2+ (brown), or 3+ (dark brown). The number of cells (macrophages or fibroblasts) was evaluated separately from the RCAS1-Ir in these cells. Representative images of RCAS1 staining are presented in Figure 1.

Statistical analysis. The nonparametric Mann-Whitney test was used to compare RCAS1-Ir within the subgroups studied. Correlations were calculated using the nonparametric Spearman's rho test. RCAS1-Ir in macrophages and fibroblasts relative to the patient's menopausal status was studied using the Fisher-exact test. Survival analyses were conducted using the Kaplan-Meier survival curves and the differences in patient survival were compared using log-rank test. Multivariate survival analysis was conducted using Cox proportional-hazards regression with the stepwise entering method. Statistical analysis was conducted using MedCalc 11.4.2.0 (MedCalc Software, Seoul, Republic of Korea), and GraphPad InStat 3.06 (GraphPad Software Inc., San Diego, CA, USA).

Results

Immunoreactivity of RCAS1 in cancer cells and tumor stroma

We found significantly higher RCAS1-Ir in the cytoplasm of the EOC cells of premenopausal patients compared to postmenopausal patients ($P = 0.01$); however, there were no differences between pre- and postmenopausal patients with respect to membranous RCAS1-Ir in cancer cells ($P = 0.88$) (Table 1). There were no differences in cytoplasmic RCAS1-Ir in tumor stroma macrophages and fibroblasts corresponding to menopausal status. In the case of macrophages, among the premenopausal women, 8 cases showed absent or low immunoreactivity while 9 showed moderate or high RCAS1-Ir; the results for postmenopausal women were 29 and 24, respectively ($P = 0.78$). In relation to the cytoplasmic RCAS1-Ir in fibroblasts, the results were as follows: 15 (absent or low) and 2 (moderate or high) for premenopausal, and 41 (absent or low) and 12 (moderate or high) for postmenopausal, $P = 0.49$).

The detailed results of RCAS1-Ir according to the cell types studied and the results of tumor stroma analyses are summarized in Table 1.

Immunoreactivity of RCAS1 and patients survival

Patients with high RCAS1-Ir in the cytoplasm of cancer cells had significantly worse median OS compared to patients with low RCAS1-Ir in the cytoplasm of the tumors (OS 31 months, range 0–160 *vs.* 73 months, range 1–160, $P = 0.04$). By contrast, we found no differences in patient survival with respect to high and low membranous RCAS1-Ir in cancer cells within the analyzed tumors. We identified improved survival in patients with a low quantity of fibroblasts within tumor stroma compared to patients with a moderate or high quantity of fibroblasts (median OS 91 months, range 6–160 *vs.* 32 months, range 0–160; $P = 0.03$). Patient survival was unaffected by RCAS1 cytoplasmic immunoreactivity in macrophages, RCAS1 cytoplasmic immunoreactivity in fibroblasts, stromal macrophage quantity, stromal cellularity, or the degree of lymphocytic infiltration. The survival curves are presented in Figure 2. In the multivariate survival analysis including cytoplasmic RCAS1-Ir, the stage of the disease, tumor grade and histopathological type of the tumor, only

©Polish Society for Histochemistry and Cytochemistry

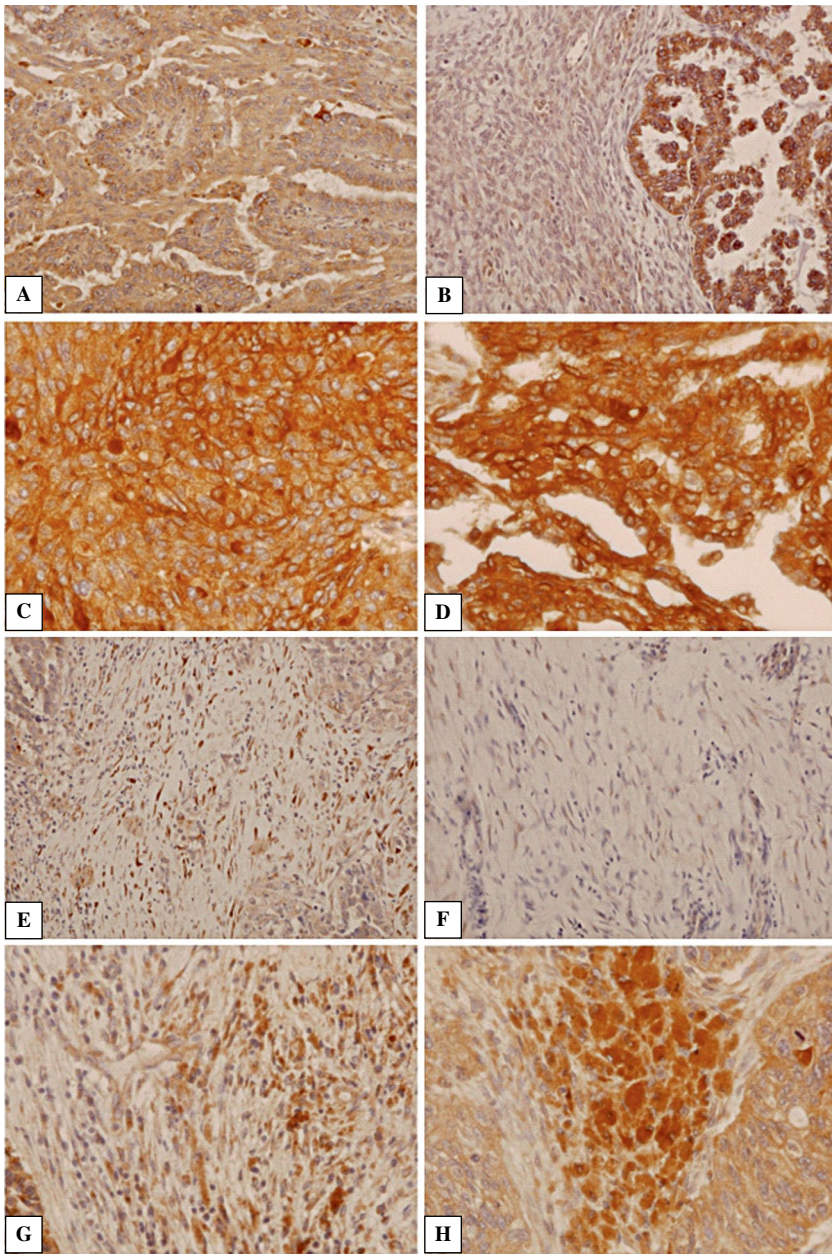

Figure 1. Representative microphotographs of RCAS1 immunoreactivity evaluated as Immunoreactive Score (RCAS1-IRS) in cancer cells and tumor stroma cells in ovarian serous adenocarcinoma. **A.** Homogeneous cytoplasmic RCAS1 immunoreactivity (RCAS1-Ir) in cancer cells assessed as 1+; and no RCAS1-Ir in cancer cell membrane (0+). **B.** Moderate (2+) and homogeneous RCAS1-Ir in cancer cells; no RCAS1-Ir in cancer cell membrane (0+). Tumor stroma contained large number (3+) of cancer-associated fibroblasts (CAFs) and a low number (1+) of tumor-associated macrophages (TAMs). Low (1+) RCAS1-Ir in TAMs. High (3+) RCAS1-Ir in CAFs. **C.** Heterogeneous RCAS1-Ir in both cancer cell cytoplasm and cell membrane. RCAS1-Ir in cancer cell cytoplasm was assessed as high (3+) in 10% of the cancer cells, moderate (2+) in 80% of the cancer cells, and low (1+) in 10% of the cells. Thus, RCAS1-IRS in this case was equal to 2 since $[(3 \times 10) + (2 \times 80) + (1 \times 10)]/100 = 2$. RCAS1-Ir in cancer cell membrane was assessed as high (3+) in 25% of the cancer cells, moderate (2+) in 5% of the cells, low (1+) in 60% of the cells and no reactivity (0) was found in 10% of the cells. Thus, RCAS1-IRS in cancer cell membrane was equal to 1.45 since $(3 \times 25) + (2 \times 5\%) + (1 \times 60) + (0 \times 10)]/100 = 1.45$. **D.** The RCAS1-IRS in cancer cell cytoplasm and cell membrane was 1.8 and 1.45, respectively. **E.** The quantities of both TAMs and CAFs in the tumor stroma were assessed as moderate (2+). Similarly, RCAS1-Ir in TAMs and CAFs was assessed as high (3+). **F.** Tumor stroma presented with a low quantity (1+) of TAMs and a moderate (2+) quantity of CAFs. RCAS1-Ir in TAMs cytoplasm was assessed as low (1+), no RCAS1-Ir (0) in CAFs. **G.** Tumor stroma with a moderate (2+) quantity of TAMs and a low (1+) quantity of CAFs. RCAS1-Ir in TAMs cytoplasm was assessed as high (2+), RCAS1-Ir in CAFs cytoplasm was assessed as low (1+). **H.** Tumor stroma with a high (3+) quantity of TAMs and a moderate quantity of CAFs (2+). RCAS1-Ir in the macrophages was assessed as high (3+), and RCAS1-Ir in CAFs as low (1+). Magnifications: A, B, E, F ×200; C, D, G, H ×400.

©Polish Society for Histochemistry and Cytochemistry

Table 1. RCAS1 immunoreactivity (RCAS1-Ir) and tumor stroma characteristics in ovarian epithelial cancer

	Immunological score (IRS) (Median and range)
Cytoplasmic RCAS1-Ir in cancer cells of premenopausal patients	1.80 (1.025–2.90)
Cytoplasmic RCAS1-Ir in cancer cells of postmenopausal patients	1.60 (0.35–2.70)
Membranous RCAS1-Ir in cancer cells of premenopausal patients	0.00 (0.00–2.00)
Membranous RCAS1-Ir in cancer cells of postmenopausal patients	0.06 (0.00–2.1)
RCAS1-Ir in stromal macrophages	**Number (%)**
Absent	10 (14%)
Low	27 (39%)
Moderate	22 (31%)
High	11 (16%)
RCAS1-Ir in stromal fibroblasts	**Number (%)**
Absent	2 (3%)
Low	54 (77%)
Moderate	11 (16%)
High	3 (4%)
Stromal fibroblast quantity in HPF	**Number (%)**
Absent	0 (0%)
Low	12 (18%)
Moderate	31 (47%)
High	23 (35%)
Stromal macrophage quantity in HPF	**Number (%)**
Absent	10 (14%)
Low	21 (30%)
Moderate	26 (37%)
High	13 (19%)
Lymphocytic infiltration	**Number (%)**
Absent	0 (0%)
Low	20 (29%)
Moderate	13 (19%)
High	36 (52%)
Stroma cellularity	**Number (%)**
Low	1 (1%)
Moderate	46 (66%)
High	23 (33%)

Cytoplasmic RCAS1-Ir and membranous RCAS1-Ir are expressed as Immunoreactivity Score (IRS) that was based on the simultaneous assessment of the number of RCAS1-positive cells and the intensity of the immunoreactivity as described in Methods. Stromal fibroblasts and macrophages quantity refer to the number of fibroblasts and macrophages, respectively, identified in tumor stroma under microscopic High-Power-Fields (HPFs) as described in Methods.

cytoplasmic RCAS1-Ir remained independent predictor of patients' overall survival (P = 0.026).

Immunoreactivity of RCAS1 and tumor stroma characteristics

Cytoplasmic RCAS1-Ir in cancer cells did not correlate with membranous RCAS1-Ir in cancer cells (R = 0.09, P = 0.44). RCAS1-Ir in the cytoplasm of fibroblasts was positively correlated with fibroblast quantity (R = 0.56, P < 0.0001). Similarly, RCAS1--Ir in macrophages was positively correlated with macrophage quantity (R = 0.75, P < 0.0001). Stroma cellularity was positively correlated with fibroblast quantity (R = 0.27, P = 0.02). On the other hand,

©Polish Society for Histochemistry and Cytochemistry

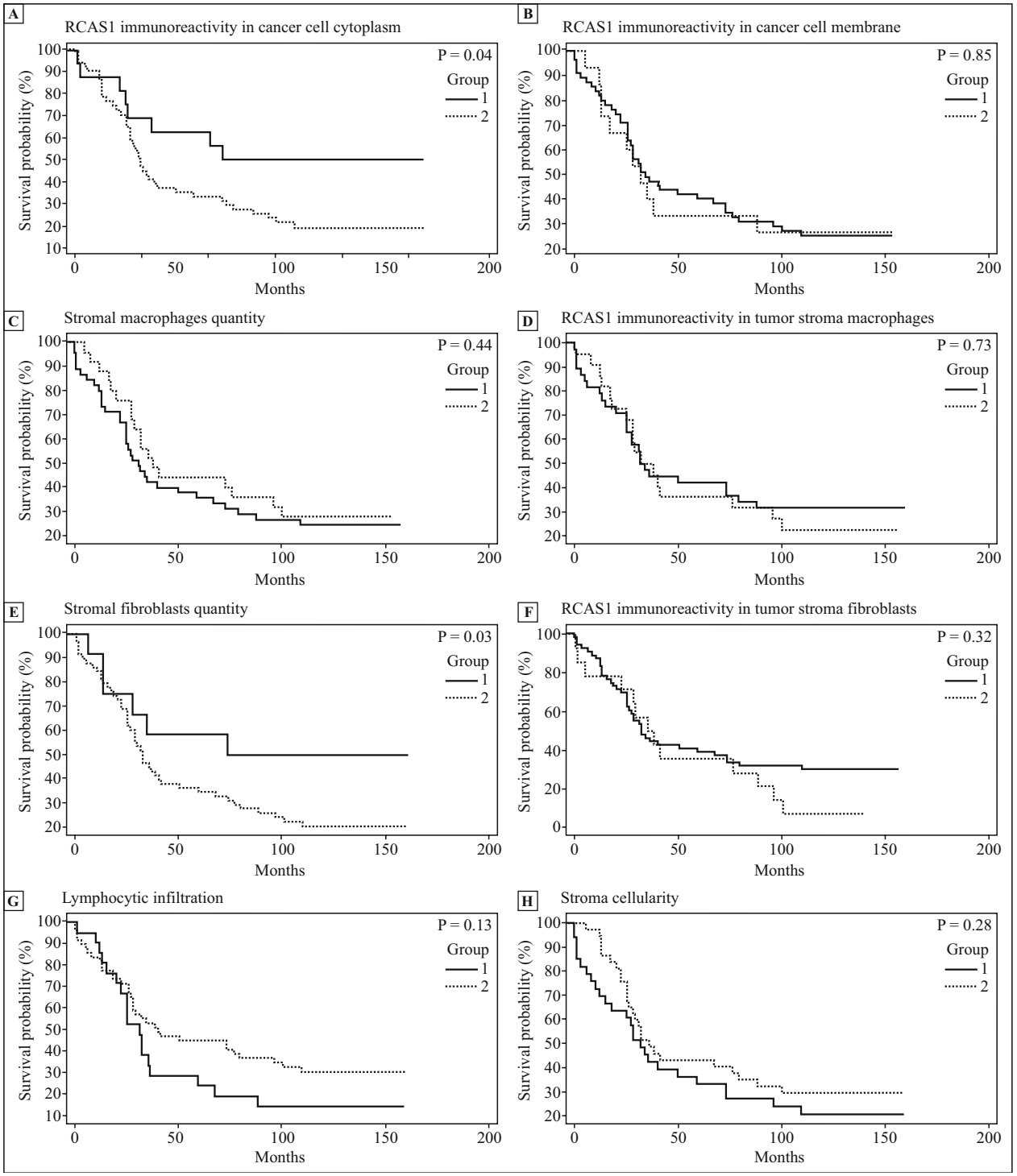

Figure 2. Survival analyses according to RCAS1 immunoreactivity (RACS1-Ir) expressed as Immunoreactive Score (RCAS1-IRS) and analyzed tumor stroma features in ovarian cancer. **A.** Group 1: low RCAS1-Ir (n = 12, median overall survival (mOS) 73 months, range 1–160) *vs.* Group 2: High RCAS1-Ir (n = 55, mOS 31 mo, range 0–160), P = 0.04. **B.** Group 1: Low RCAS1-Ir (n = 22, mOS 38 mo, range 0–160) *vs.* Group 2: High RCAS1-Ir (n = 48, mOS 32 mo, range 0–160), P = 0.85. **C.** Group 1: absent or low RCAS1-Ir (n = 31, mOS 31 mo, range 0–160 *vs.* Group 2: High and moderate RCAS1-Ir (n = 36, mOS 38 mo, range 0–156), P = 0.44. **D.** Group 1: absent or low RCAS1-Ir (n = 35, mOS 34 mo, range 0–160) *vs.* Group 2: High and moderate RCAS1-Ir (n = 32, mOS 38 mo, range 0–160), P = 0.73). **E.** Group 1: low RCAS1-Ir (n = 12, mOS 91 mo, range 6–160) *vs.* Group 2: moderate and high RCAS1-Ir (n = 55, mOS 32 mo, range 0–160), P = 0.03. **F.** Group 1: absent or low RCAS1-Ir (n = 53, mOS 32 mo, range 0–160) *vs.* Group 2: moderate and high RCAS1-Ir (n = 14,mOS 38 mo, range 0–160), P = 0.32). **G.** Group 1: absent or low RCAS1-Ir (n = 20, mOS 31 mo, range 0–160) *vs.* Group 2: moderate and high (n = 47, mOS 40 mo, range 0–160), P = 0.13. **H.** Group 1: low and moderate RCAS1-Ir (n = 44, mOS 32 mo, range 0–160) *vs.* Group 2: high RCAS1-Ir (n = 23, mOS 36 mo, range 5–160), P = 0.28). n, refers to the number of patients.

©Polish Society for Histochemistry and Cytochemistry

there was no correlation between stroma cellularity and macrophage quantity (R = 0.22, P = 0.06) and the degree of lymphocyte infiltration (R = –0.01, P = 0.93).

We found significantly higher RCAS1-Ir in the cytoplasm of cancer cells in EOC patients with a large number of macrophages and fibroblasts within the tumor stroma (Fig. 3). Cytoplasmic RCAS1-Ir in cancer cells did not differ depending on the lymphocyte infiltration rate and stroma cellularity. Similarly, the RCAS1-Ir in cancer cell cytoplasm was not associated with RCAS1 cytoplasmic immunoreactivity in tumor stroma macrophages and fibroblasts (Fig. 3).

Median membranous RCAS1-Ir in cancer cells was significantly higher in tumors with high and moderate RCAS1-Ir in stromal macrophages compared to tumors with absent or low membranous RCAS1-Ir in cancer cells (Fig. 3). A similar observation was noted in the case of RCAS1-Ir in tumor stroma fibroblasts. Membranous RCAS1-Ir in tumor cells was not associated with the quantity of fibroblasts and macrophages within the tumor microenvironment. Moreover, membranous RCAS1-Ir in cancer cells did not differ according to lymphocyte infiltration and tumor stroma cellularity (Fig. 3).

Discussion

In this study, we observed the relationships between the patterns of RCAS1 immunoreactivities and the long-term outcomes of EOC patients. We found that high RCAS1-Ir in cancer cell cytoplasm resulted in more than two-times shortened overall survival of EOC patients. On the other hand, membranous RCAS1-Ir in cancer cells did not influence patient survival. Several papers have revealed cytoplasmic and membranous RCAS1-Ir in cancer cells [22–24] which may contribute to the ability of tumor cells to evade host immune surveillance. In this study, we investigated RCAS1 expression in ovarian cancer and precancerous lesions by immunohistochemical means. We then analyzed the relationship between RCAS1 expression and clinicopathological variables, and examined whether RCAS1 expression is associated with infiltration of tumor-infiltrating lymphocytes (TILs). However, to the best of our knowledge, our observation is the first to separate cytoplasmic and membranous staining showing the different impact of these staining patterns on patient survival. This data suggests that RCAS1 located in the cytoplasm of cancer cells plays a different role than the protein within the membrane or that it may represent a different subpopulation of cancer cells.

Tumor RCAS1 expression has already been studied as a prognostic factor in various neoplasms, including gynecological malignancies [15, 25, 26]. Three separate studies have investigated RCAS1-Ir in patients with EOCs, linking it with the prognosis for ovarian cancer patients [16, 23, 24]. RCAS1 expression is related to the expression of matrix metalloprotease 1 and laminin 5 and angiogenesis. We examined whether RCAS1 contributes to connective tissue remodeling in epithelial ovarian cancer. RCAS1 expression was studied retrospectively *via* immunohistochemistry. Samples were obtained from resected tumor tissues from 65 patients with epithelial ovarian cancer. Statistical analysis was done to correlate RCAS1 expression and clinicopathologic variables. The associations between RCAS1 expression and the number of vimentin-positive cells or microvessel density were evaluated. Western blot analysis was also performed to verify the perturbation of vimentin expression in fibroblast L cells, following stimulation by soluble RCAS1. RCAS1 expression was detected in 72.3% (47/65 total cases). The first report was done by Akahira *et al*. [23]. The authors showed that the RCAS1-Ir is higher in more advanced stages of the disease. However, no significant relationship was detected between RCAS1-Ir and patient OS. Although the authors detected cytoplasmic RCAS1-Ir, they did not distinguish it from membranous immunoreactivity. Additionally, Akahira *et al*. used a different method of assessment than we did; they merely divided the tumors into RCAS1-positive and RCAS1-negative groups according to subjective assessment [23]. We used a broader assessment involving both the evaluation of the percentage of RCAS1-positive cells and the immunoreactivity intensity. Similarly, Ali-Fehmi *et al*. investigated the immunoreactivity of RCAS1 and other antigens in EOC [24]. They previously identified 65 proteins as diagnostically useful TAAs by profiling the humoral immune responses in ovarian cancer (OVCA). The authors did not observe any influence of RCAS1 immunoreactivity on patient survival. Like Akahira *et al*. [23], the authors detected cytoplasmic RCAS1-Ir, but did not distinguish it from the RCAS1-Ir on the cell surface. Furthermore, Ali-Fehmi *et al*. also used a different method of assessment than we did; they regarded tumors as RCAS1-positive when immunoreactivity was found in more than 5% of the tumor cells [24]. In their study, Sonoda *et al*. found no significant relationship between RCAS1-Ir and overall survival; however, the difference was very close to the level of significance (P = 0.06) [16]. Similarly, the method of assessment was different from the one we used; the authors classified tumors with high RCAS1-Ir when more than 25% of cells were RCAS1 positive [16]. Consequently, the discrepancy between our study and the studies

©Polish Society for Histochemistry and Cytochemistry

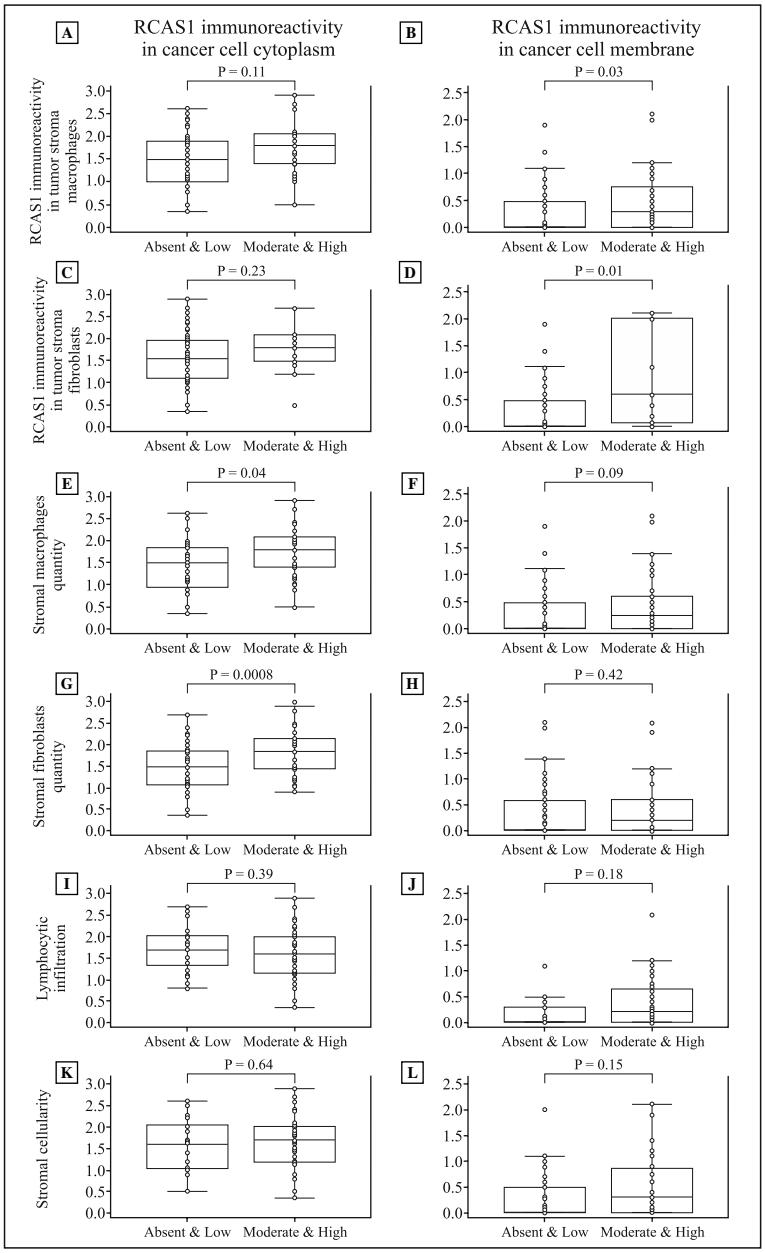

Figure 3. The relationships between Immunoreactivity Score of RCAS1 (RCAS1-IRS) in ovarian cancer cells and the analyzed tumor stroma features. A. For the patients with absent and low immunoreactivity the median RCAS1-IRS was 1.5 (range 0.35–2.6) and for moderate and high immunoreactivity IRS was 1.8 (range 0.5–2.9). **B.** For the patients with absent and low immunoreactivity the median RCAS1-IRS was 0.00 (range 0.00–2.00) and for moderate and high immunoreactivity IRS was 0.30 (0.00–2.10). **C.** For the patients with absent and low immunoreactivity the median RCAS1-IRS was 1.6 (range 0.35–2.9) and for moderate and high immunoreactivity IRS was 1.8 (0.5–2.7). **D.** For the patients with absent and low immunoreactivity the median RCAS1-IRS was 0.00 (range 0.00–1.9) and for moderate and high IRS was 0.6 (0.0–2.1). **E.** For the patients with absent and low quantity of macrophages within tumor stroma the median RCAS1-IRS was 1.5 (range 0.00–2.60) and for moderate and high IRS was 1.8 (0.50–2.90). **F.** For the patients with absent and low quantity of macrophages within tumor stroma the median RCAS1-IRS was 0.00 (range 0.00–2.00) and for moderate and high IRS was 0.25 (0.00–2.10). **G.** For the patients with low quantity of fibroblasts within tumor stroma the median RCAS1-IRS was 1.5 (range 0.35–2.70) and for moderate and high IRS was 1.95 (0.90–2.90). **H.** For the patients with low quantity of fibroblasts within tumor stroma the median RCAS1-IRS was 0.00 (range 0.00–2.10) and for moderate and high IRS was 0.20 (0.00–2.10). **I.** For the patients with absent and low tumor stroma lymphocytic infiltration the median RCAS1-IRS was 1.65 (range 0.50–2.70) and for moderate and high IRS was 1.725 (0.35–2.90). **J.** For the patients with absent and low tumor stroma lymphocytic infiltration the median RCAS1-IRS was 0.00 (range 0.00–2.10) and for moderate and high IRS was 0.23 (0.00–2.10). **K.** For the patients with low and moderate tumor stroma cellularity the median RCAS1-IRS was 1.65 (range 0.50–2.70) and for moderate and high IRS was 1.70 (0.35–2.90). **L.** For the patients with low and moderate tumor stroma cellularity the median RCAS1-IRS was 0.00 (range 0.00–2.10) and for moderate and high IRS was 0.3 (0.00–2.10).

©Polish Society for Histochemistry and Cytochemistry

mentioned above could be explained by the different methods of RCAS1-Ir assessment. We consider our method of assessment to be more accurate because it includes both the number of RCAS1-positive cells and the intensity of immunostaining. Additionally, we have distinguished cytoplasmic from membranous immunoreactivity, even though only cytoplasmic immunoreactivity had an impact on patient survival.

RCAS1 expression was also observed on noncancerous cells infiltrating the tumor microenvironment, such as macrophages and fibroblasts; however, the clinical significance of this observation is still unknown [12, 27, 28]. Due to its selective immunosuppressive activity, RCAS1 expression on tumor stroma cells could potentially be responsible for creating tumor-pervasive stroma which could in turn result in a shortened patient survival period. However, this association has not yet been proven. Jozwicki *et al*. have also showed that higher RCAS1-Ir in tumor stroma macrophages and fibroblasts was present in ovarian neoplasms with lymph node metastases [29]. Galazka *et al*. demonstrated that RCAS1 expression in macrophages and fibroblasts within cervical cancer stroma did not influence the FIGO stage of the disease and lymph node metastases; it also was not related to the grade of the tumor [12]. In our study, we did not find that RCAS1-Ir in macrophages and fibroblasts had an impact on patient survival. However, because of the positive correlation between cancer cell membranous RCAS1-Ir and RCAS1 presence in macrophages and fibroblasts, an interaction based on RCAS1 activity between these cells could exist. Further studies in this field are therefore needed.

We found significantly higher RCAS1 immunoreactivity in the cytoplasm of EOC cells of the patients who were premenopausal compared to those who were postmenopausal. Although the exact mechanism of this association is not fully understood, we speculate that RCAS1 expression may be influenced by hormonal status. RCAS1 is identical with the estrogen-responsive protein EBAG9 (estrogen receptor-binding fragment-associated gene 9), which is an estrogen-responsive gene, and the regulation of transcription is mediated by estrogen receptors [30] (1998. Moreover, in their study, Akahira *et al*. found a highly significant positive correlation between RCAS1-Ir and estrogen receptor alpha expression [23]. Thus, we speculate that RCAS1 expression is related to higher estrogen levels.

Previous data has suggested that RCAS1 can participate in tumor stroma rebuilding through interaction with noncancerous stromal cells (CAFs and TAMs), induction of apoptosis of tumor-infiltrating lymphocytes, and facilitating angiogenesis [12, 13, 26, 31]. We focused on stroma infiltration by macrophages, fibroblasts, and lymphocytes and evaluated tumor stroma cellularity as a whole. We found that RCAS1-Ir in the cytoplasm of cancer cells was positively correlated with the degree of tumor stroma infiltration by both fibroblasts and macrophages, but did not correlate with the RCAS1-Ir in these cells. On the other hand, RCAS1 membranous immunoreactivity in cancer cells positively correlated with RCAS1-Ir in fibroblasts and macrophages, but not with their quantity. Our results suggest that RCAS1 may participate in tumor stroma remodeling through the modification of tumor stroma infiltration by immune cells and fibroblasts. Additionally, this data supports the possibility of a different biological role for cytoplasmic as opposed to membranous RCAS1 localization.

The main weakness of this study was limited study group. However, we included only type-II tumors according to Shih and Kurman model [32]. Furthermore, all of our patients underwent optimal cytoreduction defined as the largest residual tumor nodule measuring 1 cm or less. Thus, in respect of patient prognosis, our study group was highly homogeneous. The homogenous character of our study group is supported by the results of multivariate survival analysis, where known risk factors were not linked with patient prognosis.

In conclusion, our results suggest that the presence of RCAS1 in cytoplasm of epithelial ovarian cancer cells seems to have a different biological function from the RCAS1 present on the membrane, as only cytoplasmic RCAS1-Ir correlated with patient overall survival. Additionally, the exact role of RCAS1-positive fibroblasts and macrophages within EOC stroma needs further elucidation, even though the presence of these cells is not associated with patient survival. Furthermore, we suggest that RCAS1 may participate in the rebuilding of the tumor microenvironment by the influence on tumor stroma infiltration by macrophages and fibroblasts.

Acknowledgments

All laboratory studies were financed by the Department of Tumor Pathology and Pathomorphology, the Ludwik Rydygier Collegium Medicum in Bydgoszcz, Nicolaus Copernicus University in Torun, Poland. We would like to thank Christine Maisto for proofreading the manuscript.

©Polish Society for Histochemistry and Cytochemistry

References

1. Torre LA, Trabert B, DeSantis CE, et al. Ovarian cancer statistics, 2018. CA Cancer J Clin. 2018; 68(4): 284–296, doi: 10.3322/caac.21456, indexed in Pubmed: 29809280.
2. Chang LC, Huang CF, Lai MS, et al. Prognostic factors in epithelial ovarian cancer: A population-based study. PLoS One. 2018; 13(3): e0194993, doi: 10.1371/journal.pone.0194993, indexed in Pubmed: 29579127.
3. Bois Adu, Reuss A, Pujade-Lauraine E, et al. Role of surgical outcome as prognostic factor in advanced epithelial ovarian cancer: A combined exploratory analysis of 3 prospectively randomized phase 3 multicenter trials. Cancer. 2009; 115(6): 1234–1244, doi: 10.1002/cncr.24149.
4. Szymankiewicz M, Dziobek K, Sznajdorwska M, et al. An analysis of the influence of infection on overall survival rates, following modified posterior pelvic exenteration for advanced ovarian cancer. Ginekol Pol. 2018; 89(11): 618–626, doi: 10.5603/GP.a2018.0106, indexed in Pubmed: 30508214.
5. Szubert S, Szpurek D, Moszynski R, et al. Extracellular matrix metalloproteinase inducer (EMMPRIN) expression correlates positively with active angiogenesis and negatively with basic fibroblast growth factor expression in epithelial ovarian cancer. J Cancer Res Clin Oncol. 2014; 140(3): 361–369, doi: 10.1007/s00432-013-1569-z, indexed in Pubmed: 24374756.
6. Czekierdowski A, Stachowicz N, Czekierdowska S, et al. Prognostic significance of TEM7 and nestin expression in women with advanced high grade serous ovarian cancer. Ginekol Pol. 2018; 89(3): 135–141, doi: 10.5603/GP.a2018.0023, indexed in Pubmed: 29664548.
7. Chen Y, Zhang L, Liu W, et al. Prognostic Significance of the Tumor-Stroma Ratio in Epithelial Ovarian Cancer. Biomed Res Int. 2015; 2015: 589301, doi: 10.1155/2015/589301, indexed in Pubmed: 26609529.
8. Sonoda K, Nakashima M, Kaku T, et al. A novel tumor-associated antigen expressed in human uterine and ovarian carcinomas. Cancer. 1996; 77(8): 1501–1509, doi: 10.1002/(SICI)1097-0142(19960415)77:8<1501::AID-CNCR12>3.0.CO;2-3, indexed in Pubmed: 8608535.
9. Sonoda K, Miyamoto S, Hirakawa T, et al. Clinical significance of RCAS1 as a biomarker of uterine cancer. Gynecol Oncol. 2006; 103(3): 924–931, doi: 10.1016/j.ygyno.2006.05.047, indexed in Pubmed: 16842844.
10. Nishinakagawa T, Fujii S, Nozaki T, et al. Analysis of cell cycle arrest and apoptosis induced by RCAS1. Int J Mol Med. 2010; 25(5): 717–722, doi: 10.3892/ijmm_00000396, indexed in Pubmed: 20372814.
11. Sonoda K, Miyamoto S, Nakashima M, et al. The biological role of the unique molecule RCAS1: a bioactive marker that induces connective tissue remodeling and lymphocyte apoptosis. Front Biosci. 2008; 13: 1106–1116, indexed in Pubmed: 17981616.
12. Galazka K, Opławski M, Windorbska W, et al. The immunohistochemical analysis of antigens such as RCAS1 and B7H4 in the cervical cancer nest and within the fibroblasts and macrophages infiltrating the cancer microenvironment. Am J Reprod Immunol. 2012; 68(1): 85–93, doi: 10.1111/j.1600-0897.2012.01134.x, indexed in Pubmed: 22530960.
13. Sonoda K, Miyamoto S, Hirakawa T, et al. Association between RCAS1 expression and microenvironmental immune cell death in uterine cervical cancer. Gynecol Oncol. 2005; 97(3): 772–779, doi: 10.1016/j.ygyno.2005.02.025, indexed in Pubmed: 15943986.
14. Sonoda K, Miyamoto S, Yamazaki A, et al. Biologic significance of receptor-binding cancer antigen expressed on SiSo cells (RCAS1) as a pivotal regulator of tumor growth through angiogenesis in human uterine cancer. Cancer. 2007; 110(9): 1979–1990, doi: 10.1002/cncr.23015, indexed in Pubmed: 17849467.
15. Sonoda K, Miyamoto S, Hirakawa T, et al. Invasive potency related to RCAS1 expression in uterine cervical cancer. Gynecol Oncol. 2005; 99(1): 189–198, doi: 10.1016/j.ygyno.2005.06.061, indexed in Pubmed: 16112176.
16. Sonoda K, Miyamoto S, Kobayashi H, et al. The level of RCAS1 expression is inversely correlated with the number of vimentin-positive stromal cells in epithelial ovarian cancer. Int J Gynecol Cancer. 2009; 19(5): 838–843, doi: 10.1111/IGC.0b013e3181a5ff6a, indexed in Pubmed: 19574770.
17. Szubert S, Koper K, Dutsch-Wicherek MM, et al. High tumor cell vimentin expression indicates prolonged survival in patients with ovarian malignant tumors. Ginekol Pol. 2019; 90(1): 11–19, doi: 10.5603/GP.2019.0003, indexed in Pubmed: 30756366.
18. Sonoda K, Miyamoto S, Hirakawa T, et al. Association between RCAS1 expression and clinical outcome in uterine endometrial cancer. Br J Cancer. 2003; 89(3): 546–551, doi: 10.1038/sj.bjc.6601126, indexed in Pubmed: 12888828.
19. Jóźwicki W, Brożyna AA, Siekiera J, et al. Expression of RCAS1 correlates with urothelial bladder cancer malignancy. Int J Mol Sci. 2015; 16(2): 3783–3803, doi: 10.3390/ijms16023783, indexed in Pubmed: 25674852.
20. Szubert S, Koper K, Dutsch-Wicherek MM, et al. The potential predictive value of serum srCaS1 levels for overall survival in endometrial cancer. Ginekol Pol. 2019; 90(3): 134–140, doi: 10.5603/GP.2019.0024, indexed in Pubmed: 30950002.
21. Jozwicki W, Domaniewski J, Skok Z, et al. Usefulness of histologic homogeneity estimation of muscle-invasive urinary bladder cancer in an individual prognosis: a mapping study. Urology. 2005; 66(5): 1122–1126, doi: 10.1016/j.urology.2005.06.134, indexed in Pubmed: 16286151.
22. Nakamura Y, Yamazaki K, Oizumi S, et al. Expression of RCAS1 in human gastric carcinoma: a potential mechanism of immune escape. Cancer Sci. 2004; 95(3): 260–265, doi: 10.1111/j.1349-7006.2004.tb02213.x, indexed in Pubmed: 15016327.
23. Akahira JI, Aoki M, Suzuki T, et al. Expression of EBAG9/RCAS1 is associated with advanced disease in human epithelial ovarian cancer. Br J Cancer. 2004; 90(11): 2197–2202, doi: 10.1038/sj.bjc.6601832, indexed in Pubmed: 15164121.
24. Ali-Fehmi R, Chatterjee M, Ionan A, et al. Analysis of the expression of human tumor antigens in ovarian cancer tissues. Cancer Biomark. 2010; 6(1): 33–48, doi: 10.3233/CBM-2009-0117, indexed in Pubmed: 20164540.
25. Wicherek L, Jozwicki W, Windorbska W, et al. Analysis of Treg cell population alterations in the peripheral blood of patients treated surgically for ovarian cancer - a preliminary report. Am J Reprod Immunol. 2011; 66(5): 444–450, doi: 10.1111/j.1600-0897.2011.01024.x, indexed in Pubmed: 21624000.
26. Dutsch-Wicherek M, Tomaszewska R, Lazar A, et al. The association between RCAS1 expression in laryngeal and pharyngeal cancer and its healthy stroma with cancer relapse. BMC Cancer. 2009; 9: 35, doi: 10.1186/1471-2407-9-35, indexed in Pubmed: 19175908.
27. Dutsch-Wicherek M, Lazar A, Tomaszewska R. The Involvement of RCAS1 in Creating a Suppressive Tumor Microen-

©Polish Society for Histochemistry and Cytochemistry

vironment in Patients with Salivary Gland Adenocarcinoma. Cancer Microenviron. 2010; 4(1): 13–21, doi: 10.1007/s12307-010-0051-6, indexed in Pubmed: 21505558.
28. Adamek D, Radwańska E, Gajda M. Expression of RCAS1 protein in microglia/macrophages accompanying brain tumours. An immunofluorescence study. Folia Neuropathol. 2009; 47(3): 240–246, indexed in Pubmed: 19813143.
29. Jozwicki W, Windorbska W, Brozyna AA, et al. The analysis of receptor-binding cancer antigen expressed on SiSo cells (RCAS1) immunoreactivity within the microenvironment of the ovarian cancer lesion relative to the applied therapeutic strategy. Cell Tissue Res. 2011; 345(3): 405–414, doi: 10.1007/s00441-011-1216-4, indexed in Pubmed: 21845402.
30. Ikeda K, Sato M, Tsutsumi O, et al. Promoter analysis and chromosomal mapping of human EBAG9 gene. Biochem Biophys Res Commun. 2000; 273(2): 654–660, doi: 10.1006/bbrc.2000.2920, indexed in Pubmed: 10873660.
31. Biedka M, Nowikiewicz T, Dziobek K, et al. The analysis of Treg lymphocytes in the blood of patients with breast cancer during the combined oncological treatment. Breast J. 2019; 26(1).
32. Shih IM, Kurman RJ. Ovarian tumorigenesis: a proposed model based on morphological and molecular genetic analysis. Am J Pathol. 2004; 164(5): 1511–1518, doi: 10.1016/s0002-9440(10)63708-x, indexed in Pubmed: 15111296.

Submitted: 18 March, 2019
Accepted after reviews: 19 July, 2019
Available as AoP: 2 August, 2019

©Polish Society for Histochemistry and Cytochemistry

FOLIA HISTOCHEMICA ET CYTOBIOLOGICA
Vol. 57, No. 3, 2019
pp. 127–138

ORIGINAL PAPER

VIA MEDICA

Stem cells and metformin synergistically promote healing in experimentally induced cutaneous wound injury in diabetic rats

Lamiaa M. Shawky[1], Eman A. El Bana[2], Ahmed A. Morsi[3]

[1]Department of Histology and Cell Biology, Benha Faculty of Medicine, Benha University, Benha, Egypt
[2]Department of Anatomy, Benha Faculty of Medicine, Benha University, Benha, Egypt
[3]Department of Histology and Cell Biology, Faculty of Medicine, Fayoum University, Fayoum, Egypt

Abstract

Introduction. Diabetes mellitus (DM) is a serious, chronic metabolic disorder commonly complicated by diabetic foot ulcers with delayed healing. Metformin was found to have a wound healing effect through several mechanisms. The current study investigated the effect of both bone marrow-derived mesenchymal stem cells (BM-MSCs) and metformin, considered alone or combined, on the healing of an experimentally induced cutaneous wound injury in streptozotocin-induced diabetic rats.

Material and methods. Forty adult male albino rats were used. Diabetes was induced by single intravenous (IV) injection of streptozotocin (STZ). Next, two circular full thickness skin wounds were created on the back of the animals, then randomly assigned into 4 groups, ten rats each. BM-MSCs were isolated from albino rats, 8 weeks of age and labeled by PKH26 before intradermal injection into rats of Group III and IV. Groups I (diabetic positive control), II (metformin-treated, 250 mg/kg/d), III (treated with 2×10^6 BM-MSCs), and IV (wounded rats treated both with metformin and BM-MSCs cells). Healing was assessed 3, 7, 14, and 21 days post wound induction through frequent measuring of wound diameters. Skin biopsies were obtained at the end of the experiment.

Results. Gross evaluation of the physical healing of the wounds was done. Skin biopsies from the wound areas were processed for hematoxylin and eosin (H&E), Masson's trichrome staining and immunohistochemical staining for CD31. The results showed better wound healing in the combined therapy group (IV) as compared to monotherapy groups.

Conclusions. Although both metformin and BM-MSCs were effective in the healing of experimentally induced skin wounds in diabetic rats, the combination of both agents appears to be a better synergistic option for the treatment of diabetic wound injuries. *(Folia Histochemica et Cytobiologica 2019, Vol. 57, No. 3, 127–138)*

Key words: rat; stem cells, BMSCs; STZ diabetes; metformin; skin wound; healing; angiogenesis; CD31

Introduction

Diabetes mellitus (DM) is a serious, chronic endocrine disorder affecting more than 380 million people worldwide by 2013, and is expected to rise to 592 million by 2035 [1]. The growing population of diabetic patients has increased the risk of development of complication such as nephropathy, retinopathy, neuropathy, and macroangiopathy which leads to diabetic foot ulcers with delayed healing and subsequent amputation [2]. Reduced angiogenesis and impaired production of cytokines by local inflammatory cells are crucial factors for delayed healing [3].

The clinical need to develop recent strategies of treatment to improve the healing of diabetic ul-

Correspondence address: Dr. Ahmed Abdel-Rahman Morsi, MD
Department of Histology and Cell Biology,
Faculty of Medicine, Fayoum University,
Fayoum Governorate, Fayoum, Egypt
tel.: 00966597899168
e-mail: ahmed_saqr4@yahoo.com

©Polish Society for Histochemistry and Cytochemistry

cerative wounds becomes mandatory. Metformin, a biguanide, is one of the most commonly prescribed oral anti-hyperglycemic agents for treating type 2 diabetes mellitus [4]. It exerts its therapeutic effects through multiple mechanisms of actions, including inhibition of glucose production in the liver. In addition, metformin is an insulin enhancer and can increase insulin sensitivity [5]. Hence, it might be beneficial for wound healing as tissue resistance to insulin has been found to interfere with the healing of excisional skin wounds by delaying the contraction and re-epithelialization [6].

Bone marrow-derived mesenchymal stem cells (BM-MSCs) are self-renewing and expandable stem cells. BM-MSCs have several applications in regenerative medicine as they have the capacity to differentiate into different types of cells such as adipocytes, osteoblasts, chondrocytes, hepatocytes, and cardiomyocytes [7]; however, their applications, in healing and repair of skin wounds are still under research.

Due to the urgent need to develop new treatment modalities to improve the healing of diabetic ulcerative wounds, the current study was designed, as a novel research issue, to investigate the effect of combined administration of both metformin and BM-MSCs on the healing of an experimentally induced cutaneous wound injury in an animal model of streptozotocin (STZ)-induced diabetes.

Materials and methods

Animals. Forty adult male albino rats, locally bred at the animal house of Kasr El-Aini, Cairo University, Egypt, with an average weight of 200–250 g were used in the present study. The animals were housed at an ambient temperature of 25 ± 1°C, exposed to natural daily light–dark cycles, and had free access to food and water *ad libitum*. All animal handling and procedures were followed and approved by the ethical committee and the guidelines of Kasr El-Aini animal house. All animal experimental procedures were carried out in accordance with the guidelines of National Institutes of Health for the care and use of Laboratory animals [8].

Chemicals. Streptozotocin was obtained from Sigma-Aldrich (St. Louis, MO, USA). Metformin tablets (Glucophage 500 mg tablets) were purchased from Minapharm (Cairo, Egypt), under license of Merck Santé, Semoy, France). Metformin tablets were grinded and suspended in 0.5% carboxymethyl cellulose (CMC) according to previous work [9], and afterwards shaken to obtain a suspension form of 50 mg/ml.

Rat excision wound model. The fur on the back of the anesthetized rats was removed via light application of depilatory cream and cleaned with alcohol swab. According to Dunn et al., 2013 [10], two circular 10 mm (1 cm) diameter full-thickness excision wounds were made on the dorsum of each anesthetized rat (ketamine, 100 mg/kg, intraperitoneal) [9], using sterile punch biopsy forceps. Hemorrhage, if any, was controlled by pressure application of sterile gauze. The wound size was chosen to be about 10 mm to compensate for the possible decrease in the incision diameter caused by wound contraction [11]. After wounding, the exposed raw area was covered by non-adherent gauze for about 24 hours to prevent tissue fluid loss. The rats were kept in an individual cage under specific pathogen free conditions in an animal room.

Streptozotocin-induced diabetes. Diabetes was induced by a single intravenous (IV) injection of sterile STZ in sodium citrate (0.1 mol/L, pH 4.5) to overnight-fasted animals through tail vein. STZ was given immediately once prepared, at a dose of 60 mg/kg body weight as described in previous studies [12]. After 3 days, diabetic states of rats were checked via blood samples withdrawn from the tail veins of these rats to determine fasting blood glucose level using blood glucose tests strips and meter (Accu-Check; Roche Diagnostics, Penzberg, Germany). On day 21 after injection, the animals were fasted for 8 h and blood glucose was measured. Animals with fasting blood glucose level equal to or more than 250 mg/dl were considered as established STZ-induced diabetic rats [12], and were included in the experiment (Table 1).

Wound closure analysis. The wound diameters were measured on postoperative days 3, 7, 14, and 21 (Table 1). Wound closure was assessed as a percent reduction in the wound area. Progressive decrease in the wound area was followed by tracing the wound margin on a transparent paper. After that, the tracing was placed on a graph paper and the number of squares was counted. Wound closure was expressed as percentage reduction of the original wound area and was calculated using the following formula as demonstrated in previous work [13]:

$$\%\ \text{wound closure in day N} = (\text{area on day 0} - \text{area on day N})/\text{area on day 0} \times 100$$

The area on day 0 is defined by the trace obtained immediately after wounding (the original wound area).

Experimental groups. Three weeks after induction of diabetes, the diabetic rats had undergone excisional wounds on their backs as described previously [10] and were randomly assigned into four groups, ten rats each (Table 1).

Group I: diabetic group (positive control). Five rats received 0.5 ml phosphate buffer saline (PBS), injected intradermally at eight different sites in the wound margins and five rats received 0.5% CMC by gastric lavage.

©Polish Society for Histochemistry and Cytochemistry

Table 1. Illustration of the workflow of the current study

Stages	Days	Events
Diabetes induction & monitoring	D 0	STZ injection
	D 3	Checking blood glucose & verification of the diabetic status
	D 21	• Monitoring of the fasting blood glucose • Rats with blood glucose ≥ 250 mg/dl were considered diabetic and were icluded
Wound creation, treatment	D 21 (D 0 post wounding)	• Wound creation on the backs of the animals • Start Metformin treatment for 21 days • Start stem treatment, once intradermal injections in the wound margins • Start combined therapy treatment • Start vehicle treatment (positive control)
Wound Measurement & end	D 24 (D 3 post wounding)	Measurement of the wound area
	D 28 (D 7 post wounding)	Measurement of the wound area
	D 35 (D 14 post wounding)	Measurement of the wound area
	D 42 (D 21 post wounding)	• Measurement of the wound area • Euthanizing of animals • End of the experiment

Group II: metformin-treated group. Ten rats received metformin (250 mg/kg/d) for 21 days after wound creation, by gastric lavage.

Group III: mesenchymal stem cell-treated group. Ten rats received single intradermal injections of MSCs (2×10^6 in 0.5 ml of PBS) at eight different sites in the wound margins [14].

Group IV: combined therapy group. Ten rats received both metformin (250 mg/kg/d by gastric lavage for 21 days) and single intradermal injections of MSCs (2×10^6) as described for Group III.

Isolation and culture of the bone marrow derived MSCs. Rat mesenchymal stem cells were isolated according to the protocol described by Hu *et al.* [15] with minor modifications. After anesthesia of 8 week-aged rats, the femur and tibia were aseptically dissected and cleared of all muscles and connective tissue. Bone marrow was collected by flushing each long bone with complete culture medium constituted of Dulbecco's Modified Eagle's medium (DMEM) 10% fetal calf serum (FCS), 2 mM glutamine and penicillin/streptomycin (50 U/ml and 50 mg/ml, all from Sigma), supplemented with heparin at a final concertation of 5 U/ml. Collected marrow samples were mechanically disrupted by passing them successively through 18-gauge and 20-gauge needles to obtain a single cell suspension. The cells were centrifuged and resuspended with culture medium and incubated at humidified 5% CO_2 and 95% air atmosphere at 37°C. BM-MSCs were first selected by their adherent property preferentially attaching to uncoated polystyrene tissue culture dishes [16]. The non-adherent cells were removed by 2–3 washes with PBS and adherent cells were further cultured in complete medium. For cell passaging, trypsin-EDTA solution (Sigma) was used. The medium was changed after 2 days and twice a week thereafter. When large colonies of primary MSCs developed (80–90% confluence), they were trypsinized (trypsin-EDTA solution) for 5 min at 37°C. The resulting cell suspension was centrifuged at 1,500 rpm for 5 min, resuspended in complete culture medium. Fibroblast-like cells became the predominant cells in culture, characterized by their fusiform shape and plastic adhesiveness. The recovered cells were counted, using hemocytometer and cellular viability was quantified by the trypan blue exclusion test in which the viable cells appeared with clear cytoplasm (not stained) [17]. Up to 3 cell passages were used in this experiment.

Flow cytometry. Extended effort was afforded for immunophenotyping of the separated, purified MSCs using flow cytometry (Accuri, San Jose, CA, USA). The cell suspension was incubated with different fluorescently labeled monoclonal antibodies against rat CD45, CD29, and CD90 molecules [18]. The BM-MSCs were positive for the MSCs markers (CD29 and CD90) and negative for the hematopoietic-lineage marker, CD45.

Histological procedure. On day 21 after wound creation, the rats were euthanized with an overdose of ether. Skin tissue samples were collected including the wounded tissues and the surrounding normal skin. The tissues were immediately fixed in 10% neutral-buffered formalin and processed for paraffin sections. Five micrometer-thick sections were cut and stained with hematoxylin and eosin (H&E) for morphological observations, and Masson's trichrome staining for the evaluation of collagen disposition, as based on previously stated protocols [19]. Immunohistochemical (IHC) reaction was done, according to previously mentioned protocols [20], for the detection of expression of CD31 (PECAM-1) by a specific antibody, mouse monoclonal antibody (Labvi-

©Polish Society for Histochemistry and Cytochemistry

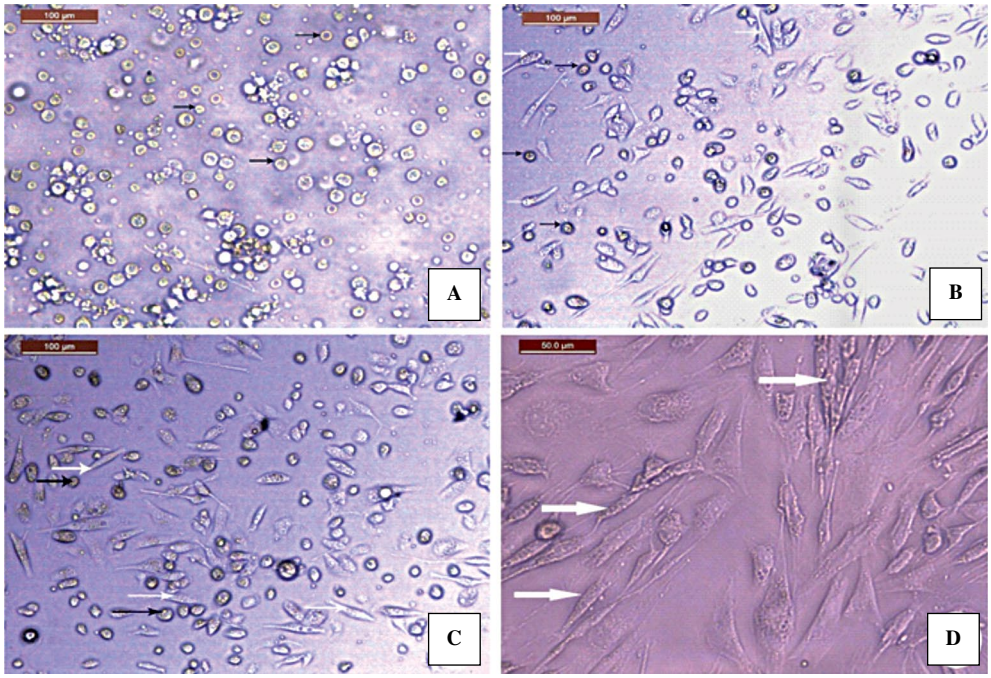

Figure 1. Inverted microscope photomicrographs of primary cultures of bone-marrow-derived mesenchymal stem cells (MSCs) on days 2 (**A** and **B**), 3 (**C**), and 7 (**D**). Panel (**A**) shows rounded nonadherent refractile cells (black arrows). Panel (**B**) shows few spindle-shaped cells (white arrow) between rounded nonadherent refractile cells (black arrow). Panel (**C**) shows many spindle cells (white arrow) between rounded nonadherent refractile cells (black arrow). Panel (**D**) shows many purer spindle shaped cells (white arrow).

sion corporation, Fremont, CA, USA). It was supplied as a prediluted antibody ready for staining formalin-fixed and paraffin-embedded tissues. The sections were incubated with the primary antibody diluted to a concentration of 1:100 in PBS for one hour, followed by a reaction with biotinylated secondary antibody. After conjugation with streptavidin–biotin–peroxidase complex, 3,3-diaminobenzidine (DAB) was used as a chromogen, and hematoxylin solution was used as a counterstain. The reaction gives brownish discoloration in the plasma membrane of capillary endothelial cells in addition to macrophages and fibroblasts [21]. Initially, immunofluorescence detection of PKH26-labeled MSCs was done by fluorescent microscope in unstained paraffin sections for tracking of stem cells.

Morphometric measurements. Quantitative morphometric measurements of the mean area percent of CD31 immunostained skin sections were done using the image analyzer computer system (Leica Qwin 500, Leica, Cambridge, England). The image analyzer was first calibrated automatically to convert the measurement units (pixels) produced by the image analyzer program into actual micrometer units. For each group, ten measuring fields in each specimen were randomly selected, using the high power magnification (×400).

Statistical analysis. All the data obtained were presented as mean ± standard deviation (SD). The normal distribution of the values in the different groups of the study was checked and the evaluation of differences between groups was performed using one-way analysis of variance (ANOVA) and *post hoc* LSD test with SPSS 19.0 software (IBM SPSS Statistics for Windows, Armonk, NY, USA). Results with P-value of less than 0.05 were considered statistically significant.

Results

Characterization of bone marrow-derived MSCs in culture

Using inverted microscope, MSCs were identified in culture as spindle-shaped cells between rounded cells (Fig. 1). On day 2 of primary culture of MSCs presented as rounded nonadherent refractile cells (black arrows) (Fig. 1A, B) and few spindle-shaped cells (white arrows) (Fig. 1B). On day 3 (Fig. 1C) of primary culture many spindle cells (white arrows) were visible between rounded nonadherent refractile cells (black arrows). On day 7 (Fig. 1D), numerous spindle-shaped MSCs (white arrows) were seen.

Evaluation of wound healing

Wound areas of each diabetic rat in the studied groups were measured on day 3, 7, 14 and 21 post wounding (Table 2 and Fig. 2). The area percentage of wound

©Polish Society for Histochemistry and Cytochemistry

Table 2. Changes in the wound areas of the studied groups of diabetic rats at different days post-wounding

Groups of rats	Wound surface area (cm^2) in post excision days			
	3rd day	7th day	14th day	21st day
Control (Gr. I)	0.905 ± 0.01 (9.5%)	0.852 ± 0.12 (14.8%)	0.550 ± 0.01 (45%)	0.305 ± 0.11 (69.5%)
Metformin-treated (Gr. II)	0.848 ± 0.14[c] (15.2%)	0.705 ± 0.15[c] (29.5%)	0.405 ± 0.01[c] (59.5%)	0.260 ± 0.10[c] (74%)
MSC-treated (Gr. III)	0.846 ± 0.11[b] (15.4%)	0.75 ± 0.01[b] (24.7%)	0.347 ± 0.02[b] (65.4%)	0.251 ± 0.2[b] (74.9%)
Metformin- and MSC-treated (Gr. IV)	0.501 ± 0.19[a] (49.9%)	0.402 ± 0.01[a] (59.8%)	0.203 ± 0.01[a] (79.7%)	0.061 ± 0.11[a] (93.9%)

Diabetes was induced by streptozotocin injection of rats as described in Methods. Data express wound area in cm^2 as mean ± SD, n = 10 in each group. The approximate percentages of wound closure are demonstrated in brackets. [a]Significantly different ($P < 0.05$) when compared with metformin- (Group II) or MSC-treated rats (Group III); [b]$P < 0.05$ when compared with non-treated wounded diabetic rats (Group I); [c]$P < 0.05$ when compared with non-treated groups (control). MSCs, bone-marrow-derived mesenchymal stem cells.

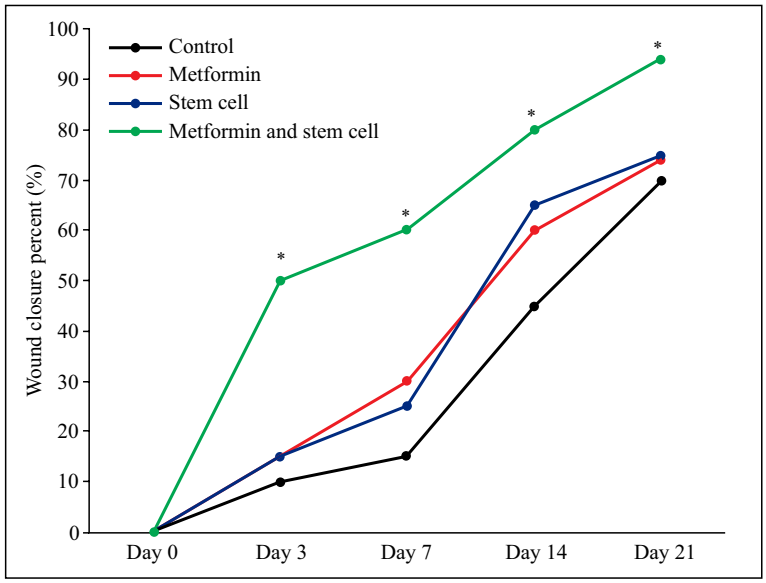

Figure 2. Rough estimation of the wound closure progress expressed as the percentages of reduction in the wound area at different time intervals (days 0, 3, 7, 14, and 21) in diabetic rats (control, metformin-, stem cells- or metformin and stem cell-treated). *Significant difference ($P < 0.05$) when compared at the same time-intervals with metformin- and mesenchymal stem cell-treated groups (Groups II and III, respectively). n =10 in each group.

closure increased significantly in the combined therapy group (MSCs plus metformin) compared to the metformin ($p < 0.05$) and MSCs ($p < 0.05$) groups at 3, 7, 14 days after wounding. On day 21 after surgery, 94% wound closure was reached in the combined therapy group, while non-treated, metformin-treated and stem cell-treated wounds reached 69.4%, 74%, and 75% closure, respectively.

Morphological study of MSCs and wound sections

Using fluorescent microscopy, examination of unstained paraffin sections was carried out to track PKH26-labeled bone marrow-derived MSCs. The PKH26-labeled stem cells emitted red fluorescence (Fig. 3).

Histological examination of H&E-stained skin sections from control diabetic rats (Group I) showed skin defect covered by poorly regenerated interrupted epidermis. The underlying papillary dermis looked loose and irregular (Fig. 4A). In both Group II and III (metformin- and MSC-treated groups, respectively), signs of partial healing were observed, such as formation of large amount of dermal granulation tissue filling the wound defect area, thin regenerated epidermis creeping over the granulation tissue, formation of new blood capillaries (Figs. 4B and

©Polish Society for Histochemistry and Cytochemistry

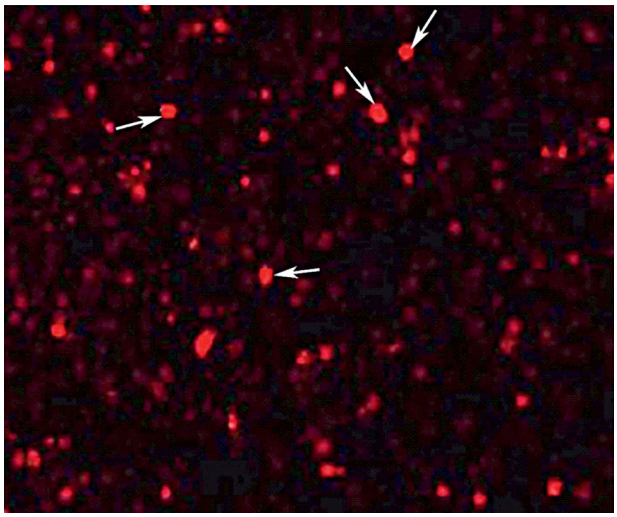

Figure 3. Fluorescence microscopy photomicrograph of a section in the skin wound area of a diabetic rat from Group III (MSC-treated) demonstrating presence of several red fluorescent PKH26-labeled bone marrow-derived mesenchymal stem cells (white arrows). Magnification: × 400.

4C, respectively). In Group IV (combined therapy group), proper healing was observed in the form of the contraction of the wound area, complete re-epithelization of the wound surface, accumulation of huge amount of granulation tissue under the re-epithelized wound surface, differentiation of the epidermal cells, re-organization (remodeling) of the collagen fibers within the granulation tissue, and formation of new more functioning (containing red blood cells) blood capillaries with good regeneration of skin appendages (Figs. 4D, E).

Trichrome stained sections showed marked prominent deposition of collagen fivers in Group IV (stem cells plus metformin-treated animals). The collagen fibers appeared deeply stained, coarse and arranged in a network like different directions (Fig. 5D). However, in Group I (positive control), collagen fibers were lightly stained and scarce (Fig. 5A), and increased gradually in metformin- (Group II) (Fig. 5B) and stem cell-treated (Group III) rats (Fig. 5C).

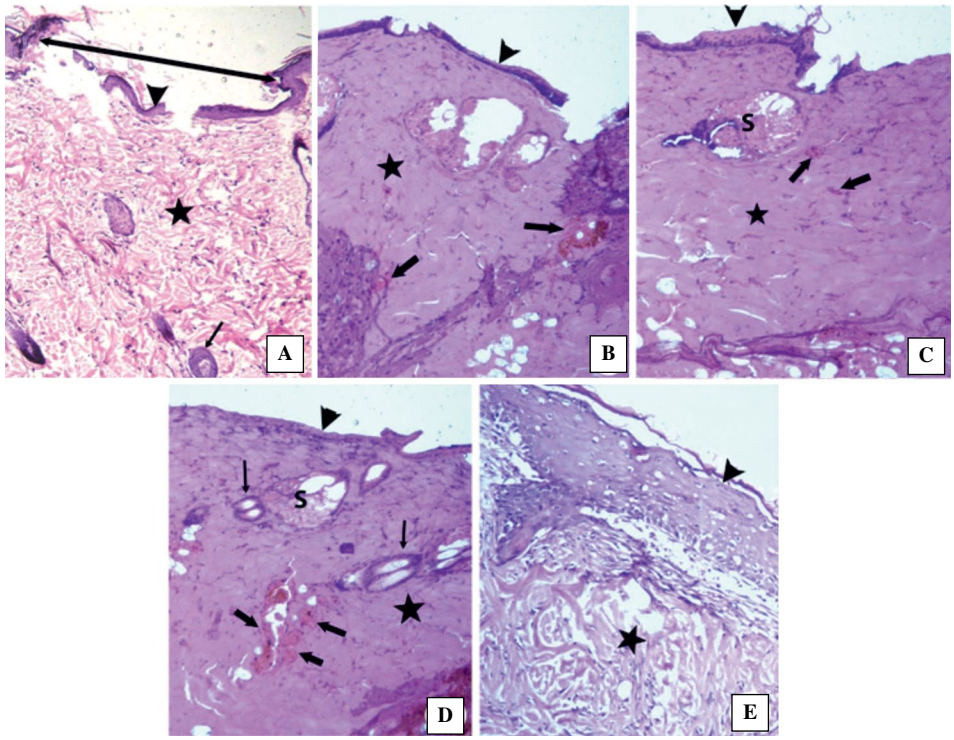

Figure 4. Photomicrographs of hematoxylin and eosin-stained skin sections of diabetic rats from different experimental groups. (**A**). Rat from the control group presents the wound defect area (double headed arrow) with thin poor healing epidermis (arrowhead) and less cell-dense connective tissue underlying dermal granulation tissue (star). (**B**). Skin of metformin-treated rat (Group II) discloses more cellular granulation tissue (star) and congested blood vessels (thick arrows). Regenerating thin epidermis (arrowhead) is seen overlying the granulation tissue. (**C**) Mesenchymal stem cell-treated rat (Group III) shows the dermal granulation tissue (star). Thin regenerated migratory epidermis (arrowhead) is seen extending to cover the granulation tissue. Small sized blood vessels are seen. (**D**) and (**E**). Rat treated with metformin and MSCs (Group IV) shows almost complete re-epithelization of the wound surface (arrowhead), dermal granulation tissue formation (star). Clear differentiation of the epidermal cells and re-organization of the granulation tissue are seen in some sections. Congested blood vessels and formation of new small-sized blood capillaries (thick arrows) are evident. Skin appendages (sebaceous gland (S) and hair follicles (thin arrows)) are well formed. Magnification: A–D ×100, and E ×400.

©Polish Society for Histochemistry and Cytochemistry

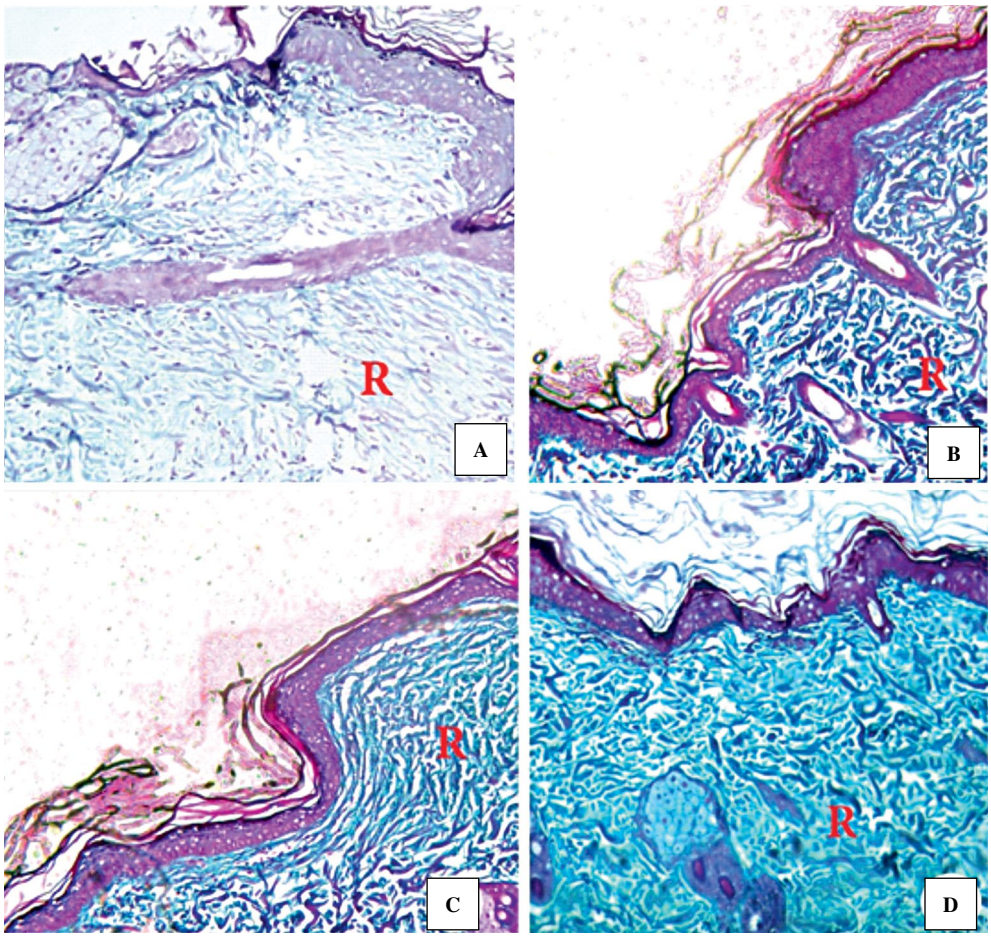

Figure 5. Masson's trichrome stained skin sections of the different groups of diabetic rats. (**A**). Rat from Group I (control) shows lightly stained collagen bundles. (**B**). Rat from Group II (metformin-treated) shows disarranged collagen bundles partially filling the wound defect area. (**C**). Rat from Group III (mesenchymal stem cell-treated) shows the dermal granulation tissue with rich collagen bundles which is disorganized under the wound area. (**D**). Rat from Group IV (combined therapy group) shows marked deposition of darkly stained, heavily distributed, coarse collagen fibers. Magnification: A–D ×100.

Immunohistochemical detection of CD31 localization during skin wound healing

Immunohistochemical staining of skin sections of diabetic rats of Group I (control) revealed moderately-intense expression of CD31 and was limited to the endothelial cells of blood vessels (Fig. 6A). However, in Groups II and III (metformin- and mesenchymal stem cell-treated animals, respectively), diffuse CD31 immunoexpression was noticed in the cells of the reticular layer of dermis such as fibroblasts and macrophages (Fig. 6B, C). In Group IV (metformin- and stem cell-treated rats), the CD31 immunoreaction was diffuse and marked with the existence of large number of CD31 positive cells in dermal connective tissue (Fig. 6D).

Histomorphological evaluation of the area percent of CD31 immunostaining

The data, demonstrated in Figure 7, revealed significant increase ($P < 0.05$) in the mean area percent of the CD31 immunostaining in combined therapy group (Group IV) when compared to either Group II (metformin-treated) or Group III (mesenchymal stem cell-treated). Compared to Group I (control), the CD31 area was significant higher for Groups II–IV ($P < 0.05$), while no difference was observed between Group II and III.

Discussion

Diabetic foot ulcer with impaired wound healing is a common complication of uncontrolled diabetes mellitus. Untreated neglected foot ulcers could be complicated by gangrene and amputation with its bad psychological impact on these patients [22, 23]. Introduction of new treatment modalities is mandatory to improve health status of diabetic patients. Bone marrow-derived stem cells are a promising stem cell source for regenerative medicine and wound repair. They can differentiate into other cell types within the

©Polish Society for Histochemistry and Cytochemistry

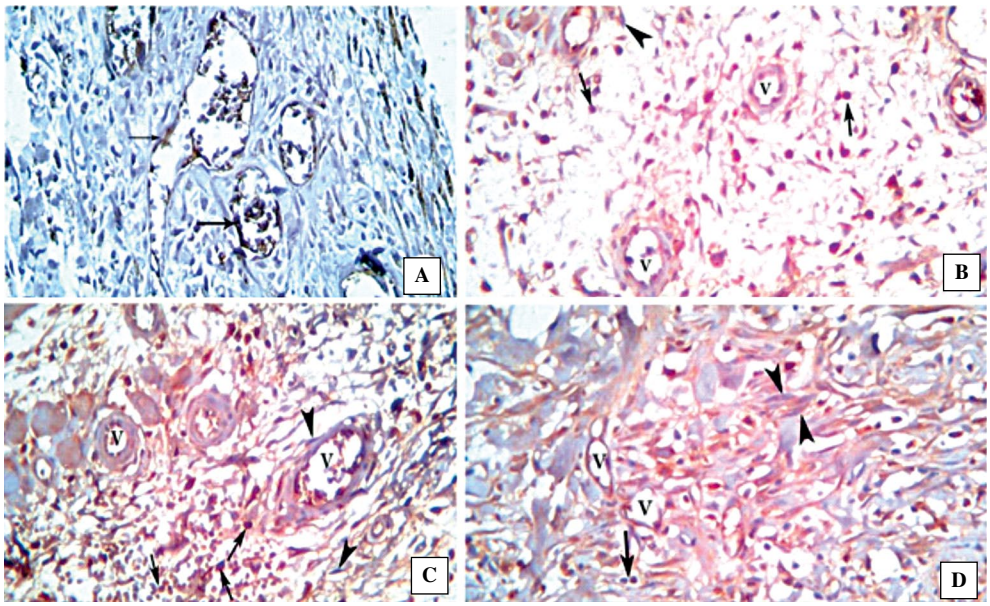

Figure 6. CD31-immunostained skin sections of diabetic rats from the studied experimental groups. (**A**). Rat from Group I (control) reveals scarce CD31 immunoreactivity limited to the endothelial cells of blood vessels (V). (**B**). Rat from Group II (metformin-treated) shows moderate CD31 immunostaining of the endothelial cells as well as dermal connective tissue cells, macrophages (arrows) and fibroblasts (arrowheads). (**C**). Rat form Group III (mesenchymal stem cell-treated) shows moderate CD31 immunostaining of the endothelial cells, fibroblasts (arrowheads) and macrophages (arrows). (**D**). Rat from Group IV (combined therapy group) shows marked CD31 positive immunoreaction including endothelial cells of blood capillaries (V) and dermal connective tissue cells. Magnification: A–D ×400.

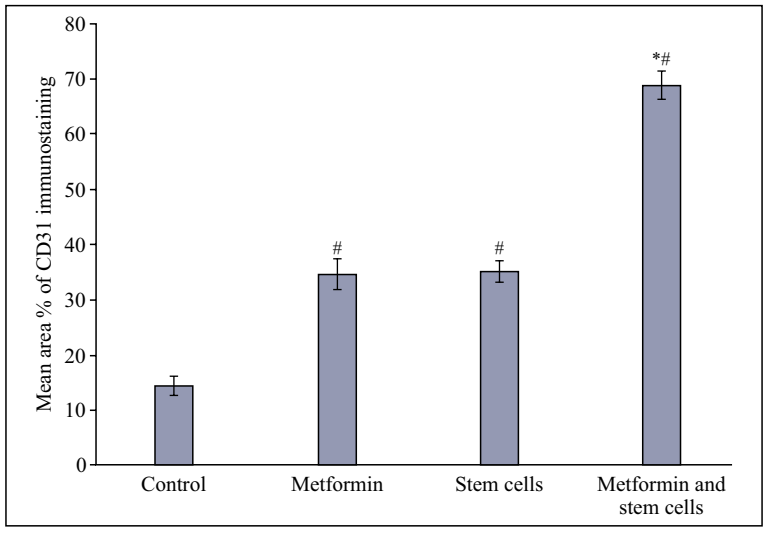

Figure 7. The mean values ± SD of the area percent of CD31 immunoreactivity in the different groups of diabetic rats, the control group, metformin-treated, mesenchymal stem-cell-treated groups, and both metformin- and MSCs-treated-group. n =10. *Significant difference ($P < 0.05$) when compared to metformin- and bone marrow-derived stem cell-treated groups. #significant difference ($P < 0.05$) when compared to the control group.

injured tissue to promote repair and regeneration of the skin [7, 24]. Metformin is a well-known, commonly prescribed oral hypoglycemic drug [4], and was found in healthy animals to have a wound healing effect against cutaneous skin injuries [25]. For this reason, the current study was designed to investigate the effect of metformin and stem cells treatment on skin wound healing in diabetic rats.

©Polish Society for Histochemistry and Cytochemistry

Skin has a remarkable accelerated capacity for spontaneous wound healing. Sex hormones, in particular estrogens, play an important role in the regulation of biological processes involved in tissue regeneration and wound healing [26, 27]. In the current study, the male gender of the experimental animals was preferred to minimize the accelerating effect of endogenous estrogens on wound healing [26]. Experimental diabetes was induced to evaluate the therapeutic effects of new agents in rats in which the cutaneous wound healing was impaired by the underlying disease [28]. In order to mimic the clinical manifestations of human DM, streptozotocin was chosen to induce diabetes in the experimental animals as it selectively destroys the beta cells of the pancreatic islets [12]. Each rat was later exposed to experimental creation of a full thickness excisional wound using a sterile punch biopsy. Given that wound healing was accelerated in partial thickness skin injury, the full thickness excision was preferred as an experimental skin wound model, rather than partial thickness skin injury to abolish the effect of endogenous stem cells located within hair follicles and sebaceous glands [29].

In the present work, there were no great gross or histological differences between the wounded skin of rats injected with PBS or those which received orally streptozotocin solvent (CMC) in the diabetic control group, so that these groups were considered the same.

Regarding the gross evaluation of wound healing and closure of the wound defect area at different time intervals throughout the experiment (days 3, 7, 14, and 21), it was found that approximately complete reduction in the wound defect area was reached in combined therapy group (Group IV) on day 21. There were no significant differences between metformin treatment (Group II) and BM-MSCs transplantation (Group III) in wound closure area. However, the combination of metformin and BM-MSCs showed significantly better curative effect over the single treatment modality. The current result indicated that stem cells, combined with metformin improved wound healing which was in accordance with findings of Seo *et al.* [30] who reported better effects on wound healing when they utilized stem cells, in combination with an another antidiabetic agent, exendin-4.

Histological analysis of the H&E stained skin sections obtained from the diabetic non-treated rats (Group I) revealed poor wound healing, delayed closure of the wound area. Poorly regenerated interrupted epidermis was also noted covering the wound floor. The papillary layer of the dermis showed less dense, deficient underlying dermal granulation tissue, which was evidenced by the lightly stained scarce collagen fibers visualized by trichrome staining. Furthermore, it was correlated with gross wound gapping and poor healing in the same group. Similar to the current findings, other investigators [31] revealed delayed cutaneous wound healing in non-treated diabetic rats. These findings could be supported by the explanation of Serra *et al.* who demonstrated the effect of diabetes on the different phases of wound healing: the inflammatory phase (with compromised immune system reactivity), the proliferative phase (suppressed collagen deposition and formation of new blood vessels) and the remodeling phase in which re-organization of collagen occurs to restore the tissue structural integrity [32].

In the treated diabetic groups of rats we noted that both metformin and stem cells improved healing process in experimentally induced skin wounds. In metformin-treated and stem cell-treated (Group II and Group III, respectively), histological examination revealed similar findings in the form of the accumulation of granulation tissue partially filling the wound defect area with thin regenerated creeping epidermis and formation of new blood vessels. Masson's trichrome stain showed more abundant collagen bundles than in injured control diabetic rats. However, the combination of both stem cells plus metformin (in Group IV) showed nearly complete re-epithelialization of the wound surface in comparison to either agent alone, formation of more cellular granulation tissue and formation of numerous blood capillaries. As well, darkly stained coarse abundant collagen fibers were evident in Masson's trichrome stained skin sections. Collagen is an important extracellular matrix component that provides integrity and structure of skin and other tissues [33]. This notion supported the finding of granulation tissue formation and collagen deposition in H&E and trichrome stainings, respectively. The finding of combined therapy group suggested better curative effect not only through increasing rate of wound healing, but also ensured normalization of the wound through effective re-epithelialization. These findings were in agreement with the results of Elsharawy *et al.*, (2011) [34], who reported better epidermal healing and accelerated revascularization of the wound when they utilized umbilical cord blood-derived CD34+ stem cells injected into the wound bed. Thus, MSCs from various sources can accelerate healing of skin wounds in diabetic rats, which offers a new possibility of diabetic ulcers treatment in humans.

To our best knowledge the application of bone marrow-derived stem cells, in combination with metformin, in the current study, is the first such attempt aimed at the improvement of the health status of diabetic patients through aiding diabetic wound repair and regeneration.

©Polish Society for Histochemistry and Cytochemistry

Different mechanisms were postulated to explain the action by which BM-MSCs transplantation leads to tissue repair. One of these mechanisms was the differentiation of the stem cells into mature endothelial cells leading to angiogenesis, or the paracrine stimulation of neovascularization through the release of angiogenic growth factors and chemical mediators [35]. Differentiation into healing tissue components is also an important mechanism. BM-MSCs can differentiate into fibroblasts and myofibroblasts so that better healing and contraction of the wound defect area can be achieved. Moreover, there was evidence suggesting that BM-MSCs could recruit more fibroblasts and stimulate their migration from the surrounding tissues *via* chemotaxis [36, 37]. Immunohistochemical staining of CD31, in the present work, seems to confirm these mechanisms. In stem cell-treated animals (Group III), significant difference was found when compared to control group (Group I). Furthermore, the CD31 immunoexpression was more intense in the combined therapy group when compared to metformin- or stem cell-treated groups, where the positive reaction was observed in the endothelial cells of the blood capillaries and large number of fibroblasts and macrophages. This observation could support the angiogenic mechanisms and differentiating potential of the applied BM-SCs.

In metformin-treated diabetic rats, significant difference was found when compared to the control group. The wound healing effect of metformin may be related to the formation of new blood capillaries as confirmed by H&E and CD31 immunohistochemistry. This explanation was confirmed by other researchers [9] who suggested that metformin promoted angiogenesis via improving the angiogenic functions of endothelial progenitor cells (EPCs) in diabetic mice. In addition, other authors [38] clarified that the EPCs decreased in number and functions in diabetic patients with subsequent vascular complications and impaired wound healing. Moreover, another mechanism was postulated to explain the wound healing effect of metformin. The insulin tissue resistance had been found to interfere with the healing of excisional skin wounds by delaying wound contraction and surface re-epithelialization, as shown by other investigators [6]. Metformin is a true insulin sensitizer affecting insulin action in peripheral tissues [5], which contributed to the indirect effect of metformin on wound healing.

Interestingly, in an another animal model opposite results were reported [39]. The authors reported reduction in the proliferation of HaCaT keratinocytes in culture media in presence of metformin. This was due to an alteration of the cell cycle without induction of apoptosis, as proven by means of flow cytometry. Furthermore, in a physiological setting, the authors revealed reduced healing process and wound closure progress in metformin-treated ulcers in diabetic patients. They explained their findings by suggestion that metformin interfered with surface re-epithelization of the wound area by reducing cell proliferation of keratinocytes [39]. The discrepancy between our and their results could be attributed to the different experimental design, methods and dosage of metformin.

The angiogenic response is essential for wound healing. Formation of new blood vessels is necessary to sustain the newly formed granulation tissue and the survival of keratinocytes [40]. In agreement with this notion, the congested blood vessels scattered among the granulation tissue, in the current study, particularly in the combined therapy group confirmed the importance of neovascularization in maintaining the vitality of the newly formed granulation tissue.

Finally, the different mechanisms of wound healing encountered in each group of the single treatment modality can be summarized to synergistically promote better wound healing in the group of combined treatment modality.

In summary, the results of the current study indicated a synergistic effect of both combined BM-MSCs and metformin on skin healing in this animal wound model of STZ-induced diabetes. This combination accelerated wound healing and increased wound closure progress by stimulation of surface re-epithelization, differentiation, and promoting angiogenesis. The combined approach could be considered as a novel treatment modality for the management of patients with diabetic foot ulcers to enhance wound healing and to decrease the risk of progression of gangrene.

Acknowledgment

Great consideration and deep gratitude were expressed to all our colleagues in the Histology departments, Faculties of Medicine, Benha and Fayoum Universities, Benha and Fayoum Governorates respectively, Egypt, for their support and valuable information.

Conflict of interest

The authors have no conflicts of interest to declare.

References

1. Guariguata L, Whiting DR, Hambleton I, et al. Global estimates of diabetes prevalence for 2013 and projections for 2035. Diabetes Res Clin Pract. 2014; 103(2): 137–149, doi: 10.1016/j.diabres.2013.11.002, indexed in Pubmed: 24630390.
2. Katsuda Y, Ohta T, Miyajima K, et al. Diabetic complications in obese type 2 diabetic rat models. Exp Anim. 2014; 63(2):

©Polish Society for Histochemistry and Cytochemistry

121–132, doi: 10.1538/expanim.63.121, indexed in Pubmed: 24770637.
3. Anderson K, Hamm RL. Factors That Impair Wound Healing. J Am Coll Clin Wound Spec. 2012; 4(4): 84–91, doi: 10.1016/j.jccw.2014.03.001, indexed in Pubmed: 26199879.
4. Li DJ, Huang F, Lu WJ, et al. Metformin promotes irisin release from murine skeletal muscle independently of AMP-activated protein kinase activation. Acta Physiol (Oxf). 2015; 213(3): 711–721, doi: 10.1111/apha.12421, indexed in Pubmed: 25382002.
5. Rena G, Hardie DG, Pearson ER. The mechanisms of action of metformin. Diabetologia. 2017; 60(9): 1577–1585, doi: 10.1007/s00125-017-4342-z, indexed in Pubmed: 28776086.
6. Otranto M, Nascimento AP, Monte-Alto-Costa A. Insulin resistance impairs cutaneous wound healing in mice. Wound Repair Regen. 2013; 21(3): 464–472, doi: 10.1111/wrr.12042, indexed in Pubmed: 23627416.
7. Rahmati M, Pennisi CP, Mobasheri A, et al. Bioengineered Scaffolds for Stem Cell Applications in Tissue Engineering and Regenerative Medicine. Adv Exp Med Biol. 2018; 1107: 73–89, doi: 10.1007/5584_2018_215, indexed in Pubmed: 29767291.
8. Council NR. Guide for the care and use of laboratory animals. 8th ed. Washington, DC: National Academies Press. ; 2010.
9. Yu JW, Deng YP, Han X, et al. Metformin improves the angiogenic functions of endothelial progenitor cells via activating AMPK/eNOS pathway in diabetic mice. Cardiovasc Diabetol. 2016; 15: 88, doi: 10.1186/s12933-016-0408-3, indexed in Pubmed: 27316923.
10. Dunn L, Prosser HCG, Tan JTM, et al. Murine model of wound healing. J Vis Exp. 2013(75): e50265, doi: 10.3791/50265, indexed in Pubmed: 23748713.
11. Kumar V, Abbas AK, Aster JC. Inflammation and repair. In: Kumar V, Abbas AK, Aster JC, editors. Robbins Basic Pathology. 10th ed. Elsevier Health Sciences; 2017. p. 57.
12. Furman BL. Streptozotocin-Induced Diabetic Models in Mice and Rats. Curr Protoc Pharmacol. 2015; 70: 5.47.1–5.4720, doi: 10.1002/0471141755.ph0547s70, indexed in Pubmed: 26331889.
13. Lee CH, Hsieh MJ, Chang SH, et al. Enhancement of diabetic wound repair using biodegradable nanofibrous metformin-eluting membranes: in vitro and in vivo. ACS Appl Mater Interfaces. 2014; 6(6): 3979–3986, doi: 10.1021/am405329g, indexed in Pubmed: 24568239.
14. Basiouny HS, Salama NM, Maadawi ZM, et al. Effect of bone marrow derived mesenchymal stem cells on healing of induced full-thickness skin wounds in albino rat. Int J Stem Cells. 2013; 6(1): 12–25, indexed in Pubmed: 24298370.
15. Hu Y, Lou B, Wu X, et al. Comparative Study on Culture of Mouse Bone Marrow Mesenchymal Stem Cells. Stem Cells Int. 2018; 2018: 6704583, doi: 10.1155/2018/6704583, indexed in Pubmed: 29760732.
16. Baghaei K, Hashemi SM, Tokhanbigli S, et al. Isolation, differentiation, and characterization of mesenchymal stem cells from human bone marrow. Gastroenterol Hepatol Bed Bench. 2017; 10(3): 208–213, indexed in Pubmed: 29118937.
17. Strober W. Trypan Blue Exclusion Test of Cell Viability. Current Protocols in Immunology. 2015: A3.B.1–A3.B.3, doi: 10.1002/0471142735.ima03bs111.
18. Ghaneialvar H, Soltani L, Rahmani HR, et al. Characterization and Classification of Mesenchymal Stem Cells in Several Species Using Surface Markers for Cell Therapy Purposes. Indian J Clin Biochem. 2018; 33(1): 46–52, doi: 10.1007/s12291-017-0641-x, indexed in Pubmed: 29371769.
19. Bancroft JD, Lyton C. The Hematoxylins and Eosin. In: Suvarna SK, Bancroft JD, Lyton C, editors. Theory and practice of histological techniques. 8th ed, Ed. 2018. p. 126–38.
20. Kiernan JA. Immunohistochemistry. In: Kiernan J, editor. Histological and histochemical methods Theory and practice. 4–th ed. Scion Publishing Ltd; 2015. p. 454–90.
21. Reis RM, Reis-Filho JS, Longatto Filho A, et al. Differential Prox-1 and CD 31 expression in mucousae, cutaneous and soft tissue vascular lesions and tumors. Pathol Res Pract. 2005; 201(12): 771–776, doi: 10.1016/j.prp.2005.08.010, indexed in Pubmed: 16308102.
22. Armstrong DG, Boulton AJM, Bus SA. Diabetic Foot Ulcers and Their Recurrence. N Engl J Med. 2017; 376(24): 2367–2375, doi: 10.1056/NEJMra1615439, indexed in Pubmed: 28614678.
23. Vileikyte L, Crews RT, Reeves ND. Psychological and Biomechanical Aspects of Patient Adaptation to Diabetic Neuropathy and Foot Ulceration. Curr Diab Rep. 2017; 17(11): 109, doi: 10.1007/s11892-017-0945-5, indexed in Pubmed: 28942488.
24. Ojeh N, Pastar I, Tomic-Canic M, et al. Stem Cells in Skin Regeneration, Wound Healing, and Their Clinical Applications. Int J Mol Sci. 2015; 16(10): 25476–25501, doi: 10.3390/ijms161025476, indexed in Pubmed: 26512657.
25. Zhao P, Sui BD, Liu Nu, et al. Anti-aging pharmacology in cutaneous wound healing: effects of metformin, resveratrol, and rapamycin by local application. Aging Cell. 2017; 16(5): 1083–1093, doi: 10.1111/acel.12635, indexed in Pubmed: 28677234.
26. Čriepoková Z, Lenhardt L', Gál P. Basic Roles of Sex Steroid Hormones in Wound Repair with Focus on Estrogens (A Review). Folia Veterinaria. 2016; 60(1): 41–46, doi: 10.1515/fv-2016-0006.
27. Vig K, Chaudhari A, Tripathi S, et al. Advances in Skin Regeneration Using Tissue Engineering. Int J Mol Sci. 2017; 18(4), doi: 10.3390/ijms18040789, indexed in Pubmed: 28387714.
28. Wong SL, Demers M, Martinod K, et al. Diabetes primes neutrophils to undergo NETosis, which impairs wound healing. Nat Med. 2015; 21(7): 815–819, doi: 10.1038/nm.3887, indexed in Pubmed: 26076037.
29. Li Y, Zhang J, Yue J, et al. Epidermal Stem Cells in Skin Wound Healing. Adv Wound Care (New Rochelle). 2017; 6(9): 297–307, doi: 10.1089/wound.2017.0728, indexed in Pubmed: 28894637.
30. Seo E, Lim JS, Jun JB, et al. Exendin-4 in combination with adipose-derived stem cells promotes angiogenesis and improves diabetic wound healing. J Transl Med. 2017; 15(1): 35, doi: 10.1186/s12967-017-1145-4, indexed in Pubmed: 28202074.
31. Kuo YR, Wang CT, Cheng JT, et al. Adipose-Derived Stem Cells Accelerate Diabetic Wound Healing Through the Induction of Autocrine and Paracrine Effects. Cell Transplant. 2016; 25(1): 71–81, doi: 10.3727/096368915X687921, indexed in Pubmed: 25853951.
32. Serra MB, Barroso WA, da Silva NN, et al. From Inflammation to Current and Alternative Therapies Involved in Wound Healing. Int J Inflam. 2017; 2017: 3406215, doi: 10.1155/2017/3406215, indexed in Pubmed: 28811953.
33. Miller EJ. Collagen types: structure, distribution, and functions. In: Collagen. CRC Press; 2018. p. 139–56.
34. Elsharawy MA, Naim M, Greish S. Human CD34+ stem cells promote healing of diabetic foot ulcers in rats. Interact Cardiovasc Thorac Surg. 2012; 14(3): 288–293, doi: 10.1093/icvts/ivr068, indexed in Pubmed: 22159252.

©Polish Society for Histochemistry and Cytochemistry

35. Das SK, Yuan YiF, Li MQ. An Overview on Current Issues and Challenges of Endothelial Progenitor Cell-Based Neovascularization in Patients with Diabetic Foot Ulcer. Cell Reprogram. 2017; 19(2): 75–87, doi: 10.1089/cell.2016.0050, indexed in Pubmed: 28266867.
36. Pacelli S, Basu S, Whitlow J, et al. Strategies to develop endogenous stem cell-recruiting bioactive materials for tissue repair and regeneration. Adv Drug Deliv Rev. 2017; 120: 50–70, doi: 10.1016/j.addr.2017.07.011, indexed in Pubmed: 28734899.
37. Hu MS, Borrelli MR, Lorenz HP, et al. Mesenchymal Stromal Cells and Cutaneous Wound Healing: A Comprehensive Review of the Background, Role, and Therapeutic Potential. Stem Cells Int. 2018; 2018: 6901983, doi: 10.1155/2018/6901983, indexed in Pubmed: 29887893.
38. Hernandez S, Gong J, Chen L, et al. Characterization of Circulating and Endothelial Progenitor Cells in Patients With Extreme-Duration Type 1 Diabetes. Diabetes Care. 2014; 37(8): 2193–2201, doi: 10.2337/dc13-2547.
39. Ochoa-Gonzalez F, Cervantes-Villagrana AR, Fernandez-Ruiz JC, et al. Metformin Induces Cell Cycle Arrest, Reduced Proliferation, Wound Healing Impairment In Vivo and Is Associated to Clinical Outcomes in Diabetic Foot Ulcer Patients. PLoS One. 2016; 11(3): e0150900, doi: 10.1371/journal.pone.0150900, indexed in Pubmed: 26963096.
40. Lian Z, Yin X, Li H, et al. Synergistic effect of bone marrow-derived mesenchymal stem cells and platelet-rich plasma in streptozotocin-induced diabetic rats. Ann Dermatol. 2014; 26(1): 1–10, doi: 10.5021/ad.2014.26.1.1, indexed in Pubmed: 24648680.

Submitted: 28 March, 2019
Accepted after reviews: 26 August, 2019
Available as AoP: 5 September, 2019

©Polish Society for Histochemistry and Cytochemistry

FOLIA HISTOCHEMICA ET CYTOBIOLOGICA
Vol. 57, No. 3, 2019
pp. 139–145

ORIGINAL PAPER

VIA MEDICA

Nucleolin and nucleophosmin expression in seminomas and non-seminomatous testicular tumors

Marek Masiuk[1, 2], Magdalena Lewandowska[1], Leszek Teresinski[2], Ewa Dobak[1], Elzbieta Urasinska[1]

[1]Department of Pathology, Pomeranian Medical University, Szczecin, Poland
[2]Laboratory of Pathology, Multispecialty Hospital, Gorzow Wielkopolski, Poland

Abstract

Introduction. Testicular tumors are heterogeneous group of neoplasms divided mainly into two types: seminomas and non-seminomas. Nucleolin (NCL) and nucleophosmin (NPM) are abundant nucleolar proteins involved in many physiologic and pathologic processes including cancer. Their overexpression was found in many tumors but it was not studied in testicular cancer.

Material and methods. The study was performed on tissue microarrays of 19 seminomas, 21 embryonal carcinomas and 11 yolk sac tumors. The expression of NCL and NPM was detected with monoclonal antibodies and visualized with EnVision FLEX/HRP technique. Immunohistochemical reactions were measured with Aperio ImageScope Software and analyzed as means of percentages of all immunopositive cells in three groups of reaction intensity, *i.e.* 3+, 2+, and 1+ as well as of H-score.

Results. Seminomas showed higher expression of nucleolin indicated by higher H-score and higher percentage of positive cells than non-seminomas. The differences in subpopulations of NCL-positive cells were also found. Embryonal carcinomas and yolk sac tumors showed lower expression of NCL than seminomas indicated by H-score. The percentage of NCL-positive cells did not differ between embryonal carcinomas and seminomas while there were significant differences in subpopulations of cells. The percentage of NCL-positive cells in yolk sac tumors was lower than in seminomas. The results show different heterogeneity of subpopulations of NCL-positive cells in embryonal carcinomas and yolk sac tumors compared to seminomas. The analysis of nucleolin expression in embryonal carcinomas and yolk sac tumors showed no differences between these two tumor types. No differences in nucleophosmin expression between seminomas and non-seminomas were found.

Conclusions. The differences in the expression of nucleolin between two groups of germ cell testicular tumors found in the current study indicate a new aspect of biology of these neoplasms and require further studies on the role of nucleolin in germ cell tumorigenesis. *(Folia Histochemica et Cytobiologica 2019, Vol. 57, No. 3, 139–145)*

Key words: nucleolin; nucleophosmin; germ cell tumor; seminoma; testis; IHC

Introduction

Testicular tumors are the most common cancer in young men between puberty and forties in Europe and they account for 1–3% of all cancers in men. The incidence and death rate in Poland are among the highest in European countries [1]. Germ cell testicular tumors are heterogeneous group of neoplasms and based on their diverse histology and biological behavior they can be divided into seminomas and non-seminomas. Median age of patients with seminoma is 35 years and ones with non-seminomas is 25 years [2]. Compared to non-seminomas, seminomas present relatively uniform histology with large cells containing regular nuclei with one or more nucleoli [3]. Non-seminomas is diverse group of neoplasms that among others include embryonal carcinoma and yolk sac tumors as a pure malignancies or elements of mixed germ cell tumors. Embryonal carcinomas vary in histologic presentation from sheets of primitive-appearing cells to glandular or papillary structures with highly pleomorphic atypical nuclei with many nucleoli

Correspondence address: Marek Masiuk MD, PhD
Department of Pathology, Pomeranian Medical University
Unii Lubelskiej Street 1
71–252 Szczecin, Poland
e-mail: marek.masiuk@gmail.com

©Polish Society for Histochemistry and Cytochemistry

and frequent mitoses. Less common in adult men yolk sac tumors show numerous histologic patterns from solid through microcystic and glandular to classic one with Schiller-Duval bodies [3, 4]. The most common histologic and molecular precursor of seminomas and non-seminomas is germ cell neoplasia *in situ* (GCNIS), which arises from primordial germ cells that failed to differentiate into spermatogonia. One of the first events in neoplastic transformation of germ cells is an expression of Oct4. Different programming of GCNIS results in transformation to seminoma or to embryonal carcinoma that is a neoplastic counterpart of the human embryonal stem cell [5–7]. GCNIS express several stem cell related markers such as Oct4, NANOG, c-KIT, PLAP, TSPY [2, 6, 8]. Seminoma cells have limited capacity to differentiate while embryonal carcinoma cells can differentiate into embryonic somatic lines or extraembryonal and trophoblastic structures [8]. Both embryonal carcinoma cells and seminoma cells express Oct4 and NANOG. Difference between seminomas and non-seminomas include expression of Sox17, high hTERT expression and high telomerase activity in seminomas and Sox2 expression in embryonal carcinomas [2, 9, 10].

Nucleolus seen within the nucleus in standard histologic staining with hematoxylin and eosin is a structure composed of three elements: fibrillar centers (FC), dense fibrillar components (DFC) and granular components (GC) and it is a site of ribosome biogenesis [11]. Nucleolin (NCL), highly conservative protein, is a three-domain structure involved in many processes such as nucleolus formation, transcription of rDNA, maturation of rRNA, ribosomal assembly and nucleocytoplasmic transport, regulation of apoptosis and cell differentiation [11–13]. NCL is involved in wide variety of pathologic processes including cancer (as a promotor or suppressor), inflammation, neurodegeneration [12]. This protein is mainly detected in nucleolus but also in nucleoplasm outside nucleolus [11, 14], cytoplasm and cell membrane [12]. Nucleophosmin (NPM) is another abundant nucleolar protein with possible aberrant cytoplasmic localization. Similarly to NCL it shuttles between nucleolus and nucleoplasm. Both proteins function as chaperones and they interact with numerous protein partners including themselves [15]. NCL and NPM overexpression was found in many tumors [16, 17]; however, their expression in testicular tumors has yet not been analyzed.

Materials and methods

The study was approved by the Bioethical Commission of the Pomeranian Medical University in Szczecin, Poland (approval number KB-0012/267/09/18).

All cases of germ cell testicular tumors diagnosed in Departments of Pathology of the 1st and the 2nd Clinical Hospitals of Pomeranian Medical University, Szczecin, Poland and Multispecialty Hospital, Gorzów Wielkopolski, Poland between May 2004 and April 2018 were re-analyzed by one pathologist (MM) and representative slides and paraffin-embedded tissue blocks were selected for constructing tissue microarrays (TMA). All tissue samples for routine pathologic diagnosis were formalin-fixed and paraffin embedded. Two main tumor types were selected for further studies — pure seminomas and mixed germ cell tumors. Due to high heterogeneity of the latter ones, cases containing only embryonal carcinomas and yolk sac tumor elements were selected for the study. 19 cases of seminomas and 27 cases of mixed germ cell tumors (21 cases of embryonal carcinoma elements and 11 cases of yolk sac tumor elements) were included in the study.

Immunohistochemistry. All immunohistochemical (IHC) studies were performed on tissue microarray (TMA) slides. During histological evaluation areas of interest were encircled on a glass slide and afterwards cores of tissue were taken from representative sites of original paraffin blocks and were inserted into recipient paraffin blocks. To ensure the representativeness of the material 3 cores were taken from each area of interest. Each TMA were cut into 3 μm-thick section, deparrafinized and antigens were retrieved for IHC reactions (PT Link, Dako, Glostrup, Denmark). Endogenous peroxidase was blocked with hydrogen peroxide and slides were incubated with primary antibody. Two mouse anti-human antibodies were used for detecting studied proteins — anti-nucleolin (monoclonal antibody; clone 4E2; Abcam, plc., Cambridge, UK; 1:2000 dilution, 37°C for 90 min) and anti-nucleophosmin (monoclonal antibody; clone FC82291; Abcam, plc.; 1:2500 dilution, 37°C for 90 min). Antigens retrieval procedures were tested and antibodies were titrated for optimal IHC reactions that were visualized with EnVision FLEX/HRP (Dako). Slides were counterstained with hematoxylin, dehydrated and sealed with coverslips. One section of each TMA was also stained with hematoxylin and eosin for microscopic control of cores quality. Slides were immediately scanned with ScanScope slide scanner (Aperio Technologies Inc., Vista, CA, USA) and the analyses of IHC reactions were performed with Aperio ImageScope software (Aperio Technologies Inc.) (Fig. 1). Each evaluated area was selected manually to avoid analysis of necrotic areas or non-neoplastic tissues encountered in cores. Results of the analysis were measured and calculated by the software and were presented in three forms: a) mean percentage of all positive cells, b) percentage of cells with different expression of proteins [+3 (highly positive), +2 (medium positive), +1 (low positive) and 0 (negative)] and c) H-score, which was calculated with following formula: *H-score = (% of +3-positive cells × 3) + (% of +2-positive cells × 2) + (% of +1-positive cells)*.

©Polish Society for Histochemistry and Cytochemistry

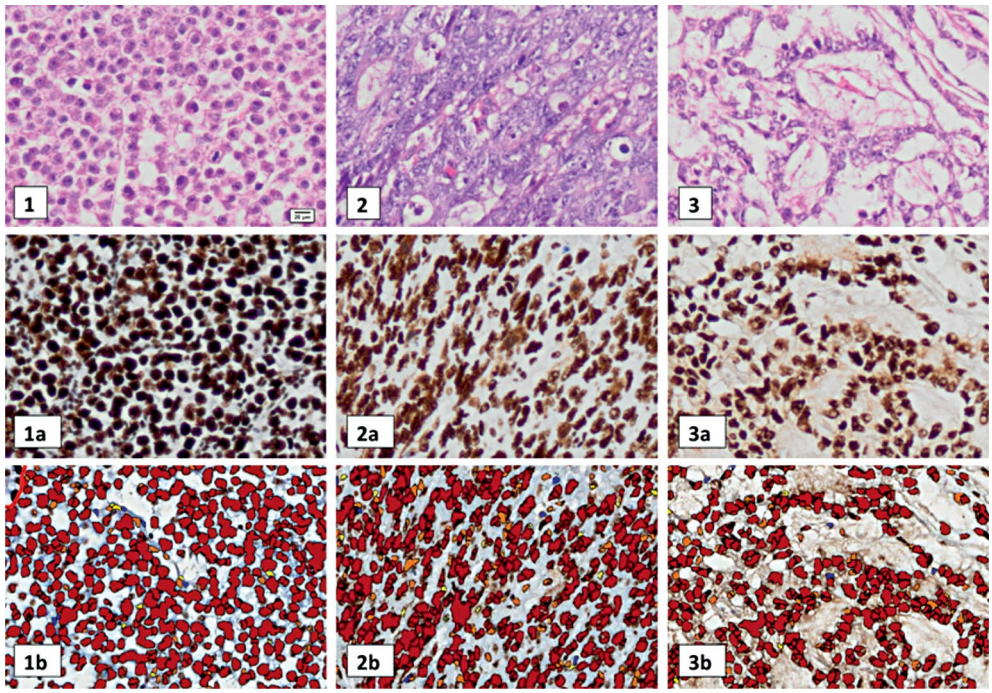

Figure 1. Nucleolin (NCL) expression in seminoma, embryonal carcinoma and yolk sac tumor. **1–3** hematoxylin and eosin staining; **1** — seminoma, **2** — embryonal carcinoma, **3** — yolk sac tumor. Microphotographs **1a–3a** present NCL immunoreactivity, whereas figures **1b–3b** present analyses of the NCL immunoreactivity by Aperio Scan Scope software in respective tumors. Sections were stained by immunohistochemistry as described in Materials and Methods.

Statistical analysis. Data distribution was tested with Shapiro-Wilks test. Some data showed non-Gaussian distribution thus Kruskal-Wallis test was used for finding differences between more than two groups and subsequently U-Mann-Whitney test for differences between two groups. All analyses were performed with STATISTICA for Windows 13.1 (StatSoft, Kraków, Poland).

Results

The mean age of patients with testicular tumors analyzed was 35.5 ± 12.3 years (mean ± SD) while mean tumor size was 35.5 ± 19.1 mm. Detailed data is presented in Table 1.

Patients with seminomas were older than patients with non-seminomas but the difference did not reach statistical significance ($p = 0.07$). When compared between separate groups of non-seminomas, patients with embryonal carcinoma component were significantly younger than patients with seminoma ($p = 0.008$) and patients with yolk sac tumor component ($p = 0.03$). There were no age differences between patients with yolk sac tumor component and patients with seminoma ($p = 0.86$). Tumor size showed no statistically significant differences between any groups studied. Mean number of nuclei measured in each case was 4941 ± 1874 (mean ± SD).

Nucleolin expression and subpopulation of NCL--positive cells in seminomas and non-seminomas

We analyzed the percentage of NCL-positive cells, percentages of subgroups of highly positive (+3), medium positive (+2), low positive (+1) and negative cells (0) as well as H-score in seminomas and non-seminomas. Seminomas showed higher expression of NCL indicated by higher H-score and higher percentage of positive cells than non-seminomas ($p = 0.0009$ and $p = 0.024$, respectively). Interesting results were found in subpopulations of NCL-positive cells. The percentage of +3-positive cells was higher ($p = 0.0004$) while percentages of +2, +1 and negative cells were lower in seminomas than in non-seminomas ($p = 0.001$, $p = 0.002$ and $p = 0.025$, respectively) (Table 2). Differences in percentages of subgroups of NCL-positive cells indicate the heterogeneity of expression of nucleolin between seminomas and non-seminomas.

Nucleolin expression and subpopulation of NCL-positive cells in seminomas vs embryonal carcinoma- and yolk sac tumor-component of non-seminomas

We compared NCL expression between seminomas and two subtypes of non-seminomatous tumors — embryonal carcinomas and yolk sac tumors separately. Both

©Polish Society for Histochemistry and Cytochemistry

Table 1. Patients' age and tumor size

	Seminomas	Non-seminomas	Embryonal carcinomas	Yolk sac tumors
Age (years)	38.6 ± 12.0[a]	32.4 ± 10.4	28.6 ± 7.0	39.3 ± 12.2[b]
Tumor size [mm]	36.7 ± 25.4	34.8 ± 14.3	31.7 ± 11.5	44.0 ± 19.2

The results present mean ± SD. Letters by superscripts indicate significant differences between groups: [a]p = 0.008, seminomas *vs.* embryonal carcinomas; [b]p = 0.03, yolk sac tumors *vs*. embryonal carcinomas.

Table 2. Semiquantitative analysis of the immunohistochemical expression of nucleolin in seminomas and non-seminomas of the testis

Immunoreactivity	Seminomas	Non-seminomas	p
% of positive nuclei	97.71 ± 1.6	95.88 ± 3.80	0.024
% of +3 positive nuclei	81.41 ± 7.67	68.87 ± 12.94	0.0004
% of +2 positive nuclei	13.29 ± 5.10	21.41 ± 8.80	0.001
% of +1 positive nuclei	3.01 ± 1.67	5.56 ± 3.28	0.002
% of negative nuclei	2.27 ± 1.60	4.11 ± 3.81	0.025
H-score	273.81 ± 11.94	255.03 ± 20.74	0.0009

The results present mean ± SD. +3, +2 and +1 denote highly, medium, and low positive immunoreactivity, respectively. H-score was calculated as described in Material and Methods.

Table 3. Semiquantitative analysis of the immunohistochemical expression of nucleolin in seminomas, embryonal carcinomas and yolk sac tumors of the testis

Immunoreactivity	Seminomas	Embryonal Carcinomas	Yolk Sac Tumors
% of positive nuclei	97.71 ± 1.6[a]	95.97 ± 4.45	95.70 ± 2.24
% of +3 positive nuclei	81.41 ± 7.67[b, c]	68.80 ± 11.59	69.00 ± 15.83
% of +2 positive nuclei	13.29 ± 5.10[d]	21.80 ± 7.44	20.72 ± 11.35
% of +1 positive nuclei	3.01 ± 1.67[e, f]	5.34 ± 3.00	5.98 ± 3.87
% of negative nuclei	2.27 ± 1.60[g]	4.02 ± 4.46	4.30 ± 2.23
H-score	273.81 ± 11.94[h, i]	255.35 ± 20.72	254.42 ± 21.79

Table legend as for Table 2. Letters in superscripts indicate significant differences between groups: [a]p = 0.015 seminomas *vs* yolk sac tumors; [b, c]p = 0.0002 and p = 0.049, seminomas *vs.* embryonal carcinomas and seminomas *vs.* yolk sac tumors, respectively; [d]p = 0.0005 seminomas *vs.* embryonal carcinomas; [e, f]p = 0.003 and p = 0.045, seminomas *vs* embryonal carcinomas and seminomas *vs.* yolk sac tumors, respectively; [g]p = 0.01 seminomas *vs* yolk sac tumors; [h, i]p = 0.0016 and p = 0.02, seminomas *vs.* embryonal carcinomas and seminomas *vs.* yolk sac tumors, respectively.

embryonal carcinomas and yolk sac tumors showed lower expression of NCL than seminomas indicated by H-score (p = 0.0016 and p = 0.02, respectively).

The percentage of NCL-positive cells in embryonal carcinomas did not differ from the percentage of NCL-positive in seminomas while there were significant differences in subpopulations of cells. We found lower population of +3-positive cells (p = 0.0002) and higher populations of +2-positive and +1-positive cells in embryonal carcinomas than in seminomas (p = 0.0005 and p = 0.003, respectively) (Table 3).

The percentage of NCL-positive cells in yolk sac tumors was lower than in seminomas (p = 0.015). The differences in subpopulation of cells in yolks sac tumors were slightly different than in embryonal carcinomas. We found lower population of +3-positive cells (p = 0.049) and higher populations of +1-positive cells (p = 0.045) and negative cells (p = 0.01) in yolk sac tumors than in seminomas but we found no differences in +2-positive cell subpopulation (Table 3).

The results show different heterogeneity of subpopulations of NCL-positive cells in embryonal carcinomas and yolk sac tumors compared to seminomas.

The analysis of NCL expression in embryonal carcinomas and yolk sac tumors showed no significant differences between these two tumor types either in H-score value or in percentages of respective groups of NCL-positive and negative cells (Table 3).

©Polish Society for Histochemistry and Cytochemistry

Table 4. Parameters of immunohistochemical expression of NPM in germ cell testicular tumors

Immunoreactivity	Seminomas	Non-seminomas	p
% of positive nuclei	89.89 ± 7.62	83.03 ± 17.29	0.32
% of +3 positive nuclei	42.87 ± 22.00	36.19 ± 23.85	0.35
% of +2 positive nuclei	30.33 ± 7.43	30.15 ± 10.33	0.94
% of +1 positive nuclei	16.19 ± 10.17	16.71 ± 9.42	0.75
% of negative nuclei	10.60 ± 7.23	16.97 ± 17.29	0.45
H-score	205.48 ± 45.82	185.56 ± 63.22	0.35

Table legend as for Table 2.

Nucleophosmin expression and subpopulation of NPM-positive cells in seminomas and non-seminomas

We also analyzed the percentage of NPM-positive cells, percentages of subgroups of highly positive (+3), medium positive (+2), low positive (+1) and negative cells (0) as well as H-score in seminomas and non-seminomas. We found no significant differences in any analyzed parameters for NPM expression between seminomas and non-seminomatous group (Table 4). The expression of NPM did not differ between embryonal carcinomas and yolk sac tumors (data not shown).

Discussion

In the current study, we analyzed nuclear expression of two proteins — nucleolin and nucleophosmin in seminomas and non-seminomas by standard IHC technique performed on tissue microarrays. Only NCL showed differences of expression between these tumor types. Nuclear expression of NCL was significantly higher in seminomas than in embryonal carcinomas and yolk sac tumors, while there were no statistically significant differences between the latter ones. We found no differences in NPM expression between tumor types studied. There were no previous studies on these two proteins in testicular pathology including germ cell tumors.

NCL and NPM are among most abundant nucleolar proteins forming argyrophilic nucleolar organizer regions (AgNOR) that were extensively studied since eighties in different pathologies but only few publications on AgNOR in testicular pathology can be found. Meng *et al.* analyzed area of AgNOR in testicular carcinoma *in situ* (CIS) finding higher level of AgNOR in CIS associated with non-seminomas than with seminomas. They also mentioned that mean area of AgNOR in solid tumor cells did not differ between seminomas and non-seminomas but they pointed to difficulties in objective assessing the parameters studied [18]. Ohyama *et al.* studied forty-five patients with invasive testicular tumors and they found higher number of AgNOR per nucleus in seminomas than in non-seminomas [19]. Results of the study by Ohyama *et al.* are in concordance with the results of our current study. It may be stated that higher AgNOR parameters in seminomas are related to higher NCL expression since it is one of the main AgNOR-related proteins [11, 14].

The expression of NCL in different histologic types of cancer was previously studied in limited series of tumor types. The results of our previous study on a group of 87 ductal and 11 lobular invasive breast cancers showed higher expression of NCL in nucleolus and in karyoplasm in ductal than lobular breast cancers [17]. Xu *et al.* showed higher expression of nucleolin in squamous cell lung cancers than in pulmonary adenocarcinomas but their results were not statistically significant [20].

At the molecular level seminomas differ from non-seminomas by many markers and pathways including proteins, miRNA, mRNA and DNA methylation [21]. Seminomas molecular characteristic mirrors early germ cells while embryonal carcinoma resembles embryonic stem cells [8]. Among markers of pluripotency, Sox2 is the one that is expressed in non-seminomas with no expression in seminomas [9, 10]. Experiments on glioblastoma stem-like cells showed that increased NCL expression downregulated Sox2. NCL decreased stem-like characteristics of Sox2 expression and the inhibitory effect of NCL was due to the transcription inhibition and also was observed on protein level. NCL knockout increased the expression of Sox2. Lower expression of NCL was accompanied by the upregulation of glioblastoma stem cell (GSC) markers including Sox2 [22]. The higher nucleolin expression in Sox2- negative seminomas may suggest similar molecular pathway to the one described in glioblastoma stem-like cells.

Nuclolin is a protein interacting with human telomerase reverse transcriptase (hTERT) and this

©Polish Society for Histochemistry and Cytochemistry

interaction is necessary for nucleolar localization of hTERT and its activity [23]. NCL overexpression causes nucleolar localization of telomerase in cancer cells [24]. Schrader *et al.* found high expression and high activity of hTERT in both seminomas and embryonal carcinomas (with high range of results) but lower in yolk sac tumors; however the differences between all groups studied were not statistically significant [25]. Turnbull *et al.* found some variants of SNPs in *hTERT* gene independently associated with testicular germ cell tumors, one of them showing stronger association with seminomas than with non-seminomas [26]. The differences in NCL expression between seminomas and non-seminomas found in our study may suggest the possible different interactions of nucleolin with hTERT in testicular tumors that might be modified by single nucleotide polymorphism in *hTERT* gene.

We did not find any differences in nucleophosmin expression between seminomas and non-seminomas. Published results on NPM expression in different histologic tumor types including malignant and benign ones are ambiguous. Pianta *et al.* studied 46 thyroid tumors (10 benign and 33 malignant) and they found higher NPM expression in papillary cancers than in follicular or undifferentiated cancers. On the other hand, NPM expression in benign follicular adenomas was higher than in follicular or undifferentiated carcinomas [27]. Sari *et al.* studied NPM expression in 68 renal tumors (9 benign and 59 malignant) and found nuclear NPM expression in chromophobe, papillary and clear cell cancers with no expression in benign oncocytomas and highly aggressive sarcomatoid cancers. They also found higher nucleolar NPM expression in benign oncocytomas and in highly aggressive sarcomatoid renal cell cancers than in clear cell or papillary renal cell cancers [28]. These results may suggest that NPM expression is neither related to benign *vs* malignant tumors nor to low *vs*. high malignant cancers. Relatively high standard deviation of NPM expression found in current study indicates high heterogeneity of NPM expression in all tumor types. Further studies are required for assessing the role of NPM in solid tumor pathology.

In this study, the expression of NCL and NPM in seminomas and non-seminomas as well as different subpopulations of cells expressing both proteins were analyzed for the first time. The differences in subpopulations of cells expressing NCL between seminomas and non-seminomas indicate new aspect of the biology of these tumors. However, our results should be considered as initial observations that require further studies including correlations with clinical data, also prospective ones, for the studied patients (*e.g.* disease-free survival). Moreover, the number of yolk sac tumors cases should be increased for clinical studies. Overall, our results show differences in the expression of selected nucleolar protein in testicular tumors that require further studies.

Acknowledgements

Authors are thankful to Ms. Władysława Surma for technical assistance in scanning slides with ScanScope (Aperio Technologies Inc.).

Conflict of interest

Authors declare no conflict of interest.

References

1. Bray F, Richiardi L, Ekbom A, et al. Trends in testicular cancer incidence and mortality in 22 European countries: continuing increases in incidence and declines in mortality. Int J Cancer. 2006; 118(12): 3099–3111, doi: 10.1002/ijc.21747, indexed in Pubmed: 16395710.
2. Elzinga-Tinke JE, Dohle GR, Looijenga LHj. Etiology and early pathogenesis of malignant testicular germ cell tumors: towards possibilities for preinvasive diagnosis. Asian J Androl. 2015; 17(3): 381–393, doi: 10.4103/1008-682X.148079, indexed in Pubmed: 25791729.
3. Young RH. Testicular tumors--some new and a few perennial problems. Arch Pathol Lab Med. 2008; 132(4): 548–564, doi: 10.1043/1543-2165(2008)132[548:TTNAAF]2.0.CO;2, indexed in Pubmed: 18384207.
4. Ulbright TM. Germ cell tumors of the gonads: a selective review emphasizing problems in differential diagnosis, newly appreciated, and controversial issues. Mod Pathol. 2005; 18 Suppl 2: S61–S79, doi: 10.1038/modpathol.3800310, indexed in Pubmed: 15761467.
5. Looijenga LHJ, Stoop H, de Leeuw HP, et al. POU5F1 (OCT3/4) identifies cells with pluripotent potential in human germ cell tumors. Cancer Res. 2003; 63(9): 2244–2250, indexed in Pubmed: 12727846.
6. Mitchell RT, Camacho-Moll M, Macdonald J, et al. Intratubular germ cell neoplasia of the human testis: heterogeneous protein expression and relation to invasive potential. Mod Pathol. 2014; 27(9): 1255–1266, doi: 10.1038/modpathol.2013.246, indexed in Pubmed: 24457464.
7. Moch H., Humphrey PA, Ulbright TM, Reuter VE (ed.). (2016). WHO Classification of Tumours of the Urinary System and Male Genital Organs. 4th Edition. International Agency for Research on Cancer, Lyon, pp 190-193.
8. Honecker F, Stoop H, Mayer F, et al. Germ cell lineage differentiation in non-seminomatous germ cell tumours. J Pathol. 2006; 208(3): 395–400, doi: 10.1002/path.1872, indexed in Pubmed: 16273510.
9. de Jong J, Stoop H, Gillis AJM, et al. Differential expression of SOX17 and SOX2 in germ cells and stem cells has biological and clinical implications. J Pathol. 2008; 215(1): 21–30, doi: 10.1002/path.2332, indexed in Pubmed: 18348160.
10. Looijenga LHJ. Human testicular (non)seminomatous germ cell tumours: the clinical implications of recent pathobiological insights. J Pathol. 2009; 218(2): 146–162, doi: 10.1002/path.2522, indexed in Pubmed: 19253916.
11. Ma N, Matsunaga S, Takata H, et al. Nucleolin functions in nucleolus formation and chromosome congression. J Cell Sci.

©Polish Society for Histochemistry and Cytochemistry

2007; 120(Pt 12): 2091–2105, doi: 10.1242/jcs.008771, indexed in Pubmed: 17535846.
12. Abdelmohsen K, Gorospe M. RNA-binding protein nucleolin in disease. RNA Biol. 2012; 9(6): 799–808, doi: 10.4161/rna.19718, indexed in Pubmed: 22617883.
13. Tajrishi MM, Tuteja R, Tuteja N. Nucleolin: The most abundant multifunctional phosphoprotein of nucleolus. Commun Integr Biol. 2011; 4(3): 267–275, doi: 10.4161/cib.4.3.14884, indexed in Pubmed: 21980556.
14. Masiuk M, Urasinska E, Domagala W. Simultaneous measurement of nucleolin and estrogen receptor in breast cancer cells by laser scanning cytometry. Anticancer Res. 2004;24:963-966. Indexed in Pubmed. ; 15161050.
15. Šašinková M, Holoubek A, Otevřelová P, et al. AML-associated mutation of nucleophosmin compromises its interaction with nucleolin. Int J Biochem Cell Biol. 2018; 103: 65–73, doi: 10.1016/j.biocel.2018.08.008, indexed in Pubmed: 30130654.
16. Chen S, He H, Wang Y, et al. Poor prognosis of nucleophosmin overexpression in solid tumors: a meta-analysis. BMC Cancer. 2018; 18(1): 838, doi: 10.1186/s12885-018-4718-6, indexed in Pubmed: 30126359.
17. Masiuk M. Expression and intranuclear distribution of nucleolin in estrogen receptor-negative and estrogen receptor-positive breast cancers in women measured by laser scanning cytometry]. Ann Acad Med Stetin. 2006;52:23-32. In Polish. Indexed in Pubmed. ; 17633394.
18. Meng FJ, Giwercman A, Skakkebaek NE. Investigation of carcinoma in situ cells of testis by quantification of argyrophilic nucleolar organizer region associated proteins (AgNORs). J Pathol. 1996; 180(2): 206–213, doi: 10.1002/(SICI)1096-9896(199610)180:2<206::AID-PATH640>3.0.CO;2-Y, indexed in Pubmed: 8976882.
19. Ohyama C, Ito A, Tokuyama S, et al. [Clinical significance of proliferating cell nuclear antigen (PCNA) and argyrophilic nucleolar organizer region (AgNOR) in testicular tumors]. Nihon Hinyokika Gakkai Zasshi. 1995; 86(10): 1543–1551, doi: 10.5980/jpnjurol1989.86.1543, indexed in Pubmed: 7474604.
20. Xu JY, Lu S, Xu XY, et al. Prognostic significance of nuclear or cytoplasmic nucleolin expression in human non-small cell lung cancer and its relationship with DNA-PKcs. Tumour Biol. 2016; 37(8): 10349–10356, doi: 10.1007/s13277-016-4920-6, indexed in Pubmed: 26846099.
21. Shen H, Shih J, Hollern DP, et al. Cancer Genome Atlas Research Network. Integrated Molecular Characterization of Testicular Germ Cell Tumors. Cell Rep. 2018; 23(11): 3392–3406, doi: 10.1016/j.celrep.2018.05.039, indexed in Pubmed: 29898407.
22. Ko CY, Lin CH, Chuang JY, et al. MDM2 Degrades Deacetylated Nucleolin Through Ubiquitination to Promote Glioma Stem-Like Cell Enrichment for Chemotherapeutic Resistance. Mol Neurobiol. 2018; 55(4): 3211–3223, doi: 10.1007/s12035-017-0569-4, indexed in Pubmed: 28478507.
23. Wu YL, Dudognon C, Nguyen E, et al. Immunodetection of human telomerase reverse-transcriptase (hTERT) re-appraised: nucleolin and telomerase cross paths. J Cell Sci. 2006; 119(Pt 13): 2797–2806, doi: 10.1242/jcs.03001, indexed in Pubmed: 16772337.
24. Khurts S, Masutomi K, Delgermaa L, et al. Nucleolin interacts with telomerase. J Biol Chem. 2004; 279(49): 51508–51515, doi: 10.1074/jbc.M407643200, indexed in Pubmed: 15371412.
25. Schrader M, Burger A, Müller M, et al. The differentiation status of primary gonadal germ cell tumors correlates inversely with telomerase activity and the expression level of the gene encoding the catalytic subunit of telomerase. BMC Cancer. 2002; 2(1), doi: 10.1186/1471-2407-2-32.
26. Turnbull C, Rapley EA, Seal S, et al. UK Testicular Cancer Collaboration. Variants near DMRT1, TERT and ATF7IP are associated with testicular germ cell cancer. Nat Genet. 2010; 42(7): 604–607, doi: 10.1038/ng.607, indexed in Pubmed: 20543847.
27. Pianta A, Puppin C, Franzoni A, et al. Nucleophosmin is overexpressed in thyroid tumors. Biochem Biophys Res Commun. 2010; 397(3): 499–504, doi: 10.1016/j.bbrc.2010.05.142, indexed in Pubmed: 20515654.
28. Sari A, Calli A, Altinboga AA, et al. Nucleophosmin expression in renal cell carcinoma and oncocytoma. APMIS. 2012; 120(3): 187–194, doi: 10.1111/j.1600-0463.2011.02835.x, indexed in Pubmed: 22339675.

Submitted: 2 April, 2019
Accepted after reviews: 3 September, 2019
Available as AoP: 12 September, 2019

©Polish Society for Histochemistry and Cytochemistry

FOLIA HISTOCHEMICA ET CYTOBIOLOGICA
Vol. 57, No. 3, 2019
pp. 146–154

ORIGINAL PAPER

VIA MEDICA

Diagnostic immunohistochemistry for canine cutaneous round cell tumours — retrospective analysis of 60 cases

Katarzyna Pazdzior-Czapula, Mateusz Mikiewicz, Michal Gesek, Cezary Zwolinski, Iwona Otrocka-Domagala

Department of Pathological Anatomy, Faculty of Veterinary Medicine, University of Warmia and Mazury in Olsztyn, Olsztyn, Poland

Abstract

Introduction. Canine cutaneous round cell tumours (CCRCTs) include various benign and malignant neoplastic processes. Due to their similar morphology, the diagnosis of CCRCTs based on histopathological examination alone can be challenging, often necessitating ancillary immunohistochemical (IHC) analysis. This study presents a retrospective analysis of CCRCTs.

Materials and methods. This study includes 60 cases of CCRCTs, including 55 solitary and 5 multiple tumours, evaluated immunohistochemically using a basic antibody panel (MHCII, CD18, Iba1, CD3, CD79a, CD20 and mast cell tryptase) and, when appropriate, extended antibody panel (vimentin, desmin, α-SMA, S-100, melan-A and pan-keratin). Additionally, histochemical stainings (May-Grünwald-Giemsa and methyl green pyronine) were performed.

Results. IHC analysis using a basic antibody panel revealed 27 cases of histiocytoma, one case of histiocytic sarcoma, 18 cases of cutaneous lymphoma of either T-cell (CD3+) or B-cell (CD79a+) origin, 5 cases of plasmacytoma, and 4 cases of mast cell tumours. The extended antibody panel revealed 2 cases of alveolar rhabdomyosarcoma, 2 cases of amelanotic melanoma, and one case of glomus tumour.

Conclusions. Both canine cutaneous histiocytoma and cutaneous lymphoma should be considered at the beginning of differential diagnosis for CCRCTs. While most poorly differentiated CCRCTs can be diagnosed immunohistochemically using 1–4 basic antibodies, some require a broad antibody panel, including mesenchymal, epithelial, myogenic, and melanocytic markers. The expression of Iba1 is specific for canine cutaneous histiocytic tumours, and more sensitive than CD18. The utility of CD20 in the diagnosis of CCRCTs is limited. *(Folia Histochemica et Cytobiologica 2019, Vol. 57, No. 3, 146–154)*

Key words: canine cutaneous tumours; IHC diagnosis; histiocytoma; cutaneous lymphoma; plasmacytoma; mast cell tumour; alveolar rhabdomyosarcoma, amelanotic melanoma, glomus tumour

Introduction

Canine cutaneous round cell tumours (CCRCTs) are a heterogeneous group of neoplastic processes of similar morphology, but various histologic origins, with essentially different prognoses as well as treatments. CCRCTs generally include canine cutaneous histiocytoma, cutaneous lymphoma, plasmacytoma, and poorly differentiated mast cell tumours [1, 2], but some authors have also included amelanotic melanoma, neuroendocrine tumour, transmissible venereal tumour, and histiocytic sarcoma in this group [3–5]. Due to the similar morphology of tumour cells, routine histopathological examinations are not sufficient to obtain proper diagnoses in many cases of CCRCTs. Furthermore, veterinary oncologists require more specific diagnoses, which are essential for further therapy [6]. Some studies have shown that the histo-

Correspondence address: Katarzyna Pazdzior-Czapula, PhD, DVM
Department of Pathological Anatomy,
Faculty of Veterinary Medicine,
University of Warmia and Mazury in Olsztyn,
Oczapowskiego Street 13, Olsztyn, Poland
tel. +48 (89) 524 61 44
e-mail: katarzyna.pazdzior@uwm.edu.pl

©Polish Society for Histochemistry and Cytochemistry

pathological diagnosis of a significant percentage of CCRCTs was modified after immunohistochemical (IHC) analysis [1, 7, 8].

The antibody panel for CCRCTs, described by Fernandez *et al.* (2005), includes MHCII, CD18, lymphocytic markers (CD3, CD79a), and mast cell tryptase [1]. While CD3, CD79a, and mast cell tryptase are highly specific for T-cell lymphoma, B-cell lymphoma/ /plasmacytoma, and mast cell tumours, respectively, MHCII and CD18 can be expressed by a wide range of cells [9, 10]. Although the immunoexpression of neither MHCII nor CD18 is specific for Langerhans cells of histiocytoma, the immunoexpression of both markers indicates histiocytoma, but only if tumour is negative for both CD3 and CD79a [1]. Recently, ionized calcium-binding adapter molecule 1 (Iba1), a pan-macrophage marker expressed by all subpopulations of cells of the monocyte/macrophage lineage, was shown to be specific for various cutaneous histiocytic disorders, including canine cutaneous histiocytoma and histiocytic sarcoma [11].

The diagnosis of cutaneous lymphoma is based on the immunoexpression of either CD3 or CD79a. While CD3 is a common marker of all T-cells [12], CD79a is an α-chain of the transmembrane heterodimer CD79, which is expressed exclusively by B-cells. In humans, the expression of CD79a continues throughout the phase of terminal plasma cell differentiation [13]. It was previously shown that 56–80% of canine plasmacytomas express CD79a [14, 15]. CD20, a phosphoprotein expressed from the pre-B cell stage to the activated B-cell stage, is also suitable for canine lymphoma immunophenotyping [16], but is rarely expressed in canine plasmacytomas [15].

Mast cell tryptase belongs to the group of mast cell-specific proteases that are expressed exclusively by mast cells [17] and are widely used as markers of these cells [18, 19]. Tryptase immunostaining shows high sensitivity for the detection of both normal and atypical mast cells, as shown in studies of human mastocytosis and other diseases associated with an increase in mast cells [19]. A previous report revealed that immunoperoxidase staining with monoclonal antibody AA1 (anti-tryptase) is both highly specific and sensitive for the detection of mast cells in routinely processed tissues [18].

The first aim of this study was to evaluate the utility of histochemical and immunohistochemical assessments in the diagnosis of CCRCTs. The second aim of this study was to identify tumours that should be considered at the beginning of differential diagnosis in cases of CCRCTs and tumours that are rare and unexpected but still possible. A properly structured list of conditions to be considered in differential diagnosis will allow the development of a cost-effective stepwise approach for the complementary immunohistochemical analysis of CCRCTs.

Materials and methods

The canine cutaneous tumours analysed in this study were archival diagnostic specimens (2013–2017) from the Department of Pathological Anatomy, Faculty of Veterinary Medicine, University of Warmia and Mazury in Olsztyn, Poland. Cutaneous tumours (solitary n = 55 and multiple n = 5) were collected from 59 dogs by surgical excisional or incisional biopsies. The tissue samples were fixed in 10% buffered formalin, embedded in paraffin, cut into 3-μm sections, and mounted onto silanized glass slides. The sections were processed routinely and stained with Mayer's haematoxylin and eosin (HE). All tumours were diagnosed originally by histopathologic examination, as undifferentiated round cell tumours, without specifying the tumour type. Due to the lack of features indicating the specific tumour type, a more definitive diagnosis was not obtained. Immunohistochemical examination of each tumour was performed manually using a basic antibody panel (MCHII, CD18, Iba1, CD3, CD79a, CD20 and mast cell tryptase) and a visualization system based on the immunoperoxidase method with 3,3-diaminobenzidine (DAB) as a substrate (Table 1). In cases where the final diagnosis could not be determined on the basis of the results of the basic antibody panel, an extended antibody panel was applied (vimentin, desmin, α-SMA, S-100, melan-A and pan-keratin; Table 1). The specimens were counterstained with Mayer's haematoxylin. For the positive control, normal canine tissues (tonsil for MHCII, CD18, Iba1, CD3, CD79a and CD20; colon for vimentin, desmin, α-SMA, and S-100; and skin for mast cell tryptase, melan-A and pan-keratin) were processed together with the evaluated sections. For the negative control, the primary antibody was replaced by the isotype-matched mouse IgG (Dako, Glostrup, Denmark) at the appropriate dilution (for monoclonal primary antibodies) or omitted (for polyclonal primary antibodies). Additionally, selected slides were stained using May-Grünwald-Giemsa (MGG staining kit; Bio-Optica, Milan, Italy), methyl green pyronine (MGP staining kit; Bio-Optica), or periodic acid-Schiff (Sigma-Aldrich, Steinheim, Germany).

The slides were evaluated using an Olympus BX51 light microscope (Olympus, Hamburg, Germany), and the microphotographs were prepared using the U-TVO.5XC-3 camera and cellˆB imaging software (both Olympus).

Results

All evaluated cutaneous tumours comprised a dense infiltration of round to polygonal cells with variable (low to fairly high) anisocytosis, anisokaryosis and chromatin distribution. The mitotic activity of the

©Polish Society for Histochemistry and Cytochemistry

Table 1. Primary antibodies and antigen retrieval and visualization systems

Primary antibody	Clone	Dilution	Antigen retrieval	Visualization system
HLA-DR α chain (MHCII)[a]	Monoclonal mouse anti-human TAL.1B5	1:20	Tris-EDTA buffer pH = 9[b]	EnVision+ System-HRP, Mouse (DAB)[a]
CD18[c]	Monoclonal mouse anti-canine CA16.3C10	1:10	5 min. proteinase K[a]	EnVision+ System-HRP, Mouse (DAB)[a]
Iba1[d]	Polyclonal rabbit	1:500	Tris-EDTA buffer pH = 9[b]	ImmPRESS HRP Universal Antibody (Anti-Mouse/Rabbit IgG)[e]
CD3[a]	Polyclonal rabbit anti-human	1:50	Tris-EDTA buffer pH = 9[b]	ImmPRESS HRP Universal Antibody (Anti-Mouse/Rabbit IgG)[e]
CD79a[f]	Monoclonal mouse anti-human HM57	1:100	Tris-EDTA buffer pH = 9[b]	EnVision+ System-HRP, Mouse (DAB)[a]
CD20[g]	Monoclonal rabbit anti-human SP32	1:100	Tris-EDTA buffer pH = 9[b]	ImmPRESS HRP Universal Antibody (Anti-Mouse/Rabbit IgG)[e]
Mast cell tryptase[a]	Monoclonal mouse anti-human AA1	1:200	Tris-EDTA buffer pH = 9[b]	EnVision+ System-HRP, Mouse (DAB)[a]
Vimentin[a]	Monoclonal mouse anti-bovine VIM 3B4	1:100	Tris-EDTA buffer pH = 9[b]	EnVision+ System-HRP, Mouse (DAB)[a]
Desmin[a]	Monoclonal mouse anti-human D33	1:50	Tris-EDTA buffer pH = 9[b]	EnVision+ System-HRP, Mouse (DAB)[a]
α-SMA[a]	Monoclonal mouse anti-human 1A4	1:50	Tris-EDTA buffer pH = 9[b]	EnVision+ System-HRP, Mouse (DAB)[a]
S-100[a]	Polyclonal rabbit anti-bovine	1:50	Citrate buffer pH = 6[b]	ImmPRESS HRP Universal Antibody (Anti-Mouse/Rabbit IgG)[e]
Melan-A[f]	Mouse anti-human A103	1:50	Tris-EDTA buffer pH = 9[b]	EnVision+ System-HRP, Mouse (DAB)[a]
Pan keratin[h]	Monoclonal mouse anti-human AE1/AE3/PCK26	ready to use	Tris-EDTA buffer pH = 9[b]	EnVision+ System-HRP, Mouse (DAB)[a]

[a]Dako, Glostrup, Denmark; [b]Antigen retrieval was heat-induced, conducted in a microwave oven at 650 W. Samples were microwaved twice to the boiling point, and incubated in a hot buffer for 20 min after boiling each time; [c]PF. Moore, Davis, CA, USA; [d]Wako Pure Chemical Industries, Ltd., Osaka, Japan; [e]Vector Laboratories Inc., Burlingame, CA, USA; [f]Bio-Rad Laboratories Inc., Hercules, CA, USA; [g]Abcam, Cambridge, UK; [h]Ventana, Tucson, AZ; USA.

tumour cells also varied from low to high. The majority of the evaluated tumours (55/60, 91.7%) were differentiated using the basic antibody panel. The detailed basic results of IHC analyses are presented in Table 2.

Canine cutaneous histiocytoma was diagnosed in 27/60 tumours (45%), collected from dogs aged 8 months to 12 years (mean age: 6.4). The tumours were solitary except for one case (a 1.5-year old dog presented with multiple tumours localized within the pinna). The tumour cells expressed MHCII, Iba1, and — in 23 cases — CD18, but were negative for CD3, CD79a, CD20 and mast cell tryptase (Fig. 1A). The tumour cells showed moderate epitheliotropism, which was difficult to observe in massively ulcerated tumours. In one dog, the cutaneous tumour of the paw pad showed a morphology similar to that of the simultaneously excised testicular tumour, which was diagnosed morphologically as seminoma, and therefore cutaneous metastasis of seminoma was suspected. Tumour cells massively infiltrated skin and subcutis, without any epitheliotropism. However, the IHC assessment revealed, that the neoplastic cells of the cutaneous tumour showed the membranous expression of MHCII and Iba1 (while the testicular tumour was negative to Iba1, but approximately 10% of tumour cells expressed MHCII), and were negative to CD18, CD3, CD79a, CD20 and mast cell tryptase. On the basis of these findings, histiocytic sarcoma was diagnosed (Fig. 1B).

Cutaneous lymphomas of either T-cell or B-cell origin were diagnosed in 18/60 cases (30%). These tumours were collected from dogs aged 1.5–13 years (mean age: 8.8 years). In 14 cases, cutaneous lymphoma was solitary, while in 4 — multiple (epitheliotropic T-cell lymphoma). In epitheliotropic cutaneous lymphomas (10/60 cases, 16.7%), the tumour cells showed prominent epitheliotropism. The tumour cells expressed either CD3 (9/60 cases, 15%, Fig. 1C) or CD79a (one case). In nonepitheliotropic cutaneous

©Polish Society for Histochemistry and Cytochemistry

Table 2. Basic antibody panel results in the evaluated canine cutaneous round cell tumours

No	MHCII	CD18	Iba1	CD3	CD79a	CD20	Tryptase	Diagnosis
1	+	+	+	–	–	–	–	Histiocytoma
2	+	+	+	–	–	–	–	Histiocytoma
3	+	+	+	–	–	–	–	Histiocytoma
4	+	+	+	–	–	–	–	Histiocytoma
5	+	+	ND	–	–	ND	–	Histiocytoma
6	+	+	ND	–	–	ND	–	Histiocytoma
7	+	+	+	–	–	–	–	Histiocytoma
8	+	+	+	–	–	–	–	Histiocytoma
9	+	+	+	–	–	–	–	Histiocytoma
10	+	+	+	–	–	–	–	Histiocytoma
11	+	+	+	–	–	–	–	Histiocytoma
12	+	+	+	–	–	–	–	Histiocytoma
13	+	+	ND	–	–	ND	–	Histiocytoma
14	+	+	+	–	–	–	–	Histiocytoma
15	+	+	+	–	–	–	–	Histiocytoma
16	+	+	+	–	–	–	–	Histiocytoma
17	+	+	ND	–	–	ND	–	Histiocytoma
18	+	+	+	–	–	–	–	Histiocytoma
19	+	+	+	–	–	–	–	Histiocytoma
20	+	+	+	–	–	–	–	Histiocytoma
21	+	+	ND	–	–	ND	–	Histiocytoma
22	+	+	+	–	–	–	–	Histiocytoma
23	+	+	+	–	–	–	–	Histiocytoma
24*	+	+	+	–	–	–	–	Histiocytoma
25	+	–	+	–	–	–	–	Histiocytoma
26	+	–	+	–	–	–	–	Histiocytoma
27	+	–	+	–	–	–	–	Histiocytoma
28	+	–	+	–	–	–	–	Histiocytic sarcoma
29	+	+	–	+	–	–	–	Epitheliotropic T-cell lymphoma
30	+	–	–	+	–	–	–	Epitheliotropic T-cell lymphoma
31*	+	–	–	+	–	–	–	Epitheliotropic T-cell lymphoma
32*	+	+	–	+	–	–	–	Epitheliotropic T-cell lymphoma
33	+	–	–	+	–	–	–	Epitheliotropic T-cell lymphoma
34*	+	+	–	+	–	–	–	Epitheliotropic T-cell lymphoma
35	–	–	–	+	–	–	–	Epitheliotropic T-cell lymphoma
36	–	–	ND	+	–	ND	ND	Epitheliotropic T-cell lymphoma
37*	+	+	ND	+	–	ND	ND	Epitheliotropic T-cell lymphoma
38	+	–	ND	–	+	–	–	Epitheliotropic B-cell lymphoma
39	+	–	ND	+	–	ND	–	Nonepitheliotropic T-cell lymphoma
40	–	–	–	+	–	–	–	Nonepitheliotropic T-cell lymphoma
41	–	–	–	+	–	–	–	Nonepitheliotropic T-cell lymphoma
42	+	–	–	+	–	–	–	Nonepitheliotropic T-cell lymphoma
43	–	–	–	–	+	–	–	Nonepitheliotropic B-cell lymphoma
44	–	–	ND	–	+	–	–	Nonepitheliotropic B-cell lymphoma

→

©Polish Society for Histochemistry and Cytochemistry

Table 2 (cont.). Basic antibody panel results in the evaluated canine cutaneous round cell tumours

No	MHCII	CD18	Iba1	CD3	CD79a	CD20	Tryptase	Diagnosis
45	–	ND	ND	–	+	+	–	Nonepitheliotropic B-cell lymphoma
46	+	–	–	–	+	+	–	Nonepitheliotropic B-cell lymphoma
47	+	+	–	–	+	+	–	Plasmacytoma
48	+	–	ND	–	+	–	–	Plasmacytoma
49	–	+	ND	–	+	–	–	Plasmacytoma
50	–	+	–	–	+	–	–	Plasmacytoma
51	–	–	ND	–	+	–	–	Plasmacytoma
52	–	–	ND	–	–	ND	+	Mast cell tumour
53	–	–	–	–	–	–	+	Mast cell tumour
54	–	ND	ND	–	–	ND	+	Mast cell tumour
55	–	–	ND	–	–	ND	+	Mast cell tumour
56	–	–	ND	–	–	ND	–	Alveolar rhabdomyosarcoma
57	–	–	ND	–	–	ND	–	Alveolar rhabdomyosarcoma
58	–	–	–	–	–	–	–	Amelanotic melanoma
59	–	–	–	–	–	–	–	Amelanotic melanoma
60	–	–	–	–	–	ND	–	Glomus tumour

Symbols: +, positive; –, negative; ND — not determined; * multiple tumours

lymphomas (8/60 cases, 13.3%), the tumour cells expressed either CD3 (4 cases, 6.7%) or CD79a (4 cases, 6.7%; Fig. 1D). The expression of CD20 was seen in two cases of nonepitheliotropic B-cell lymphoma. The expression of MHCII was observed in 8 cases of epitheliotropic lymphoma and 3 cases of nonepitheliotropic lymphoma, while the expression of CD18 — in 4 cases of epitheliotropic lymphoma. All evaluated lymphomas were negative to Iba1 and mast cell tryptase.

In cutaneous plasmacytomas (5/60 cases, 8.3%) collected from dogs aged 1.5–14 years (mean age: 8.3 years), the tumour cells expressed CD79a, and, in one of these cases — also CD20, but the nuclear:-cytoplasmic ratio was substantially lower than that in tumours diagnosed as cutaneous B-cell lymphomas. In four of these cases, the cytoplasm stained magenta with methyl green pyronine. The expression of MHCII was observed in 2 cases, while CD18 — in 3 cases. All evaluated plasmacytomas were negative to Iba1 and mast cell tryptase.

In four other cases (4/60, 6.7%), tumour cells expressed mast cell tryptase and were negative to other markers; therefore, their final diagnosis was mast cell tumour. The metachromatic granules, which were indiscernible in routine HE staining, were visualized by May-Grünwald-Giemsa staining in only one of these tumours.

The final diagnosis could not be assessed on the basis of the results of the basic antibody panel in 5/60 cases (8.3%), as the tumour cells did not express MHCII, CD18, Iba1, CD3, CD79a, CD20 or mast cell tryptase.

In two of these cases (3.3%), tumour cells expressed vimentin and desmin and did not express the other markers, with the final diagnosis being alveolar rhabdomyosarcoma (Fig. 1E). In one of these dogs, due to the simultaneous occurrence of another tumour on the forearm, multiple round cell neoplasia was suspected. However, after the IHC assessment, the other tumour was diagnosed as a histiocytoma.

In one of the evaluated tumours, the tumour cells expressed vimentin, S-100 and melan-A and did not express the other evaluated markers, with a final diagnosis of amelanotic melanoma. No melanin granules were found in the cytoplasm of the tumour cells. The surface of the tumour was massively ulcerated, but distinct epidermal invasion was noted. In other tumour, the tumour cells expressed vimentin and S-100, but were negative to melan-A (as well as other evaluated markers), and therefore amelanotic melanoma was suspected. Unfortunately, in this case, the size of the sample was not sufficient for further evaluation.

In one tumour located in the area of the lips, the tumour cells expressed vimentin and α-SMA and did not express the other evaluated markers, and the tumour was finally diagnosed as a glomus tumour. Round to oval neoplastic cells formed small clusters surrounded by a PAS-positive basement membrane (Fig. 1F).

©Polish Society for Histochemistry and Cytochemistry

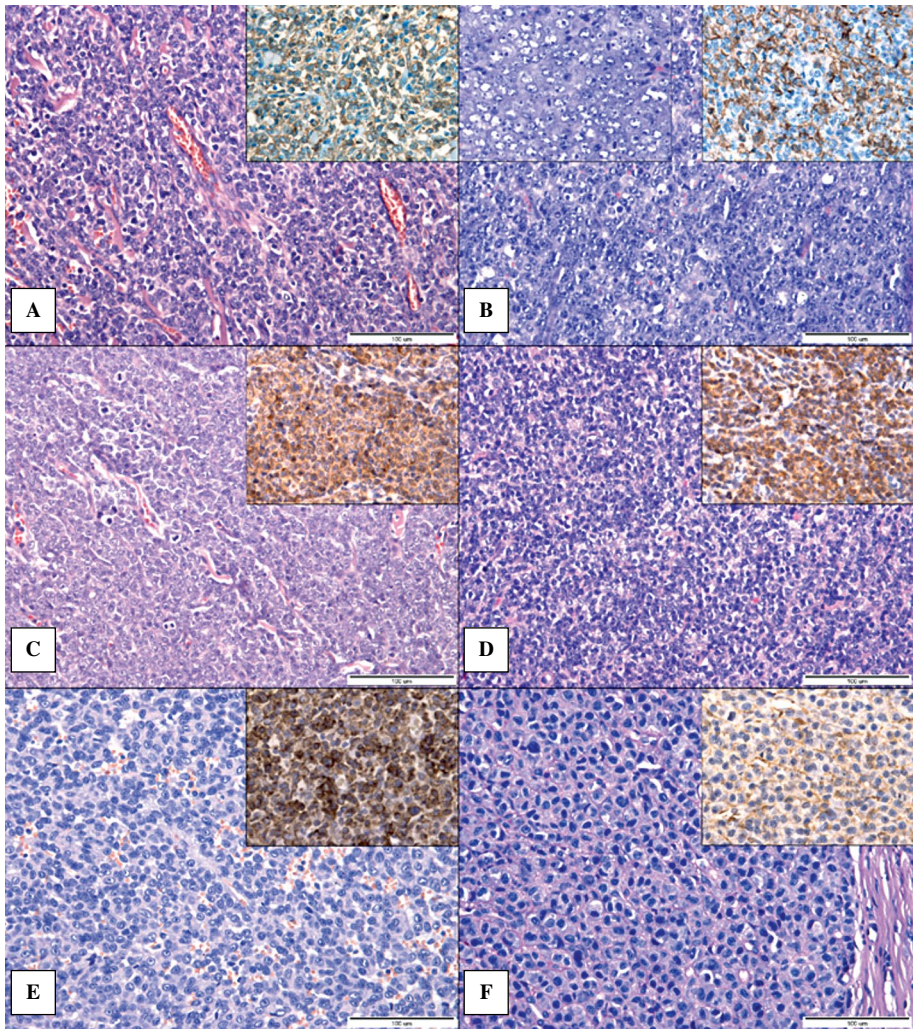

Figure 1. Microphotographs show undifferentiated canine cutaneous round cell tumours with similar histologic presentations and various definitive diagnoses. **(A)** Histiocytoma. Tumour comprised uniformly polygonal cells, with a moderately abundant, slightly eosinophilic cytoplasm (HE). Inset: Tumour cells show cytoplasmic and membranous expression of Iba1 (IHC, DAB). **(B)** Histiocytic sarcoma. Round to polygonal tumour cells with high mitotic and apoptotic rates. Morphologically, the tumour cells are similar to the testicular tumour (left inset), but these cells are packed more densely with nuclear crowding (HE). Right inset: Tumour cells showing the cytoplasmic and membranous expression of Iba1 (IHC, DAB). **(C)** Epitheliotropic T-cell lymphoma. Round to polygonal tumour cells with low-to-moderate anisocytosis and anisokaryosis and a high mitotic rate (HE). Inset: Tumour cells show the cytoplasmic expression of CD3 (IHC, DAB). **(D)** Nonepitheliotropic B-cell lymphoma. Tumour comprised uniformly round cells with low anisocytosis and anisokaryosis and small-to-moderate amounts of cytoplasm (HE). Inset: Tumour cells show the cytoplasmic expression of CD79a (IHC). **(E)** Alveolar rhabdomyosarcoma. Polygonal tumour cells with moderate anisocytosis and anisokaryosis form clusters separated by thin, highly vascularized fibrous septa (HE). Inset: Tumour cells show the cytoplasmic expression of desmin (IHC, DAB). **(F)** Glomus tumour. Small clusters of tumour cells are surrounded by a PAS-positive basement membrane (PAS). Inset: Immunoreactivity to ^SMA concentrated near the cellular membrane of the tumour cells (IHC, DAB)

Discussion

In the present study, histiocytomas and cutaneous lymphomas constituted the vast majority (75%) of the evaluated tumours. Therefore, histiocytomas and cutaneous lymphomas should be considered at the beginning of the differential diagnosis of CCRCTs. Histiocytomas are very common in dogs [2, 20], while cutaneous lymphomas occur less commonly and represent 1% of all canine skin tumours [12, 21]. In the present study, only tumours posing diagnostic difficulties were included; therefore, the number of detected tumours does not reflect their occurrence in the population.

In the present study, multiple tumours were seen in 4 cases of epitheliotropic T-cell lymphoma and in

©Polish Society for Histochemistry and Cytochemistry

one case of histiocytoma. While epitheliotropic T-cell lymphoma has a wide range of clinical presentations, and primary skin lesions, even if solitary, mostly progress into disseminated or generalized disease [12], multiple histiocytoma is very rare and occurs in less than 1% of the cases [22]. However, other CCRCTs, including non-epitheliotropic lymphoma, mast cell tumour and plasmacytoma, can also present as multiple tumours [21, 23, 24].

Epitheliotropism is an important diagnostic feature of some types of CCRCTs, allowing clinicians to narrow the list of possible diagnoses. The ability of tumour cells to invade and infiltrate the epidermis and/or adnexa results from the expression of specific adhesion molecules [25, 26]. Distinct epitheliotropism is highly indicative for epitheliotropic lymphoma and histiocytoma, but can be also seen in melanoma [2], and was reported in a few cases of mast cell tumour [26]. In the present study, epitheliotropism was a distinct feature of epitheliotropic lymphoma, but was also noted in most cases of histiocytoma and one case of amelanotic melanoma. However, the presence *versus* the lack of epitheliotropism should be interpreted with caution, as some authors claim that epitheliotropism of the epitheliotropic lymphoma may be reduced in association with progressive and severe dermal invasion [12]. Nevertheless, epitheliotropism is usually still prominent in canine tumour-stage mycosis fungoides, unlike its human equivalent [25]. Furthermore, the characteristic packets of tumour cells within the epidermis are not easy to detect in massively ulcerated tumours, as seen in the present study and in previous reports [8, 27].

The results of the present study indicate, that expression of Iba1 is specific for canine histiocytic tumours, what was also reported previously [11]. In the present study, expression of both MHCII and CD18 was not specific for histiocytoma, and was seen also in 4 cases of epitheliotropic T-cell lymphoma and one case of plasmacytoma. Furthermore, in 4 cases of histiocytoma and a histiocytic sarcoma, tumour cells were negative to CD18. The previous report revealed, that significant number of histiocytomas showed CD18 expression in only a small number of the tumour cells [8]. Therefore, we suggest, that Iba1 can easily replace both MHCII and CD18 in the basic antibody panel for the diagnosis of CCRCTs.

In the present study, the expression of CD20 was reported in two cases of nonepitheliotropic B-cell lymphoma and one case of plasmacytoma, so its sensitivity in identifying tumours of B-cell origin was much lower, than CD79a. Although CD20 is a valuable aid in immunophenotyping of canine lymphomas [16], the utility of this marker in diagnosing CCRCTs seems to be limited. Furthermore, it has been shown recently, that expression of CD20 in canine epitheliotropic T-cell lymphoma is not uncommon [28]. In the present study, one of the epitheliotropic lymphomas expressed CD79a and did not express CD3. Although epitheliotropic lymphomas are regarded to be exclusively of T-cell origin [21, 29], there is one report describing a B-cell epitheliotropic lymphoma [1].

The diagnosis of plasmacytoma in the present study was based on the immunoexpression of CD79a and the morphology, as the expression of CD79a alone cannot be used to distinguish B-cell lymphomas from plasmacytomas [1, 7]. All evaluated plasmacytomas expressed CD79a, and most of them (except for one) stained positive for MGP. Therefore, MGP staining can be used as an adjunct to the diagnosis of plasmacytomas, but cannot replace immunohistochemical markers. In a previous study, the antibody Mum-1p, used to detect multiple myeloma 1/interferon regulatory factor 4 (MUM1/IRF-4) antigen, was proven to be specific for canine plasmacytomas, superior in both sensitivity and specificity to CD79a [15]. However, the expression of MUM1/IRF-4 was also recently described in canine cutaneous histiocytomas, and therefore, this immunolabelling is recommended to be used only as a part of the round cell tumour panel, not alone [30].

Mast cell tumours frequently occur in dogs, and their diagnosis is usually straightforward due to the presence of characteristic, metachromatic granules in the cytoplasm of the tumour cells, which are easily identifiable with histochemical stains [31]. However, these granules are occasionally difficult to detect in some subsets of poorly differentiated mast cell tumours [32]. In the present study, the metachromatic granules were detected by histochemical staining (MGG) in only one of the four poorly differentiated mast cell tumours, but all of these tumours showed positive findings for mast cell tryptase. Therefore, mast cell tryptase immunolabelling should be considered superior in sensitivity to histochemical stainings for the identification of canine mast cell tumours. However, mast cell tumours that did not express tryptase but showed positivity for toluidine blue were previously described [1, 33]. Thus, the combination of mast cell tryptase immunolabelling and one of the histochemical stainings for metachromatic granule visualization would be the most appropriate method for the diagnosis of poorly differentiated mast cell tumours.

Amelanotic melanomas can be diagnostically challenging, as the cellular features of neoplastic cells may mimic poorly differentiated carcinomas, soft tissue sarcomas, and lymphomas [27, 34]. In the

©Polish Society for Histochemistry and Cytochemistry

present study, one case of CCRCT was diagnosed as amelanotic melanoma based on the immunoexpression of vimentin, S-100 and melan-A. In the other case, tumour cells expressed vimentin and S-100, but were melan-A negative. The expression of both vimentin and S-100 is not specific for melanocytes [34], and therefore the final diagnosis in that case was not obtained. However, the amelanotic melanoma can be suspected, as other possible differential diagnoses were excluded by other immunohistochemical stainings. In this case, other melanocytic markers should be applied, such as antibody PNL2, which was shown to be more sensitive than melan-A in the identification of canine melanocytic neoplasms [27, 35].

Other round cell tumours included in the present study, *i.e.*, alveolar rhabdomyosarcoma and glomus tumour, are not usually included in the differential diagnosis of CCRCTs. However, alveolar rhabdomyosarcoma can manifest as a cutaneous lesion, as described in a previous study [36]. In contrast to alveolar rhabdomyosarcoma, which, in our opinion, should be always included in the differential diagnosis of poorly differentiated CCRCTs (negative to basic antibody panel), glomus tumours seem to be extremely rare. Glomus tumours are benign neoplasms derived from glomus cells and are found frequently in humans but have been described in only single case reports in dogs [37–40].

In conclusion, histiocytoma and cutaneous lymphoma should be considered at the beginning of differential diagnosis of poorly differentiated CCRCTs. The expression of Iba1 is specific for canine cutaneous histiocytic tumours (including histiocytoma and histiocytic sarcoma), and more sensitive than CD18. The utility of CD20 in the diagnosis of CCRCTs is limited. Although most undifferentiated CCRCTs can be diagnosed immunohistochemically using 1–4 basic antibodies, some require a broad antibody panel, including mesenchymal, epithelial, myogenic, and melanocytic markers. Clinicians should also take into account the fact that many different types of CCRCTs can be morphologically indistinguishable from each other, and immunohistochemistry should be routinely recommended to confirm the morphological diagnosis, especially when there are discrepancies between the diagnosis and the clinical picture of the disease.

Acknowledgements

The project was financially co-supported by Minister of Science and Higher Education in the range of the program entitled "Regional lnitiative of Excellence" for the years 2019–2022, Project No. 010/RID/2018/19, amount of funding 12.000.000 PLN.

Conflict of Interest

The authors declared no potential conflicts of interest with respect to the research, authorship, and/or publication of this article.

References

1. Fernandez NJ, West KH, Jackson ML, et al. Immunohistochemical and histochemical stains for differentiating canine cutaneous round cell tumors. Vet Pathol. 2005; 42(4): 437–445, doi: 10.1354/vp.42-4-437, indexed in Pubmed: 16006603.
2. Meuten DJ ed. Tumours in Domestic Animals, 5th ed. Ames: Wiley Blackwell; 2017.
3. Sandusky GE, Carlton WW, Wightman KA. Diagnostic immunohistochemistry of canine round cell tumors. Vet Pathol. 1987; 24(6): 495–499, doi: 10.1177/030098588702400604, indexed in Pubmed: 3137715.
4. Cangul IT. Improved classification, diagnosis and prognosis of canine round cell tumours. Vet Sci Tomorrow. 2001; 4: 1–19.
5. Erich SA, Constantino-Casas F, Dobson JM, et al. Morphological Distinction of Histiocytic Sarcoma from Other Tumor Types in Bernese Mountain Dogs and Flatcoated Retrievers. In Vivo. 2018; 32(1): 7–17, doi: 10.21873/invivo.11198, indexed in Pubmed: 29275293.
6. Ramos-Vara JA, Kiupel M, Baszler T, et al. American Association of Veterinary Laboratory Diagnosticians Subcommittee on Standardization of Immunohistochemistry. Suggested guidelines for immunohistochemical techniques in veterinary diagnostic laboratories. J Vet Diagn Invest. 2008; 20(4): 393–413, doi: 10.1177/104063870802000401, indexed in Pubmed: 18599844.
7. Araújo M, Preis I, Lavalle G, et al. Histomorphological and immunohistochemical characterization of 172 cutaneous round cell tumours in dogs. Pesquisa Veterinária Brasileira. 2012; 32(8): 772–780, doi: 10.1590/s0100-736x2012000800016.
8. Paździor-Czapula K, Rotkiewicz T, Otrocka-Domagała I, et al. Morphology and immunophenotype of canine cutaneous histiocytic tumours with particular emphasis on diagnostic application. Vet Res Commun. 2015; 39(1): 7–17, doi: 10.1007/s11259-014-9622-1, indexed in Pubmed: 25563490.
9. Moore PF, Rossitto PV, Danilenko DM. Canine leukocyte integrins: characterization of a CD18 homologue. Tissue Antigens. 1990; 36(5): 211–220, doi: 10.1111/j.1399-0039.1990.tb01831.x, indexed in Pubmed: 1710078.
10. Day MJ. Immunophenotypic characterization of cutaneous lymphoid neoplasia in the dog and cat. J Comp Pathol. 1995; 112(1): 79–96, doi: 10.1016/s0021-9975(05)80091-x, indexed in Pubmed: 7722010.
11. Pierezan F, Mansell J, Ambrus A, et al. Immunohistochemical expression of ionized calcium binding adapter molecule 1 in cutaneous histiocytic proliferative, neoplastic and inflammatory disorders of dogs and cats. J Comp Pathol. 2014; 151(4): 347–351, doi: 10.1016/j.jcpa.2014.07.003, indexed in Pubmed: 25172051.
12. Fontaine J, Bovens C, Bettenay S, et al. Canine cutaneous epitheliotropic T-cell lymphoma: a review. Vet Comp Oncol. 2009; 7(1): 1–14, doi: 10.1111/j.1476-5829.2008.00176.x, indexed in Pubmed: 19222826.
13. Mason DY, van Noesel CJ, Cordell JL, et al. The B29 and mb-1 polypeptides are differentially expressed during human B cell differentiation. Eur J Immunol. 1992; 22(10): 2753–2756, doi: 10.1002/eji.1830221044, indexed in Pubmed: 1396979.

©Polish Society for Histochemistry and Cytochemistry

14. Schrenzel M, Naydan D, Moore P. Leukocyte differentiation antigens in canine cutaneous and oral plasmacytomas. Veterinary Dermatology. 1998; 9(1): 33–41, doi: 10.1046/j.1365-3164.1998.00078.x.
15. Ramos-Vara JA, Miller MA, Valli VEO. Immunohistochemical detection of multiple myeloma 1/interferon regulatory factor 4 (MUM1/IRF-4) in canine plasmacytoma: comparison with CD79a and CD20. Vet Pathol. 2007; 44(6): 875–884, doi: 10.1354/vp.44-6-875, indexed in Pubmed: 18039900.
16. Jubala CM, Wojcieszyn JW, Valli VEO, et al. CD20 expression in normal canine B cells and in canine non-Hodgkin lymphoma. Vet Pathol. 2005; 42(4): 468–476, doi: 10.1354/vp.42-4-468, indexed in Pubmed: 16006606.
17. de Souza Junior DA, Santana AC, da Silva EZ, et al. The Role of Mast Cell Specific Chymases and Tryptases in Tumor Angiogenesis. Biomed Res Int. 2015; 2015: 142359, doi: 10.1155/2015/142359, indexed in Pubmed: 26146612.
18. Walls AF, Jones DB, Williams JH, et al. Immunohistochemical identification of mast cells in formaldehyde-fixed tissue using monoclonal antibodies specific for tryptase. J Pathol. 1990; 162(2): 119–126, doi: 10.1002/path.1711620204, indexed in Pubmed: 2250189.
19. Horny HP, Valent P. Diagnosis of mastocytosis: general histopathological aspects, morphological criteria, and immunohistochemical findings. Leuk Res. 2001; 25(7): 543–551, doi: 10.1016/s0145-2126(01)00021-2, indexed in Pubmed: 11377679.
20. Gesek M, Rotkiewicz T, Otrocka-Domagała I, et al. Manifestation of Tumours in Domestic Animals in Warmia and Mazury (Poland) Between 2003 and 2011. Bulletin of the Veterinary Institute in Pulawy. 2014; 58(3): 439–446, doi: 10.2478/bvip-2014-0067.
21. Lee Gr, Ihrke PJ, Walder WJ, et al. Skin diseases of the dog and cat. Clinical and histopathologic diagnosis. 2th ed. Oxford: Blackwell Science Ltd. ; 2005.
22. Moore PF. A review of histiocytic diseases of dogs and cats. Vet Pathol. 2014; 51(1): 167–184, doi: 10.1177/0300985813510413, indexed in Pubmed: 24395976.
23. Rakich PM, Latimer KS, Weiss R, et al. Mucocutaneous plasmacytomas in dogs: 75 cases (1980-1987). J Am Vet Med Assoc. 1989; 194(6): 803–810, indexed in Pubmed: 2466821.
24. London CA, Seguin B. Mast cell tumors in the dog. Vet Clin North Am Small Anim Pract. 2003; 33(3): 473–89, v, doi: 10.1016/s0195-5616(03)00003-2, indexed in Pubmed: 12852232.
25. Moore PF, Olivry T. Cutaneous lymphomas in companion animals. Clin Dermatol. 1994; 12(4): 499–505, doi: 10.1016/0738-081x(94)90216-x, indexed in Pubmed: 7866943.
26. Oliveira FN, Elliott JW, Lewis BC, et al. Cutaneous mast cell tumor with epitheliotropism in 3 dogs. Vet Pathol. 2013; 50(2): 234–237, doi: 10.1177/0300985812451626, indexed in Pubmed: 22700850.
27. Smedley RC, Lamoureux J, Sledge DG, et al. Immunohistochemical diagnosis of canine oral amelanotic melanocytic neoplasms. Vet Pathol. 2011; 48(1): 32–40, doi: 10.1177/0300985810387447, indexed in Pubmed: 21078882.
28. Ewing T, Pieper J, Stern A. Prevalence of CD20+ cutaneous epitheliotropic T-cell lymphoma in dogs: a retrospective analysis of 24 cases (2011-2018) in the USA. Veterinary Dermatology. 2018; 30(1): 51–e14, doi: 10.1111/vde.12703.
29. Moore PF, Olivry T, Naydan D. Canine cutaneous epitheliotropic lymphoma (mycosis fungoides) is a proliferative disorder of CD8+ T cells. Am J Pathol. 1994; 144(2): 421–429, indexed in Pubmed: 7906096.
30. Stilwell JM, Rissi DR. Immunohistochemical Labeling of Multiple Myeloma Oncogene 1/Interferon Regulatory Factor 4 (MUM1/IRF-4) in Canine Cutaneous Histiocytoma. Vet Pathol. 2018; 55(4): 517–520, doi: 10.1177/0300985818759770, indexed in Pubmed: 29444632.
31. Ribatti D. The Staining of Mast Cells: A Historical Overview. Int Arch Allergy Immunol. 2018; 176(1): 55–60, doi: 10.1159/000487538, indexed in Pubmed: 29597213.
32. Patnaik AK, Ehler WJ, MacEwen EG. Canine cutaneous mast cell tumor: morphologic grading and survival time in 83 dogs. Vet Pathol. 1984; 21(5): 469–474, doi: 10.1177/030098588402100503, indexed in Pubmed: 6435301.
33. Ozaki K, Yamagami T, Nomura K, et al. Mast cell tumors of the gastrointestinal tract in 39 dogs. Vet Pathol. 2002; 39(5): 557–564, doi: 10.1354/vp.39-5-557, indexed in Pubmed: 12243465.
34. Smith SH, Goldschmidt MH, McManus PM. A comparative review of melanocytic neoplasms. Vet Pathol. 2002; 39(6): 651–678, doi: 10.1354/vp.39-6-651, indexed in Pubmed: 12450197.
35. Ramos-Vara JA, Miller MA. Immunohistochemical identification of canine melanocytic neoplasms with antibodies to melanocytic antigen PNL2 and tyrosinase: comparison with Melan A. Vet Pathol. 2011; 48(2): 443–450, doi: 10.1177/0300985810382095, indexed in Pubmed: 20858741.
36. Otrocka-Domagala I, Pazdzior-Czapula K, Gesek M, et al. Aggressive, solid variant of alveolar rhabdomyosarcoma with cutaneous involvement in a juvenile labrador retriever. J Comp Pathol. 2015; 152(2-3): 177–181, doi: 10.1016/j.jcpa.2014.11.004, indexed in Pubmed: 25555631.
37. Shinya K, Uchida K, Nomura K, et al. Glomus tumor in a dog. J Vet Med Sci. 1997; 59(10): 949–950, doi: 10.1292/jvms.59.949, indexed in Pubmed: 9362049.
38. Dagli MLZ, Oloris SCS, Xavier JG, et al. Glomus tumour in the digit of a dog. J Comp Pathol. 2003; 128(2-3): 199–202, doi: 10.1053/jcpa.2002.0617, indexed in Pubmed: 12634100.
39. Furuya Y, Uchida K, Tateyama S. A case of glomus tumor in a dog. J Vet Med Sci. 2006; 68(12): 1339–1341, doi: 10.1292/jvms.68.1339, indexed in Pubmed: 17213705.
40. Park CH, Kozima D, Tsuzuki N, et al. Malignant glomus tumour in a German shepherd dog. Vet Dermatol. 2009; 20(2): 127–130, doi: 10.1111/j.1365-3164.2008.00714.x, indexed in Pubmed: 19220826.

Submitted: 4 September, 2019
Accepted after reviews: 23 September, 2019
Available as AoP: 25 September, 2019

©Polish Society for Histochemistry and Cytochemistry

INSTRUCTIONS FOR AUTHORS

MANUSCRPIT SUBMISSION

Folia Histochemica et Cytobiologica accepts manuscripts (original articles, short communications, review articles) from the field of histochemistry, as well as cell and tissue biology. Each manuscript is reviewed by independent referees. Book reviews and information concerning congresses, symposia, meetings etc., are also published.

All articles should be submitted to FHC electronically online at www.fhc.viamedica.pl where detailed instruction regarding submission process will be provided.

AUTHOR'S STATEMENT

The manuscript must be accompanied by the author's statement that it has not been published (or submitted to publication) elsewhere.

GHOSTWRITTING

Ghostwriting and guest-authorship are forbidden. In case of detecting ghost written manuscripts, their actions will be taking involving both the submitting authors and the participants involved.

The corresponding author must have obtained permission from all authors for the submission of each version of the paper and for any change in authorship. Submission of a paper that has not been approved by all authors may result in immediate rejection.

COST OF PUBLICATION

The cost of publication of accepted manuscript is 800 Euro.

OFFPRINTS

PDF file of each printed paper is supplied for the author free of charge. Orders for additional offprints should be sent to the Editorial Office together with galley proofs.

ORGANIZATION OF MANUSCRIPT

The first page must include: the title, name(s) of author(s), affiliation(s), short running head (no more than 60 characters incl. spaces) and detailed address for correspondence including e-mail. Organization of the manuscript: 1. Abstract (not exceeding one typed page — should consist of the following sections: Introduction, Material and methods, Results, Conclusions); 2. Key words (max. 10); Introduction; Material and methods; Results; Discussion; Acknowledgements (if any); References; Tables (with legends); Figures; Legends to figures.

In a short communication, Results and Discussion should be written jointly. Organization of a review article is free.

TECHNICAL REQUIREMENTS

Illustrations (line drawings and halftones) — either single or mounted in the form of plates, can be 85 mm, 125 mm, or 175 mm wide and cannot exceed the size of 175 × 250 mm. The authors are requested to plan their illustrations in such a way that the printed area is eco-nomically used. Numbers, inscriptions and abbreviations on the figures must be about 3 mm high. In case of micrographs, magnification (*e.g.* × 65 000) should be given in the legend. Calibration bars can also be used. For the best quality of illustrations please provide images in one of commonly used formats e.g. *.tiff, *.png, *pdf (preferred resolution 300 dpi). Color illustrations can be published only at author's cost and the cost estimate will be sent to the author after submission of the manuscript. Tables should be numbered consecutively in Arabic numerals and each table must be typed on a separate page. The authors are requested to mark the places in the text, where a given table or figure should appear in print. Legends must begin on a new page and should be as concise as necessary for a self-sufficient explanation of the illustrations. PDF file of each paper is supplied free of charge.

CITATIONS

In References section of article please use following American Medical Association 9th Ed. citation style. Note, that items are listed numerically in the order they are cited in the text, not alphabetically. If you are using a typewriter and cannot use italics, then use underlining.

Authors: use initials of first and second names with no spaces. Include up to six authors. If there are more than six, include the first three, followed by et al. If no author is given, start with the title. **Books:** include the edition statement (ex: 3rd ed. or Rev ed.) between the title and place if it is not the first edition. **Place:** use abbreviations of states, not postal codes. **Journals:** abbreviate titles as shown in *Index Medicus*. If the journal does not paginate continuously through the volume, include the month (and day). **Websites:** include the name of the webpage, the name of the entire website, the full date of the page (if available), and the date you looked at it. The rules concerning a title within a title are *not* displayed here for purposes of clarity. See the printed version of the manual for details. For documents and situations not listed here, see the printed version of the manual.

EXAMPLES

Book:

1. Okuda M, Okuda D. *Star Trek Chronology: The History of the Future.* New York: Pocket Books; 1993.

Journal or Magazine Article (with volume numbers):

2. Redon J, Cifkova R, Laurent S et al. Mechanisms of hypertension in the cardiometabolic syndrome. *J Hypertens.* 2009; 27(3):441–451. doi: 10.1097/HJH.0b013e32831e13e5.

Book Article or Chapter:

3. James NE. Two sides of paradise: the Eden myth according to Kirk and Spock. In: Palumbo D, ed. *Spectrum of the Fantastic*. Westport, Conn: Greenwood; 1988:219–223.

When the manufacturers of the reagents etc. are mentioned for the first time, town, (state in the US) and country must be provided wheras for next referral only the name of the firm should be given.

Website:

4. Lynch T. DSN trials and tribble-ations review. Psi Phi: Bradley's Science Fiction Club Web site. 1996. Available at: http://www.bradley.edu/campusorg/psiphi/DS9/ep/503r.htm. Accessed October 8, 1997.

Journal Article on the Internet:

5. McCoy LH. Respiratory changes in Vulcans during pon farr. *J Extr Med* [serial online]. 1999;47:237–247. Available at: http:// //infotrac.galegroup.com/itweb/nysl_li_liu. Accessed April 7, 1999.